Bergvesenet

Postboks 3021, N-7441 Trondheim

Rapportarkivet

Bergvesenet rapport nr	Intern Journal nr	Internt arkiv nr	Rapport lokalisering	Gradering
5354				

Kommer fra ..arkiv	Ekstern rapport nr	Oversendt fra	Fortrolig pga	Fortrolig fra dato:
Grong Gruber AS		Grong Gruber a.s.		

Tittel

THE GEOLOGY OF THE MOLYPDENIUM MINERALIZED AREA AT FREMSTFJELL, GRONG DISTRICT, CENTRAL NORWAY

Forfatter	Dato År	Bedrift (oppdragsgiver og/eller oppdragstaker)
A.R.I. Mohamed Elamin	1984	Grong Gruber AS

Kommune	Fylke	Bergdistrikt	1: 50 000 kartblad	1: 250 000 kartblad
Grong	Nord-Trøndelag	Trondheimske	18231	Grong

Fagområde	Dokument type	Forekomster (forekomst, gruvefelt, undersøkelsesfelt)
Geologi		Fremstfjell

Råstoffgruppe	Råstofftype

Sammendrag, innholdsfortegnelse eller innholdsbeskrivelse

Contents.

THE GEOLOGY OF THE MOLYBDENUM MINERALIZED AREA AT FREMSTFJELL, GRONG DISTRICT, CENTRAL NORWAY

Abdel Rahman Ibrahim Mohamed Elamin

B.Sc. (Honours) Khartoum

Thesis submitted for the Degree of

Master of Philosophy

Council for National Academic Awards

Portsmouth Polytechnic

Department of Geology

October 1984

I dedicate this work to my family,

most especially for the sacrifices they made

The geology of the molybdenum mineralized area at Fremstfjell, Grong District, Central Norway

Abdel R.I. Mohamed

ABSTRACT

The Fremstfjell area contains rocks of Middle Ordovician age thrust onto Precambrian gneisses of the Grong Culmination of the Baltic Shield. The Palaeozoic rocks comprise volcanics (basalt-rhyolite) with associated sediments, intruded by a trondhjemite complex that consists of gabbro, diorite and trondhjemite with minor granite. A zone of Mo-Cu stockwork mineralization surrounded by propylitic alteration is associated with the granite in the centre of the area. This complex is intruded by a set of post-mineralization dolerite dykes.

The present work is based on a field and laboratory study of these rocks. Two hundred rock samples including drill core were collected, sixty five samples were analysed for major and trace elements by XRF techniques, 24 polished sections were studied by reflected light microscopy and 8 sections were stained for feldspar discrimination at the Department of Geology, Portsmouth Polytechnic. A representative suite of 9 samples was selected for electron microprobe analysis which was carried out at the Department of Earth Sciences, Cambridge University.

The petrography and major and trace element geochemistry suggest that these rocks are part of a tholeiitic sequence with a distinct tendency towards calc-alkaline affinities and that they were generated in an island-arc. A model for the genesis of the trondhjemite magma is proposed in which mantle derived rocks such as island-arc basalts or ocean-floor low K tholeiites are partially melted to give the gabbro-trondhjemite suite.

The presence of indistinct mineral zoning, poorly defined alteration patterns and the Mo-Cu ore mineral assemblages suggest that porphyry-type mineralization occurs in the Fremstfjell area. A tentative model involving the derivation of ore-bearing fluids from a descending lithospheric slab and subsequent addition of material in a crustal circulating hydrothermal environment is proposed.

CONTENTS

LIST OF FIGURES

LIST OF TABLES

LIST OF PLATES

ACKNOWLEDGEMENT

I thank the Director General of the Geological and Mineral Resources Department of the Sudan for nomination for a Chevron Oil Fellowship which financed the work and for kind support. Grong Mines Ltd., Norway kindly allowed access and gave logistical support during the field work.

Thanks are due to Professor J.R. Vail who suggested the project and for the facilities and assistance which were provided in the Department of Geology at Portsmouth Polytechnic. I much appreciated and enjoyed the supervision and guidance of Dr. M.J. Ryan. I thank Dr. D.J. Hughes for his most useful criticism, discussion and reading of the manuscript and the other academic staff who helped me. Thanks are also due to Professor Frank Vokes and Herr Arve Haugen for their hospitality and to all my colleagues, especially Salih, Shazally and Toum. I enjoyed the companionship of my friends Richard Hocking, Steve Swatton, Pete Davis and Jane Enderby.

I am grateful to the technical staff, especially J. Vigay, J. Davidson, R. Pulley, D. Weights, D. Rowe and Mrs. L. Holland, for their help in various ways. I extend my thanks to Jackie Duggua for typing the thesis.

CHAPTER 1

Introduction

1.1 Location

Grong lies at latitude 64°30'N and longitude 12°45'E, approximately 150 km northeast of Trondheim, Nord Trøndelag, central Norway (Fig. 1). It lies in a large glaciated valley at the convergence of the Sanddøla and Namsen rivers. The Namsen has formed the main valley in the district and drains to the sea near Namsos. Grong is surrounded by steeply rising mountains that attain a maximum height of 1160 m in the north.

The area mapped lies 25 km east of Grong and occurs within the mountainous terrain of the Caledonides. To the south the area is bounded by the Sanddøla river which runs east-west along the southern contact between the Caledonides and the Precambrian supracrustal rocks of the Grong Culmination.

1.2 Topography and drainage

The investigated area has an altitude of between 640 and 690 m. It lies above the tree line and exhibits typical post-glacial topography but much of the topography is still governed by the geology. The ground level in the area drops gradually from 900 m north-east of Korttjern at Skarfjell to 500 m at Fremsttjern in the south-west (Fig. 2). Shear zones dissect the area, forming gullies or linear features that often run east to west and can be traced on the aerial photographs more clearly than on the ground (Plate 1).

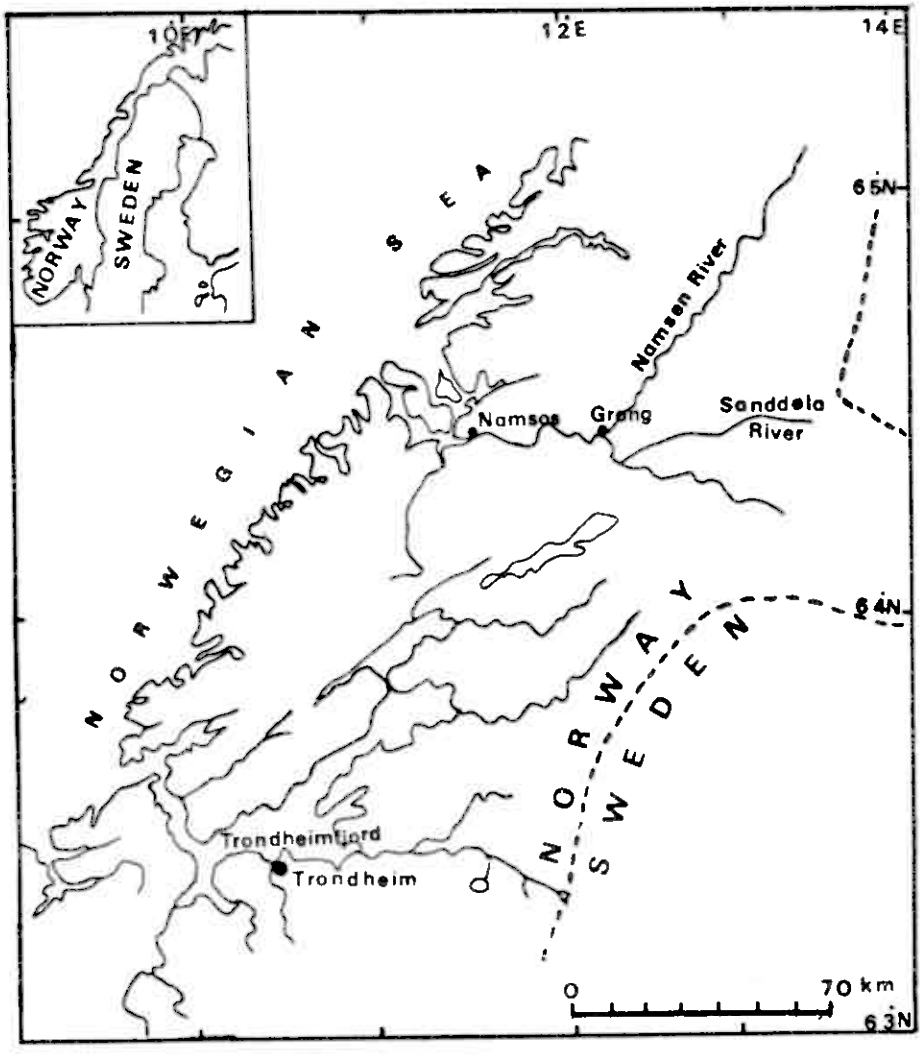

Fig 1 Location Map

The area is characterized by the development of numerous lakes. These lakes are oriented along the shear zones and they also widen at the intersection of the shear zones with major thrust zones.

The area is traversed by two local watersheds, one runs north-south from near Korttjern to a triangulation point (688, Fig. 2), and the other lies to the west and runs north-west between Bergtjern and Skarsfjellet. The area south of Langtjern is drained to the Sanddøla river by many parallel streams, however south-west of this lake the drainage pattern and distribution of lakes is controlled by thrust faulting (Fig. 2). Generally, the drainage pattern contains both dendritic and rectilinear elements and the latter is controlled by the underlying structure.

The terrain is smooth with rounded peaks. Frost action has emphasised jointing, producing a tabular appearance to the rocks which occasionally show evidence of ice gouging.

1.3 Climate, vegetation and accessibility

Because of its altitude, its position some eighty kilometers from the Atlantic Coast of Norway and some two degrees of latitude south of the Arctic Circle the area has sub-arctic climate with cool temperate summers. The 1981 field season was hindered by poor weather in August and September which followed all-time record high temperatures in July of that year. In 1982 one week was lost to bad weather with the rest of the season warm and dry.

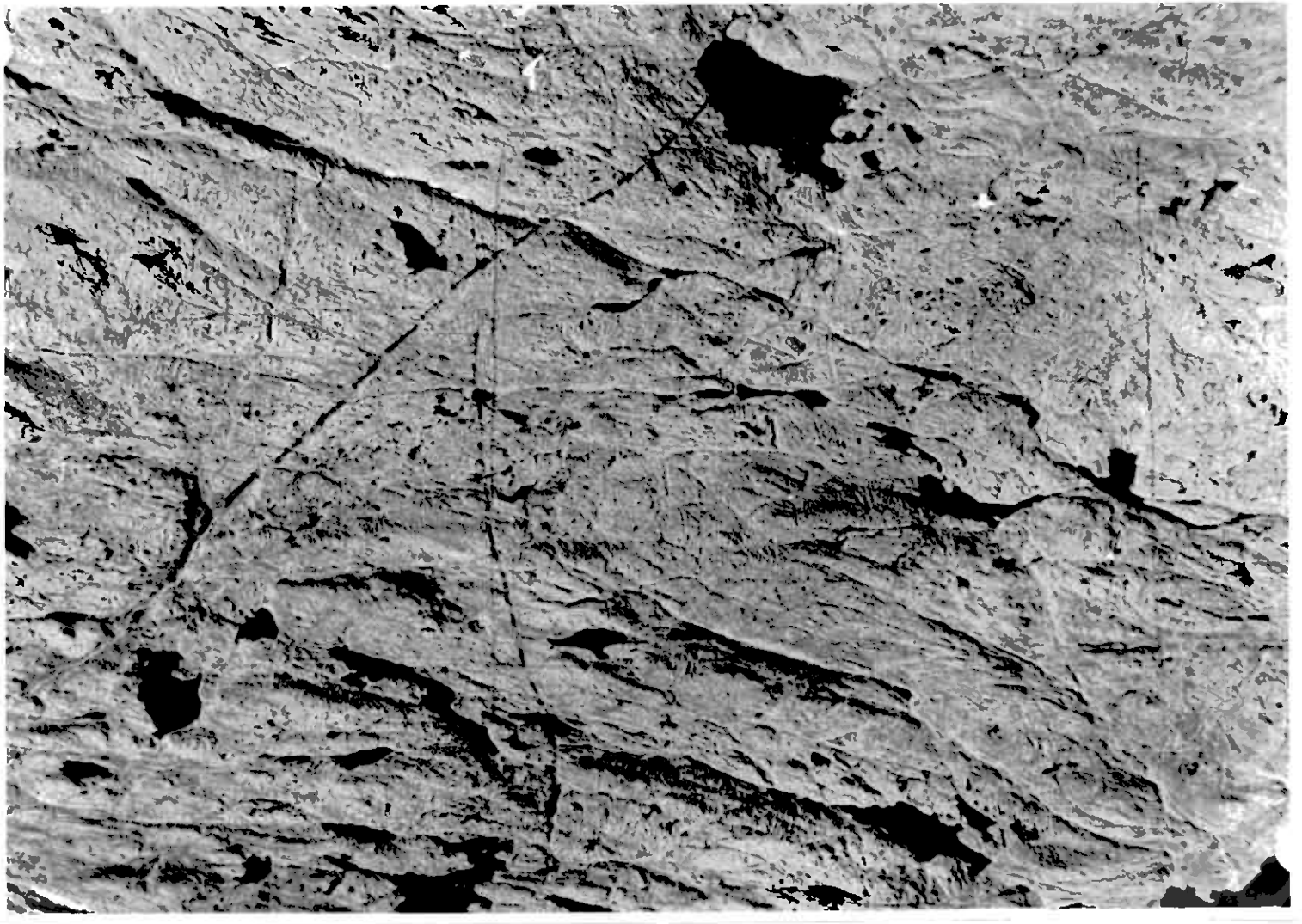

Plate(1): Aerial photograph showing intense NW-SE linear shear zones, broken by faults and joints. (North is top). Large lake at the top of the photograph is Korttjern (see map 1). Scale approx. 1:20,000.

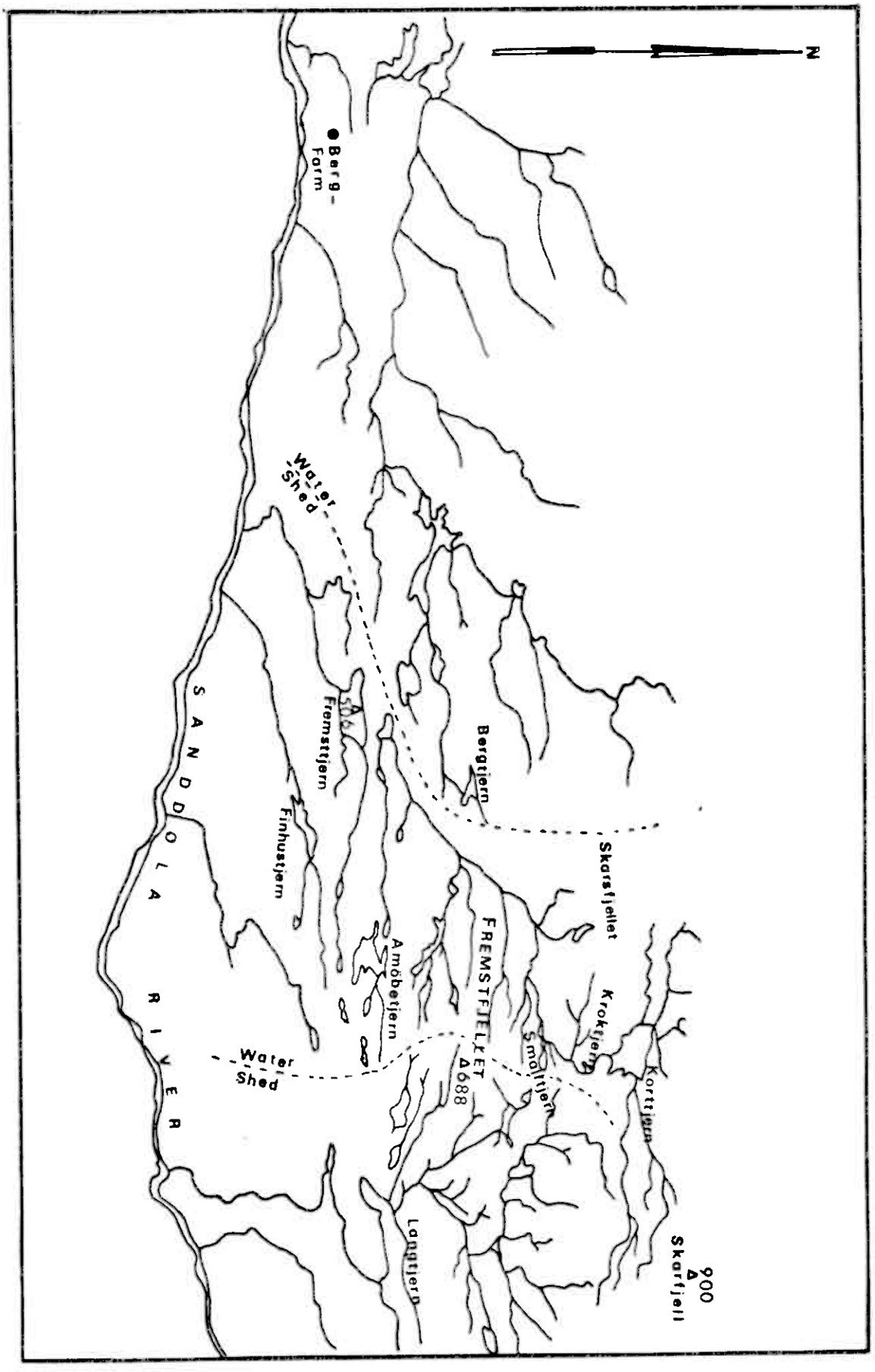

Scale 1:40000

Fig 2 Drainage Map

As the area lies above the tree-line it is vegetated mainly by coarse grass, reindeer moss, heather, bracken and swamp vegetation. Occasional dwarf birch and dwarf conifers also occur. The terrain supports an abundant insect fauna, principally mosquitoes and black-flies with clegs down towards the fringes of the forest.

Access was by vehicle to the abandoned hill farm of Berg (Fig. 2), about 7-8 kilometers west-southwest of the area and then a 2-3 hour hike was required up to the field-camp. Grong Gruber A/S provided a small cabin and camping equipment on the mountain. In 1981 most of the rock samples were flown out by helicopter; apart from that, everything had to be back-packed into and out of the area.

1.4 Previous work

The main features of the geology of the Grong District are known through the mapping of Steiner Foslie (1920-1930) at 1:50,000 scale. In 1951 Norges Geologiske Undersøkelse (N.G.U.) published geological map sheets at a scale of 1:100,000. The northernmost of these map sheets (Namsvatnet med en del av Frøyningsfjell), was described by Strand (Foslie and Strand, 1956), with some later additions in 1963. In 1956 Chr. Oftedahl discussed some of the main features of the tectonics and in 1958 he described the ore occurrences in the district. Zachrisson mapped Jämtland and Västerbotten in Sweden in 1969, and produced the basis for the succession in the Köli Nappe which forms the main structural element in the region.

During the 1970's mineral exploration activity was intensified in the area. The "Grong Project" was undertaken by the Grong Gruber and Skorovas Gruber mining companies, in co-operation with N.G.U. in the period 1970-75. This resulted in mapping an area that extends from Namsvann-Huddingsdalen in the north to Grong-Sanddøla-Nordli in the south, bounded by the Swedish border to the east. As part of the Grong Project Gale (1972) mapped the Fremstfjell area. Recently, mapping in the area has been carried out by R. Kvien between Huddingsdalen and Limingen and A. Reymer in the Nordli area (N.G.U. unpublished work). In 1975 R. Greiling carried out a tectonic study based on photogeology in the area north of Huddingsdalen and some results from the Skorovaton area were subsequently published (Halls et al., 1977).

In 1975 an N.G.U. team carried out geochemical stream sampling and this work was published at 1:20,000 scale by N.G.U. The map shows the occurrence of copper and molybdenum mineralization. Also, Gale (1973) reported the occurrence of molybdenite in the Fremstfjell area. Consequently, the Fremstfjell area attracted Grong Gruber A/S to explore the area and prospect for molybdenum ores. In 1979 F. Vokes (University of Trondheim) and A. Haugen (Grong Gruber) visited the area and Vokes reported that there was a possibility of porphyry-type molybdenum mineralization (Grong Gruber, unpublished report). In 1980 Grong Gruber made an induced polarisation survey of the area and also carried out a programme of trenching. Also in 1980, M. Ryan and M. Holman

(Portsmouth Polytechnic) mapped and grab-sampled the area. Since 1981, M. Ryan and the present author have been investigating the area.

1.5 Present work

Data for this investigation have been collected by the present author who visited the area with M. Ryan of Portsmouth Polytechnic during two five-week field seasons in August/September 1981 and July/August 1982. 1:5,000 scale topographic sheets and 1:20,000 scale aerial photographs were used as base maps to prepare a 1:5,000 scale geological map that has been reduced to 1:10,000 (pocket).

More than two hundred rock samples, including drill cores, were collected for petrographical, geochemical and ore petrographical studies (Chapters 3, 4 and 5 respectively). Sixty-five samples representing the rock units were analysed by X-ray fluorescence techniques for 10 majors and a number of trace elements. These samples, plus drill core and grab-samples from trenches, were analysed for Mo and Cu by Mercury Analytical Ltd. of Ireland using a technique involving solution in HNO_3 + $HClO_4$ and then atomic absorption spectrophotometry - with addition of Al to avoid Mo-suppression by Ca (P. Cazalet, Mercury Analytical, written comm.).

Twenty-four polished sections have been studied microscopically in an attempt to elucidate the mineralization and its relationships with the enclosing rocks (Chapter 5). Forty-nine mineral analyses were made using the Electron Microprobe at the Department of Earth Science, Cambridge University and

they are presented in Appendix 2. Eight thin sections were stained using the technique Bailey and Stevens (1960) in order to determine K-feldspar and plagioclase in granite and trondhjemite (see Chapter 3).

CHAPTER 2

Regional Geology

2.1 Introduction

Norway is an integral part of the Scandinavian Peninsula. It is a mountainous country rich in metalliferous deposits. Its present morphology is probably due to uplift accompanied by marginal faulting in Cenozoic times (Holtedahl, 1960).

Norwegian rocks fall into two major groups: namely Precambrian and Caledonian (Oftedhal, 1980).

2.2 The Precambrian Rocks

The Precambrian of Norway is a part of the Baltic Shield that forms the north-western extremity of Fennoscandia (Miyashiro, 1973) and contains widespread metalliferous deposits. Geochronologically, these rocks can be divided into an older Northern and a younger Southern province (Fig. 3).

2.2.1 Northern Precambrian Province

This province can be divided (Oftedhal, 1980) into two main regions: the Varanger-Finnmark region and the coastal Lofoten-Vesterålen-Tromsø region, dominantly east and west of the Caledonian zone respectively. Precambrian windows are also widespread within the Caledonides of Finnmark (Oftedhal, op. cit.).

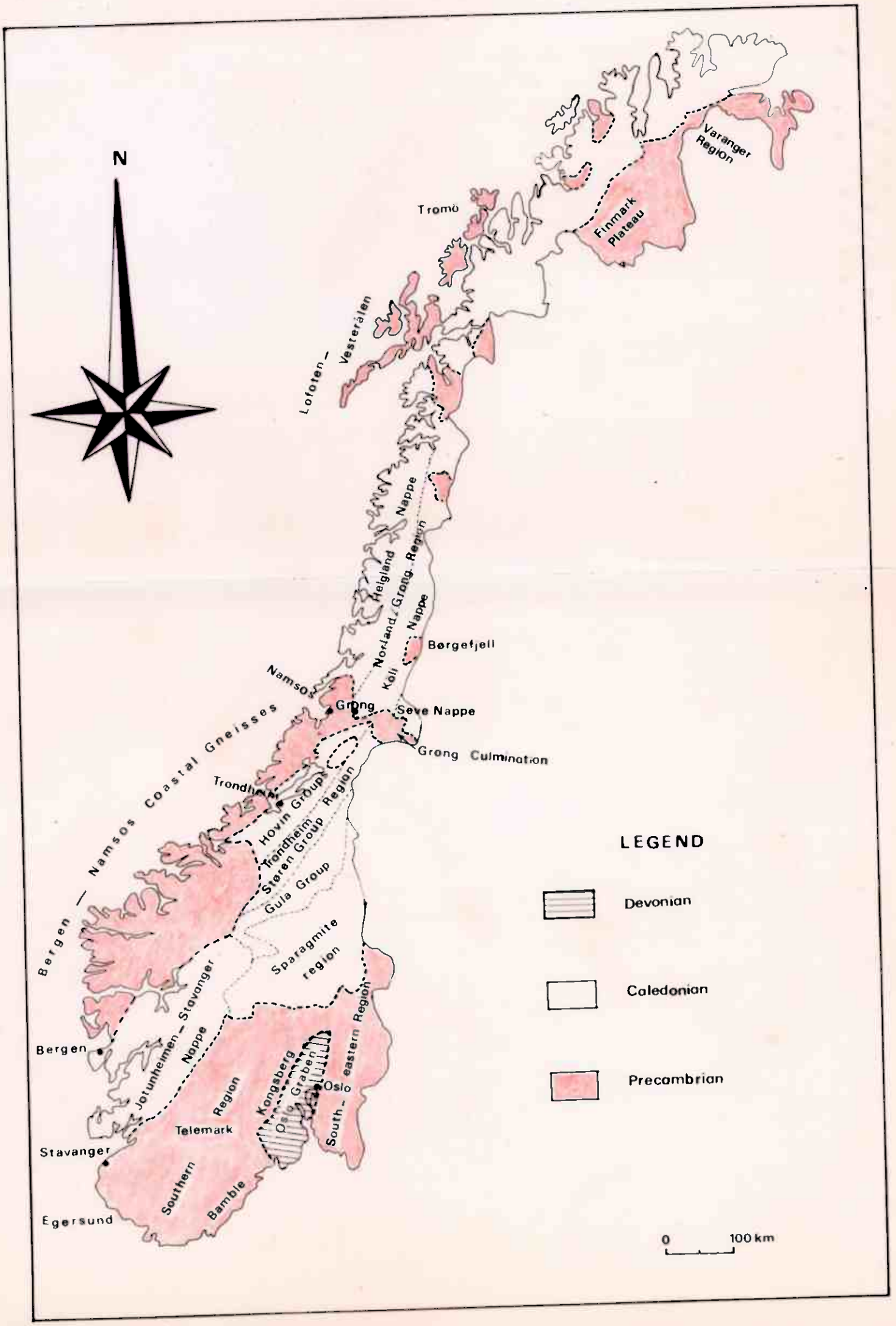

Fig 3 Sketch map of the main geological division of Norway

(modified from Chr. Oftedahl, 1980)

11

2.2.1.1 Varanger-Finnmark region

This region is mainly underlain by a 2800 Ma old basement (The Jarfjord complex, Oftedhal (op. cit.), unconformably overlain by two metamorphosed supracrustal groups 2600 and 2000-1800 Ma old respectively. The basement rocks comprise granitic and migmatitic gneisses with subordinate schists and amphibolites. Both supracrustal units are composed of sedimentary rocks sometimes intercalated with volcanic rocks. They are all generally mildly folded and regionally metamorphosed in the greenschist facies.

2.2.1.2 Lofoten-Vesterålen-Tromsø region

This region, on the western side of the Caledonian zone (Fig. 3), (Griffin et al., 1978) is underlain by strongly deformed migmatites which are 2700 Ma old and which have mainly nebulitic structures.

Weakly deformed supracrustal volcanic and sedimentary units above are thought to belong to a continental orogenic suite related to an Andean-type subduction zone (Oftedhal, 1980). The highest grade of metamorphism in the supracrustals occurred around 1830 Ma (Oftedhal, op. cit.), culminating in granulite and amphibolite facies in the southwestern and northeast parts of the region.

All of the above sequences were cut by a plutonic suite comprising gabbro, mangerite and granite which were emplaced within the period 1800-1700 Ma (Malm and Ormaasen, 1978).

2.3.1 Southern Precambrian Province

This province (including part of the project area) comprises the younger Precambrian rocks. It generally lacks basement older than 1800 Ma (Oftedhal, 1980) and it covers the Nordland, Namsos-Bergen, Central-Southern and the South-eastern Precambrian areas (Oftedhal, op. cit.).

2.3.1.1 The Nordland area

The Nordland Precambrian rocks occur as windows in the Caledonides from Narvik to Trondelag that pass into Bergen-Namsos coastal massif (Oftedhal, op. cit.).

These windows consist of supracrustal biotite-quartz schist, biotite-quartzites and andesitic to dacitic meta-volcanics. These rocks frequently occur as folded roof pendants and enclaves within granite and syenite plutons of 1700 Ma age.

2.3.1.2 Namsos-Bergen coastal area

This area is divided by Trondheimsfjord (Fig. 3) into two parts.

From the fjord north to Namsos the predominant units are migmatitic and granitic gneisses with migmatitic pelites of upper amphibolite facies.

From the fjord south to Bergen the area consists of two main complexes, a basement group and a supracrustal cover. The basement rocks are predominantly migmatitic gneisses. The supracrustal units comprise amphibolite facies meta-

sediments with lenses of dunite, anorthosite and eclogite all cut by meta-dolerite sills. However, according to Brueckner (1979) rocks from both complexes yield a Rb/Sr isochron age of 1700 Ma.

2.3.1.3 The Central-Southern Precambrian area

This area is bounded in the south by the Norwegian coast, in the east by the Oslo Graben (Barth and Reitan, 1963) and is overlain by the Caledonian thrust nappes from the north and northwest (Fig. 3). Oftedhal (1980) divided the area into lithological complexes: the Egersund Complex in the southwest, the Kongsberg-Bamble and the Telemark Supracrustal Complexes in the east and in the centre respectively and the Southern Basement Gneisses with associated post-tectonic granite.

The Egersund Complex comprises anorthosite with subordinate norite, monzonite and mangerite all cut by two generations of dolerite dykes. The anorthosites are thought to have evolved as anatectic magmas derived from an anorthositic layer in the lower crust (Pasteels et al., 1979).

Mixed gneisses, amphibolite and a variety of metasedimentary lithologies represent the most widespread rock units characteristic of the Kongsberg-Bamble Complex. Intrusive into these units are gabbros and dolerite sills cross cut by later orogenic granite and granitic pegmatites. All of these rocks are poly-metamorphosed (Jacobsen and Heier, 1978), complexly folded on various axes and faulted parallel to the

Oslo Rift (Oftedhal, 1980). Acidic and basic lavas occur at a number of localities and have island-arc geochemical affinities (Jacobsen and Heier, op. cit.).

The Telemark Supracrustal suite consists mainly of continental volcanic rocks interbedded with quartzitic sandstones. The volcanics are of tholeiitic to mild alkaline affinity (Sigmond, 1978). The Telemark volcanics and sedimentary rocks may have been formed between 1300-1200 Ma (Oftedhal, 1980).

The southern extremity of Norway is made up of mixed basement gneisses devoid of Telemark Supracrustals. The basement unit is cross-cut by basic plutonic rocks analogous to the Bamble gabbros (Oftedhal, 1980) which are nickel-bearing. All of the above mentioned rocks are intruded by either cross-cutting post-tectonic or concordant late-tectonic granites.

2.3.1.4 The Southeastern Precambrian

The outcrop area of Precambrian rocks in southeastern Norway is bounded by Oslofjord and the Swedish border in the west and east respectively (Fig. 3). Petrographically it comprises a varied suite of gneisses intruded by minor gabbros and granites. However, these Precambrian rocks disappear beneath Cambrian shales to the north.

2.4 Caledonides

2.4.1 Introduction

Prior to the late Mesozoic opening of the Atlantic Ocean the Appalachian-Caledonian orogen formed a continuous belt from N. America through the British Isles to the Scandinavian Peninsula (Dewey and Kay, 1969). The Caledonides are bounded by the Baltic Shield to the east and by the Hercynian orogen to the south (Miyashiro, 1973).

The evolution of the Scandinavian Caledonides involved two major stages of tectono-metamorphic events: the Finnmarkian and the Scandinavian phases (Ramsay and Sturt, 1976; Roberts and Gale, 1978; Sturt et al., 1978). The Finnmarkian phase was broadly contemporary with the Grampian phase in the British Isles to the west (Ryan and Sturt, 1981), referred to as zone A by Dewey (1969) and with the obduction of ophiolitic assemblages onto the Baltic Shield in the west (Furnes et al., 1979). The Scandinavian phase was responsible for transport of great thrust nappes which presently dominate the pattern of the tectono-stratigraphic units in the Scandinavian Caledonides (Andersen et al., 1982).

In the Norwegian Caledonides, volcanic rocks are generally thin in the north, being represented by amphibolites of probable submarine origin. Similar rocks thicken in central and south Norway with the predominant basaltic lavas showing frequent pillow structures, again indicative of an aqueous environment of extrusion (Vokes and Gale, 1976). The lithological diversity of the Norwegian Caledonides can be grouped

(Oftedhal, 1980) into the following tectonic regions (Fig. 3): the Trondheim, the Nordland, the Troms and Finnmark and the Jotunheimen-Stavanger.

2.4.2 Trondheim region

This region is a key area in the Norwegian Caledonides. The rocks of the Trondheim region comprise unmetamorphosed Cambro-Silurian sediments (Trondheim Supergroup, Gale and Roberts, 1974), underlain by allochthonous rocks preserved in a depression within the Precambrian basement. The Trondheim Supergroup has been subdivided by the same authors (Gale and Roberts op. cit.) into lithostratigraphic units: the Gula; Støren; Lower Hovin; Upper Hovin and Horg Groups.

2.4.2.1 Gula Group

This group is heterogeneous in both age and derivation. It is mainly composed of metamorphosed igneous and sedimentary units which together form a sequence of gneisses, calc-silicate rocks, migmatites, mica schists, marbles, calcareous quartzites, quartzites, quartz conglomerates, metagraywackes, phyllites, amphibolites and minor serpentinized ultramafic bodies. These units may range in age from Precambrian to Cambrian and correspond to more than one orogenic cycle (Roberts and Sturt, 1980).

2.4.2.2 Støren Group

The Støren group is dominated by a low-grade metavolcanic terrain comprising greenstones and quartz-keratophyres with subordinate layered jasper, chert and phyllites implying a submarine origin. The greenstones, which sometimes contain

relict pillow structures, are intruded in some places by gabbros, trondhjemites and sheeted dolerite dykes. According to Gale and Roberts (1974) the above sequences are Palaeozoic ophiolite fragments having both ocean-floor and island-arc geochemical affinities.

2.4.2.3 Lower and Upper Hovin Groups and Horg Group

The Lower Hovin Group comprises basal conglomerates (derived mainly from the Støren rocks), metasandstones, siltstones, metagraywackes, pelites, marbles, intraformational conglomerates, greenstones and rhyolite tuffs. Fossils indicate an Ordovician (Arenig to Caradocian) age (Wolff, 1980).

These sequences are succeeded by polymict conglomerates alternating with flysch-type metagraywackes, sandstones, conglomerates and pelites with local marbles and tuffs all belonging to the Upper Hovin Group (Roberts, 1978).

The Horg Group consists of low-grade metasandstones and slates above quartzitic conglomerates and graptolite-bearing pelites. These groups comprise a volcanic-arc/back-arc basin assemblage overlying the Støren oceanic crust (Roberts, op. cit.).

2.4.3 Nordland/Grong Region

The Grong region is an extension of the Trondheim zone. It represents a depression between two Precambrian massifs: The Børgfjell Massif and the Grong Culmination to the north and south respectively (Kollung, 1979). It comprises three

lithotectonic units: the Seve, the Köli and the Helgeland Nappes (Roberts, op. cit.).

2.4.3.1 The Seve Nappe

The Seve Nappe lies to the east of the Grong Culmination (Fig. 3) and it largely comprises a supracrustal complex divided on lithological and metamorphic grounds into Eastern, Central and Western tectonic units all of which have been subjected to two phases of deformation (Aukes et al., 1979).

The Eastern belt consists of garnet-mica schists alternating with minor marble layers, meta-arkoses and amphibolites. The rocks have been metamorphosed in the upper greenschist facies with local attainment of amphibolite facies. The Central belt structurally overlies the Eastern belt and it consists of amphibolite facies rocks (migmatitic gneisses and amphibolites). The Western belt is relatively thin and is composed mainly of garnet-mica schist having the same metamorphic grade as the Eastern belt. The Seve nappe wedges out against the Grong Culmination to the west.

2.4.3.2 The Köli Nappe

This Nappe is structurally underlain by the Seve Nappe and is comparable to the Köli Nappe in Sweden (Zachrisson, 1969). It extends beyond the Grong Culmination to the south and to the north of the Børegefjell window (Fig. 3). It is composed largely of low grade regionally metamorphosed volcanic and sedimentary sequences. The metavolcanics comprise

keratophyres, tuffs, hornblende schists and amphibolites with subordinate metagabbros. The metasediments include graphitic phyllites and marble horizons. Trondhjemites cut through both sequences and serpentinites are locally developed in the lower part of the Nappe (Oftedahl, 1980).

2.4.3.3 The Helgeland Nappe

This nappe is underlain by low-grade rocks of the Grong Culmination to the west and in the north by Rødingfjell Nappe (Ramberg, 1967). It consists of gneisses, mica schists with subordinate marbles and amphibolites. These rocks were intruded by acid rocks including the Bindal Granite, the biggest Caledonian granite massif in Norway. Small lenses of peridotite are also encountered and all of these rocks have been subjected to polyphase deformation and have been metamorphosed into lower to middle almandine amphibolite facies (Oftedahl, 1980).

2.4.4 Troms and Finnmark Region

2.4.4.1 Troms Region

This region comprises the northern Norwegian Caledonides and contains a number of lithostratigraphic units. These from oldest to youngest are: the Rombak, the Narvik, the Evenes, the Bogen and the Niingen Groups (Oftedhal, 1980).

The Rombak Group is underlain by an Archaean basement (Kulling, 1972) and it consists predominantly of mica schists

with subordinate marble and thin amphibolite horizons. These units are separated by a major thrust from the Narvik and Evenes Groups which are themselves over-thrust by the Bogen and Niingen Groups.

The Narvik Group is mainly composed of mica schist with quartzite largely intruded by granitic veins while the Evenes Group consists mainly of limestone with subordinate mica schist and quartzite.

The Bogen Group is made up of alternating mica schists, quartzites, marbles and dolomitic marbles and horizons of meta-sedimentary iron ore and the overlying Niingen Group consists of mica schist intruded by granitic rocks.

In general, mica schist with marbles form the bulk of the Troms region. However, intrusive rocks which consist predominantly of gabbros and diorites which relate to the nearby trondhjemites (Kulling, op. cit.) commonly occur.

2.4.4.2 Finnmark Region

The structure of the Finnmark region is dominated by a succession of nappes that have various structural and metamorphic relationships with the underlying basement. The nappes comprise the following units from oldest to youngest which have been dated by fossil evidence (Holland and Sturt, 1970): the Klubben, Storels, Afjord and Hellefjord Groups. The Klubben Group unconformably overlies Precambrian gneisses in a nappe structure (Ramsay and Sturt, 1977). It is mainly composed of

cross-bedded quartzites with layers of semi-pelites and marble all of which are regionally metamorphosed in higher amphibolite facies (Sturt and Roberts, 1978). The Klubben Nappe structurally overlain by the Storels and Afjord Groups. These Groups are predominantly composed of mixed garnet bearing psammites and pelites with subordinate graphitic schist and quartzites. The highest structural unit, the Hellefjord Group (Sturt et al., 1978) consists of metagraywackes with minor horizons of diopside-bearing schists.

The Caledonian rocks of Troms and Finnmark of northern Norway are thought to have been emplaced during the Finnmarkian phase of the Caledonian orogeny (Sturt and Roberts, 1978).

2.4.5 The Jotunheim-Stavanger (Nappe) region

This region contains the highest mountains in Norway and it consists of three nappes: the Jotun, the Bergsdalen and the Ryfylke Nappes.

The Jotun rocks (Goldschmidt, 1916) predominantly comprise gabbros with subordinate ultrabasic rock and anorthosites. According to Battey and McRitchie (1975) the gabbros were produced by magmatic differentiation from a melt and were later intruded by minor trondhjemite. The Jotun gabbros have been metamorphosed at granulite facies and retrogressed to amphibolite and greenschist assemblages. They are more or less deformed and often mylonitized predominantly along NE-SW trends (Battey and McRitchie, 1973).

The Bergsdalen Nappes represent the southwestern linear extension of the Jotun Nappe. They comprise a stack of sliced-off plates of Precambrian rocks with a Cambrian argillaceous sediment cover (Kvale, 1960). The Precambrian rocks include quartzites and metarhyolites with dolerite sills and are cut by a granite.

Cambro-Ordovician phyllite and mica schist form the bulk of the Ryfylke Nappe and discordantly overlie a Precambrian basement (Sigmond and Andresen, 1976). In some parts this group is interlayered with meta-andesite and overlain by albite gneiss, both of which have undergone low grade metamorphism. Acid and basic charnockitic rocks are sporadically developed within the gneiss.

2.5 Intrusive rocks

2.5.1 Introduction

Both the Precambrian terrains and structurally overlying Caledonian rocks of Norway (section 2.2, 2.3) have been disrupted by a variety of intrusive rocks which exhibit both lithological and structural diversity. The Norwegian intrusives cover a wide spectrum of ages which range from Precambrian to Palaeozoic. Geochemically, most of the intrusive rocks have either alkaline or calc-alkaline affinities although tholeiitic and transitional intrusives have been widely reported. Most of these rocks have already been described (in this chapter) in relation to their host rocks. However,

some of these rocks which are predominantly of Caledonian age will be briefly reviewed in this section with respect to some selected regions.

2.5.2 Trondheim region

Intrusives of Caledonian age occur throughout the Trondheim region and vary in composition from basic to acidic. A variety of gabbros occur associated with the Trondheim Supergroup (Wolff, 1967; Rui, 1972). Some of these rocks exhibit a clear differentiation trend from peridotite through olivine gabbro and gabbro/norite to granodiorite and granite (Willson and Olesen, 1975). Ultrabasic rocks are rare, they occur with minor intrusives in the Støren and Gula Groups and the Köli Nappe. Intermediate and acid rocks that include diorites, trondhjemites, monzonites, granodiorites and rare granites, occur in the Gula and Støren Groups. Metadolerites occur west of Trondheimsfjord and they are comparable in their ages and their geological characteristic with the intrusive rocks of Särs in Sweden (Andreasson et al., 1979).

2.5.3 Nordland region

The volcanic rocks of the Grong area are cut by widely distributed intrusives that vary in composition, predominantly from gabbros through diorite to trondhjemite. They occur as concordant sheets of various sizes, as minor lenses and circular bodies. The trondhjemites usually cross-cut the gabbros which sometimes occur as large roof pendants (Kollung, 1979).

Macroscopic textures in the gabbros include primary layering and igneous lamination (Hallset al., 1977) and most of the rocks are foliated parallel to the regional structural trends of the host rocks, suggesting their development as pre- or syn-tectonic intrusives (Kollung, op. cit.). Other intrusive rocks include granite, granodiorite, syenite and metadolerite in northern Grong and Børgefjell. The metadolerites probably represent the youngest intrusive phases in the region.

2.5.4 The Tromsø and Finnmark region

Intrusive rocks in the Tromsø region comprise two distinct suites: a Pre-Caledonian gabbro complex and a syn-orogenic plutonic suite. The Tromsø gabbro complex has been cut by a Caledonian thrust in the Lyngen Peninsula (Oftedhal, 1980). The Syn-orogenic plutonic province in the Oksfjord Peninsula is unique within the Caledonides. It comprises multiple intrusions of ultrabasic, basic and evolved rocks. These rocks generally range from sub-alkaline layered gabbros to calc-alkaline rocks and local gradation from diorite through syenite to monozonite is also apparent. These rocks were emplaced during the first phase of deformation and the intrusion terminated with alkaline differentiates including nepheline syenite, pegmatites and carbonatites (Sturt and Ramsay, 1965; Robins and Gardner, 1974).

The Finnmark volcano-sedimentary succession was disrupted by various intrusions during the Finnmarkian tectonothermal event (Section 2.4.1). They are represented by layered gabbros, basic dykes succeeded by diorite, massive gabbros and peridotite. A later alkaline complex has been reported (Zwaan and Roberts, 1978) comprising nepheline syenite and carbonatite. Several phases of tholeiitic dyke swarms of various sizes predominate in the east of Finnmark (Roberts, 1975) while layered gabbroic bodies occur in the west. The latter are pre-Caledonian and were probably fractionated from an alkaline olivine basalt magma (Robins, 1982).

Various intrusive rocks occur elsewhere in the Caledonides of Norway. For example the Jotun nappes already discussed in (Section 2.4.5) contain a variety of intrusive rocks ranging in composition from peridotites and anorthosites through gabbros, diorites to trondhjemites.

2.6 The Geology of Molybdenum Mineralization

The naturally occurring sulphide of molybdenum, molybdenite (MoS_2) was discovered by Carl Wilhexim Scheele two hundred years ago and the metal was first extracted by Peter Jacob Hjelm (Sutulov, 1975). Due to the tungsten shortage during World War II, molybdenum was first used as an alloying metal. It is now widely used in low-alloys, high speed alloys dies, as a lubricant, in electronic tubes and electrodes, in chemical catalysts, and in pharmaceutical and fertilizer manufacture.

Since World War II the demand and hence the production have been irregular. During the period 1972-1982 there has been a strong demand for molybdenum and therefore extensive exploration, mine-evaluation and development programs (Bilhorn, 1983). However, 1982 was the worst year of that decade for the production of molybdenum as well as being a recession year for metals trading in general. The molybdenum prices peaked in 1980 and declined in 1981 to reach a low in 1982. The performance for iron and steel worldwide is reflected in lower molybdenum consumption. However, the advanced technological uses of molybdenum suggest a recovery in demand in the near future (Bilhorn, op. cit.).

Molybdenum deposits occur throughout the world in rocks ranging in age from Precambrian to late Tertiary. Economically viable molybdenum deposits are usually found in acid porphyries such as, for example, the porphyry belt that extends from Chile through U.S.A., Canada to Alaska.

Norway was the world's first molybdenum producer, and its operation started at the end of the 18th century at the Knaben mines in the south of the country. During the last century Norway was one of three main producing countries, along with Australia and the United States. Beside the Knaben mines molybdenum has been discovered and worked in the Drammen area near Oslo and at Sorumsaasen in the north. The production efficiency was improved due to the application of a flotation process (Sutulov, 1975) to concentrate the molybdenum ores. The total production of molybdenum in Norway since the earliest

days up to the 1973 closure of the Knaben mines was 10,500 tonnes.

The United States is the world's first producer and exporter. The deposits at Climax in Colorado have been supplying the world for many years with this ore. The molybdenite at Climax occurs in a multiply injected granitic intrusion. Molybdenite is also mined in other parts of Colorado (e.g. Henderson) and elsewhere in the United States.

Canada is the world's second producer and exporter. The entire production of molybdenum comes from metamorphic rocks. In British Columbia, molybdenum production started during the mid 1960's and the metal is mined from deformed molybdenum and copper porphyry deposits.

Molybdenite is a common accessory mineral in Australian tin and tungsten deposits and is produced as a by-product of tungsten mining. Also it is associated with wolframite, native bismuth, arsenopyrite and fluorite in pipes and isolated pockets in a variety of altered granites.

The Southern Province of the Red Sea Hills (Sudan) is comprised of crystalline Precambrian rocks that mostly consist of migmatites, gneisses, schists and volcanosedimentary sequences all of which have been later intruded by granitoid plutons of batholithic dimensions (Ali, 1979). Showings of molybdenum mineralization occur associated with the later granitic intrusions in this sequence (Geological Map of Sudan, 1981).

CHAPTER 3

Fremstfjell Geology

3.1 Introduction

The Fremstfjell area contains rocks of Middle Ordovician age defined as the Gjersvik Nappe (Oftedhal, 1956; Halls et al., 1977). The Gjersvik Nappe is a segment of the larger Köli Nappe bordered by the Grong Culmination and Börgefjell basement rocks to the south and north respectively (Halls et al., op. cit.; Roberts, 1978; see Fig. 3).

The principal component of the Gjersvik Nappe is a volcanosedimentary sequence (basalt-rhyolite (spilitic-keratophyric) volcanics and calcareous sediments and arkoses) that is intruded by gabbro, diorite and trondhjemite. The Gjersvik Nappe and Seve-Köli Nappe cannot be correlated precisely because the former has yielded no fossils (Lutro, 1979). In the Fremstfjell area there is also no established stratigraphic column but by analogy with the work of Gale (1975) and Halls et al. (1977) this area comprises the following sequence:-

	Conglomerate	
Gjersvik Nappe	Intrusive Complex	dykes granite trondhjemite diorite gabbro
	Gjersvik Greenstone	Mixed sequence of basalts to rhyolites with associated sediments
		major thrust
	Basement (Precambrian)	

In this chapter field relationships and petrography will be discussed. The geochemistry of the Caledonian rocks will be discussed in chapter 4 and the detailed petrography of a selection of the thin sections is listed in the appendix 1.

3.2 Precambrian Rocks

The Precambrian rocks occur south of the Sanddøla river and pass into the Bergen-Namsos coastal gneisses (Fig. 3, Barth and Reitan, 1963). These rocks have yielded 1653 ± 84 Ma by Rb-Sr whole rock isochron methods (Raheim et al., 1979). They occupy the south-eastern corner of the map-area (map 1) and during the course of the present work they have not been investigated in detail. They are referred to as the Offerdal Nappe (Gee, 1974; Reymer, 1979) and are a part of the Baltic Shield. They comprise granitic gneisses intercalated with quartzite and schist layers. They are overthrust by the greenstones of the Gjersvik Nappe and the course of the Sanddøla River approximately follows the contact.

3.3 Gjersvik Nappe Greenstones

The Grong greenstone belt (Gjersvik Nappe) is an easterly transported tectonic slice (Gale and Pearce, 1982) and on lithological grounds these authors distinguish two types: the Gjersvik sequence and the Joma sequence. The Fremstfjell greenstones form the thickest part of the Gjersvik sequence (Kollung, 1979).

Lithologically, the Fremstfjell greenstone consists of metavolcanic and metasedimentary units. The metasediments are mainly calcareous while the metavolcanics consist of basalts to rhyolites of spilitic to keratophyric affinity similar to those in the Skorvas area (Gjelsvik, 1968).

3.3.1 Basalts and basaltic andesites

Basalts and basaltic andesites are dominant over other components of the greenstone and they occur as ill-defined layers interfingering with more acid volcanics. They are exposed from east of Korttjern to north of Langtjern, and south of this lake to the west of Finhustjern (map 1). These rocks are thrust over the basement along the course of the Sanddøla River. West of Langtjern they are in fault contact with calcareous rocks and the conglomerate west of the lake, although in part the relationship with the conglomerate is unconformable. The contacts with the extensive trondhjemite in the area are, in part intrusive (plate 2) and in part faulted. Pillows and other primary volcanic structures are not well exposed in this area but elsewhere in the region they have been recognized (Halls et al., 1977).

These rocks are dark green, fine-grained and highly schistose (plate 3). The general trend of schistosity is east-west and dipping to north and apparently does not define any complete large scale structure in the area.

Plate (2): Sharp contact (probably intrusive) between greenstone in the foreground and trondhjemite south of Cyprustjern.

Plate (3): Dark green highly schistose greenstone (basalt and basaltic andesite) east of Cyprustjern.

3.3.1.1 Petrography of basalts and basaltic andesite

In hand specimen the basalts and basaltic andesites are dark green, fine-grained, massive or intensively schistose rocks.

Under the microscope these rocks are almost totally altered, recrystallised and regionally metamorphosed in the greenschist facies. Nevertheless, relics of primary textures and mineral phases may be observed. The more basic varieties have been transformed to the assemblage: chlorite + albite + epidote + carbonate + green amphiboles + sphene ± quartz ± opaques (which are generally oriented). Pyrite occurs in late veins oriented along the foliation. However, plagioclase (albite to andesine), biotite and hornblende commonly occur in the less altered basaltic andesites (TS 3/10, 4/7, see appendix 1). Metamorphosed andesites are not uncommon in the volcanic greenstone. They are composed of albite + biotite + amphiboles and opaques with rare, minute, quartz grains.

3.3.2 Dacites and Rhyolites

Dacites and rhyolites (keratophyres) are of minor volume. They occur as thin layers north of Langtjern and as a lensoid mass 1 km long and up to 150 m wide. This lensoid mass extends from south-west of Amöebtjern to the west of Fremsttjern. A tectonic relationship exists between the keratophyre in the north and the trondhjemite (plate 4) and with the calcareous sediments in the south (plate 5). A contrast in vegetation colours marks the two units and their tectonic relationship (plate 6). The rocks are silicic, fine-grained and schistosity is displayed by numerous minute quartz veins. The general trend is 070° dipping to the north.

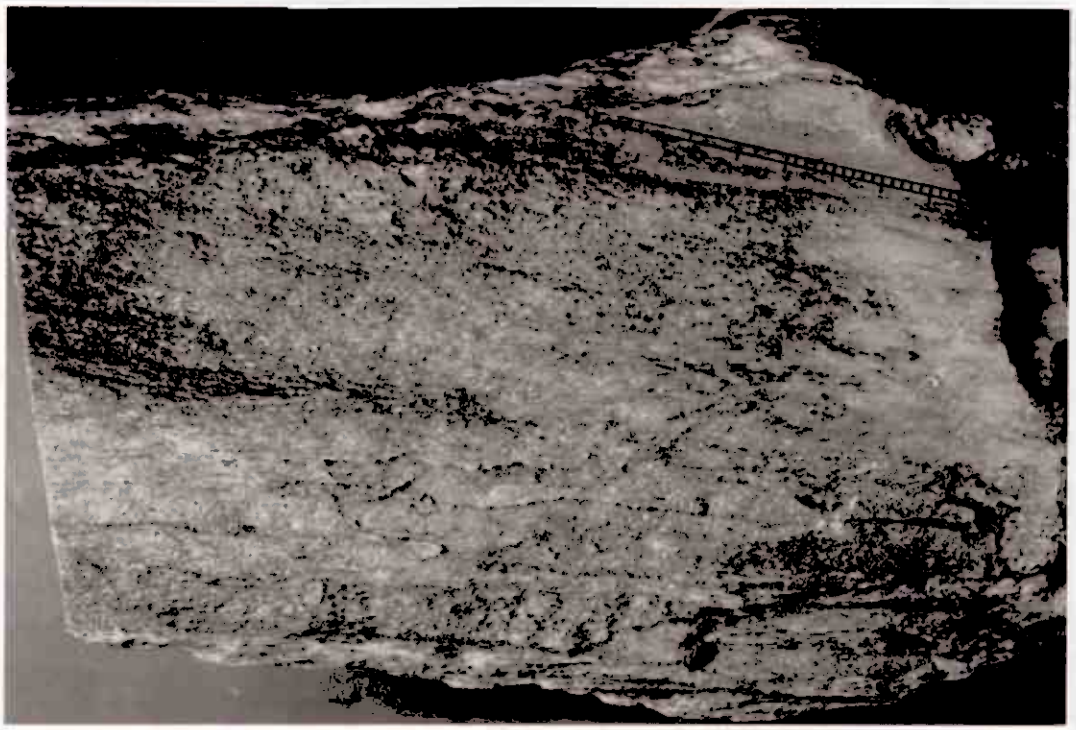

Plate (4): Slickensided surface from the contact between trondhjemite and 'keratophyre' showing quartz and sericite growth (near lake, grid 544).

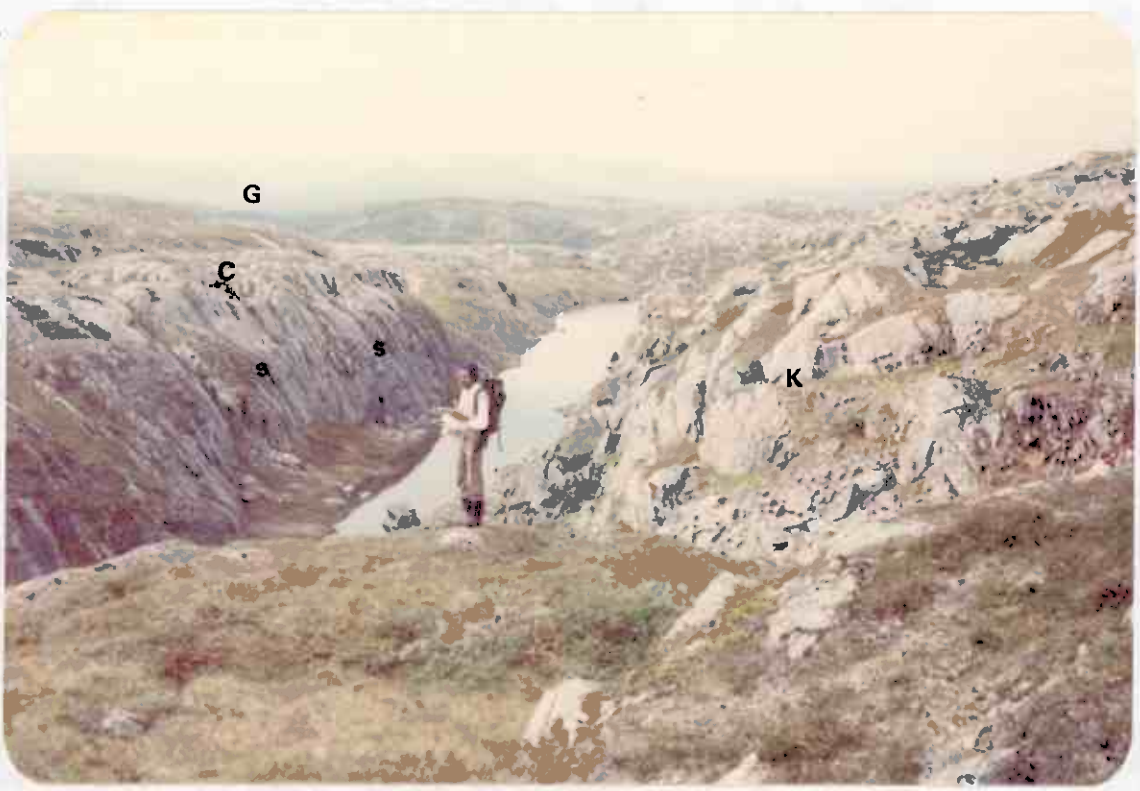

Plate (5): Outcrops of 'keratophyre' (K) faulted against calcareous metasediment (C) (slickensided surface, S) and showing basement of the Grong Culmination (G) looking west from grid 544.

3.3.2.1 Petrography of the dacites and rhyolites

In hand specimen the keratophyric dacites and rhyolites are fine-grained, mesocratic and they are more or less schistose.

Under the microscope the predominant unit is typically fine-grained, massive rock which consists of albite (modal 60%), quartz (modal 25%), biotite (modal 5-10%) as primary mineral phases and opaques, sphene, apatite and zircon as minor constituents. Secondary sericite, epidote and calcite occur overgrowing albite or as discrete veins. Chlorite, actinolite-tremolite occur along shear planes and sometimes marking a strong mylonitic fabric, particularly from adjacent to the contact between the trondhjemite and the keratophyre.

3.3.3 Metasediments

Calcareous metasediments form a considerable proportion of the outcrops. They outcrop as a linear band extending west from Littletjern to Fremsttjern and continue to Berg farm beyond the mapped area (Gale, 1975). These calcareous sediments are in fault contact with conglomerate north of Littltjern. The metasediments have a faulted relationship with the keratophyric dacites and rhyolites (plate 5). The slickensided surface shown in plate 5 indicates the sense of movement.

In the northeast of the mapped area these rocks also occur, but the contact between them and the metavolcanics is not clear. Here they display cross-bedding and slumping and it appears that they were rapidly deposited in a shallow marine environment. These rocks are fine-grained and variously

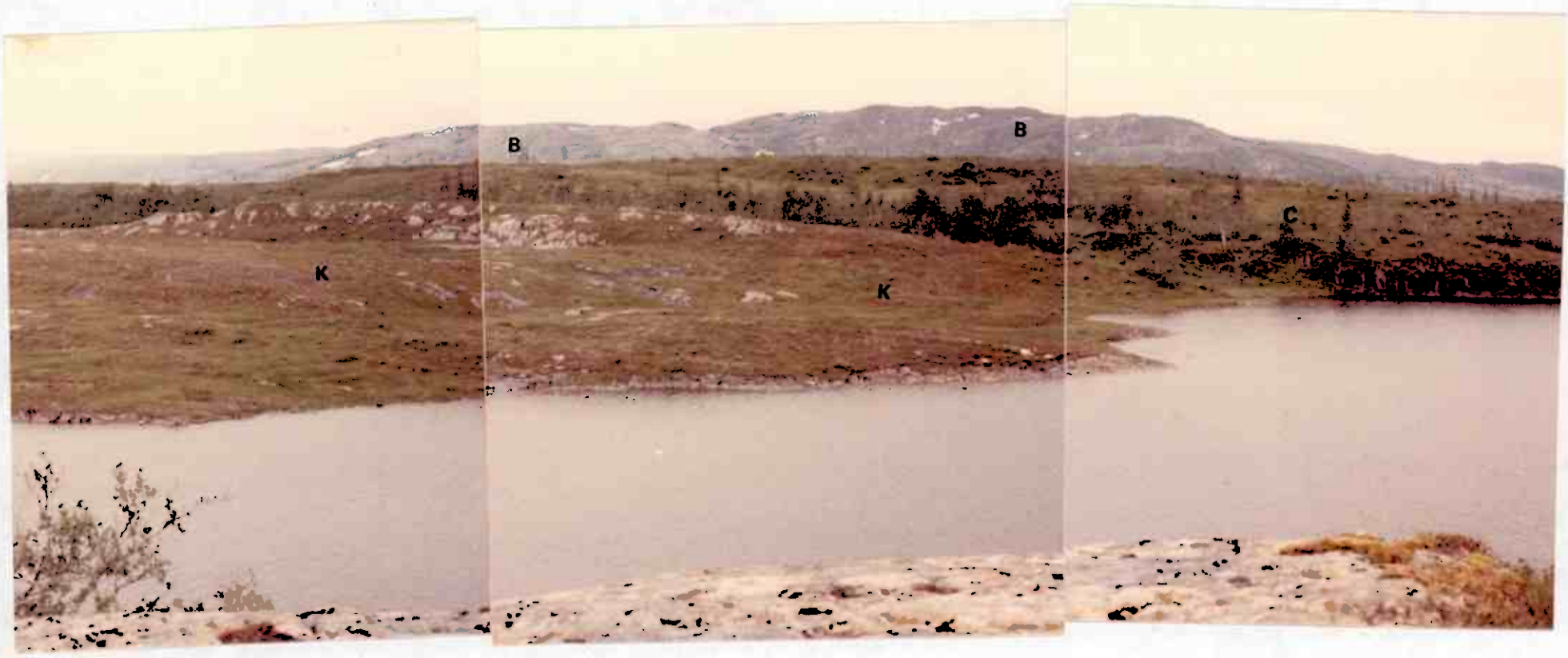

Plate (6): Panoramic view across southeastern Fremsttjern showing grey mountains of Precambrian gneisses (B) green, wooded calcareous metasediments (C) brownish 'keratophyre' (K).

coloured green, grey to white due to small changes in composition. Their general strike is 120° and they dip about 70°N.

3.3.3.1 Petrography

Calcareous sediments comprising limestones, calcareous marls and calcareous pelites are intimately associated with Gjersvik metavolcanics. They are generally fine-grained, thinly laminated with preserved bedding planes and other primary sedimentary structures. In some units the beds are contorted, displaying pinch and swell structures. In others the bedding planes are generally regular and both graded bedding and cross-bedding can be seen.

Under the microscope the rocks are generally fine-grained and recrystallised in the greenschist facies. The predominant mineral parageneses are:

a) clinozoisite + calcite + epidote + amphibole ± quartz,
b) clinozoisite + tremolite + calcite + plagioclase ± quartz and
c) sericite + epidote + chlorite + calcite + quartz ± albite.

3.4 Intrusives

Intrusive rocks occur throughout the Norwegian Caledonides. A variety of plutonic rocks ranging in composition from acid to basic intrudes the Gjersvik greenstone. Acid and basic members dominate over the intermediate ones (Gale, 1975; Halls et al., 1977; Kollung, 1979). Around Fremstfjell these rocks occupy more than half of the mapped area.

3.4.1 Gabbro

According to Halls et al. (1977) and Kollung (1979), gabbro is the dominant member of the plutonic suite intruding the Gjersvik greenstone. It is generally rare around Fremstfjell but is widespread in the Nord-Trondelag region adjacent to the project area.

It is the oldest member of the intrusive rocks in the area mapped and it occurs either as ridges or xenolithic blocks of various size that are more or less confined to the contact zone between the trondhjemite (section 3.6) and the greenstone (map 1). Gabbro blocks are frequently encountered between trench 2 and Korttjern (map 1). Gabbroic ridges cover the area north of Korttjern. In the Grøndalsfjell area to the north and the Heimdalshaugen area to the west the gabbros have a similar mode of occurrence to that in the Fremstfjell area.

Generally the contact between the gabbroic blocks and the later granites (section 3.7) is concealed under zones of debris but where it is exposed the latter is clearly chilled against the former (plate 7). The gabbros are also cut by numerous veins of trondhjemite. Although the gabbro has been reported intruding the greenstone in some localities in the Nord-Trondelag region (Halls et al., 1977), clear gabbro cutting greenstone relationships have not been observed in Fremstfjell area. The gabbros occasionally show crude-indistinct layering and elsewhere in the region layering has been recognized (Halls et al., op. cit.).

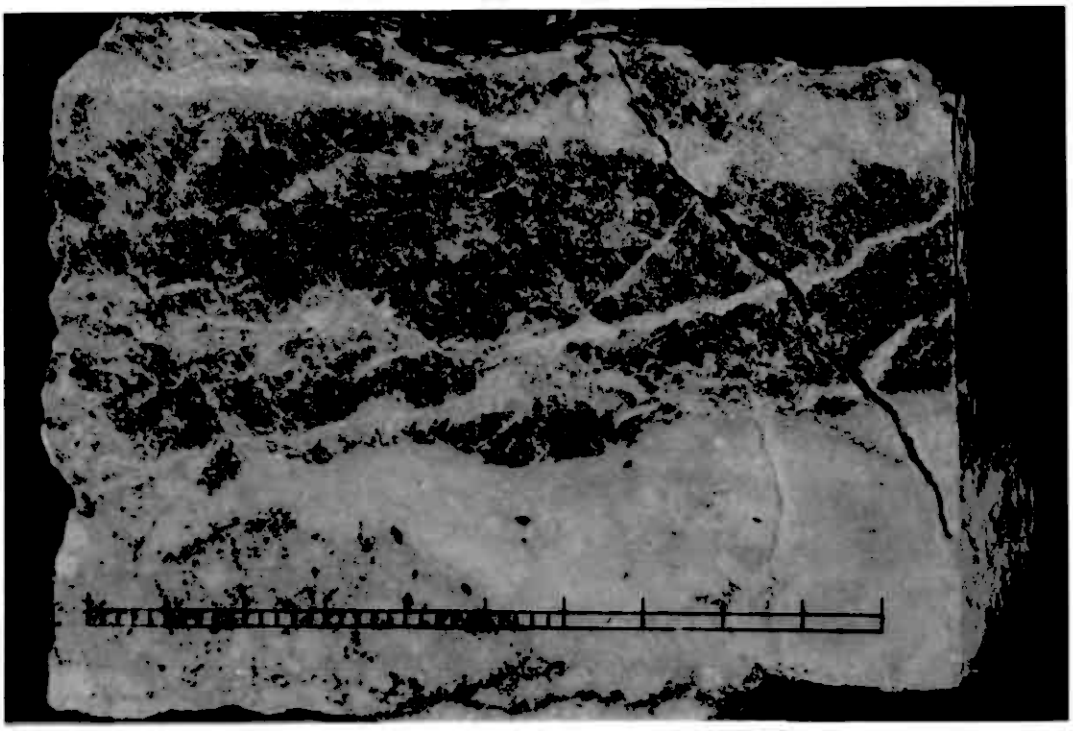

Plate (7): Sharp and chilled contact of granite (light colour) against gabbro (dark). Note also pyrite veining cutting across the sample. (Trench 2, map 1) (Scale in cm).

3.4.1.1 Petrography

In hand specimen melanocratic varieties predominate. These rocks are coarse-grained, comprising crystals of mafic minerals and interlocked felsic components. They are more or less massive gabbros but in some places a crude igneous lamination can be observed in the orientation of the mafic minerals.

Under the microscope they cover a wide spectrum of mineralogical compositions ranging from pyroxenite through hornblendite, cumulate gabbro to hornblende gabbro. This wide range of composition is also reflected in their geochemical characteristics (chapter 4). They are mainly composed of plagioclase, pyroxene and hornblende with biotite, apatite, sphene and iron ores as minor phases. Chlorite, epidote, sericite, hematite and actinolite-tremolite are the secondary minerals.

Pyroxene occurs as both clino- and ortho- varieties although clinopyroxene predominates. It forms more than modal 50% of the pyroxenite (T.S. N4 appendix 1) and the cumulate gabbro (T.S. N6 appendix 1) and is the second most important ferromagnesian phase in hornblendite. In the pyroxenite, pyroxenes form well developed crystals often displaying exsolution lamellae (plate 8). In most cases calcium rich pyroxenes (parent) exsolve either ortho- or calcium-poor ones (daughter) (Cox et al., 1981). Ten microprobe analyses (appendix 2) suggest that most of the pyroxenes are diopsidic-augite (Deer et al., 1966). They are often uralitized and

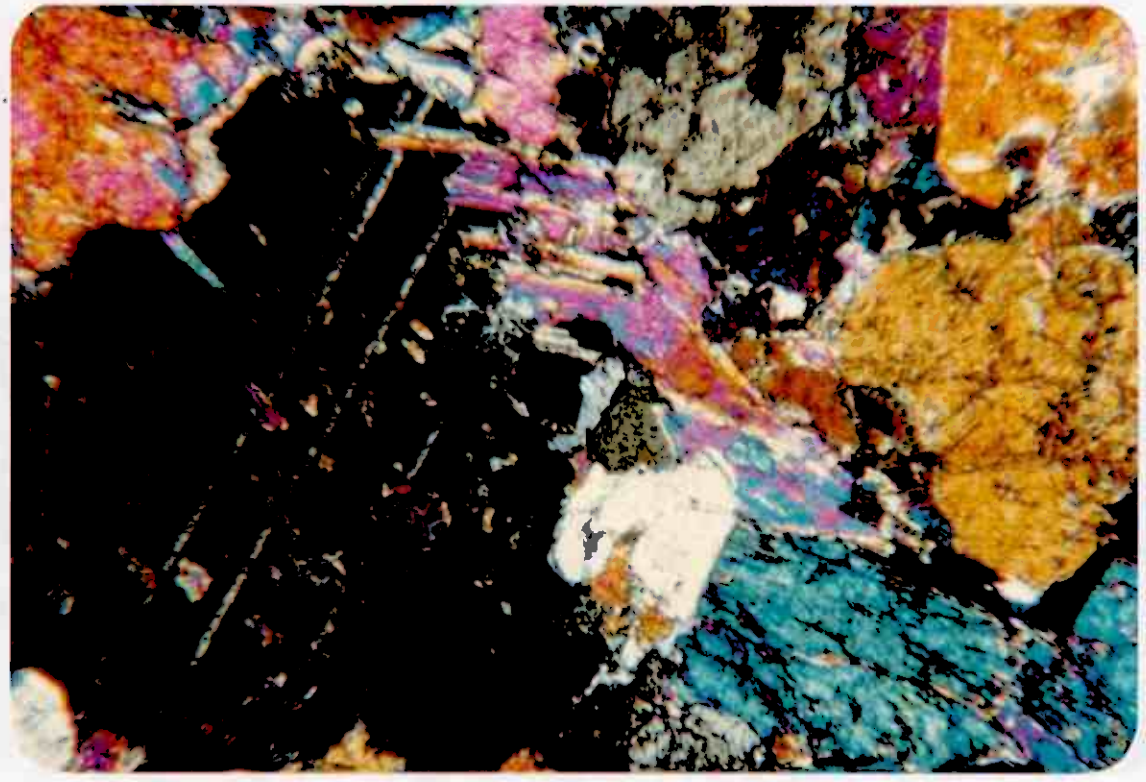

Plate (8): Twinned, exsolved clinopyroxene with altered feldspar. Gabbro. XPL x 27 (T.S. N4).

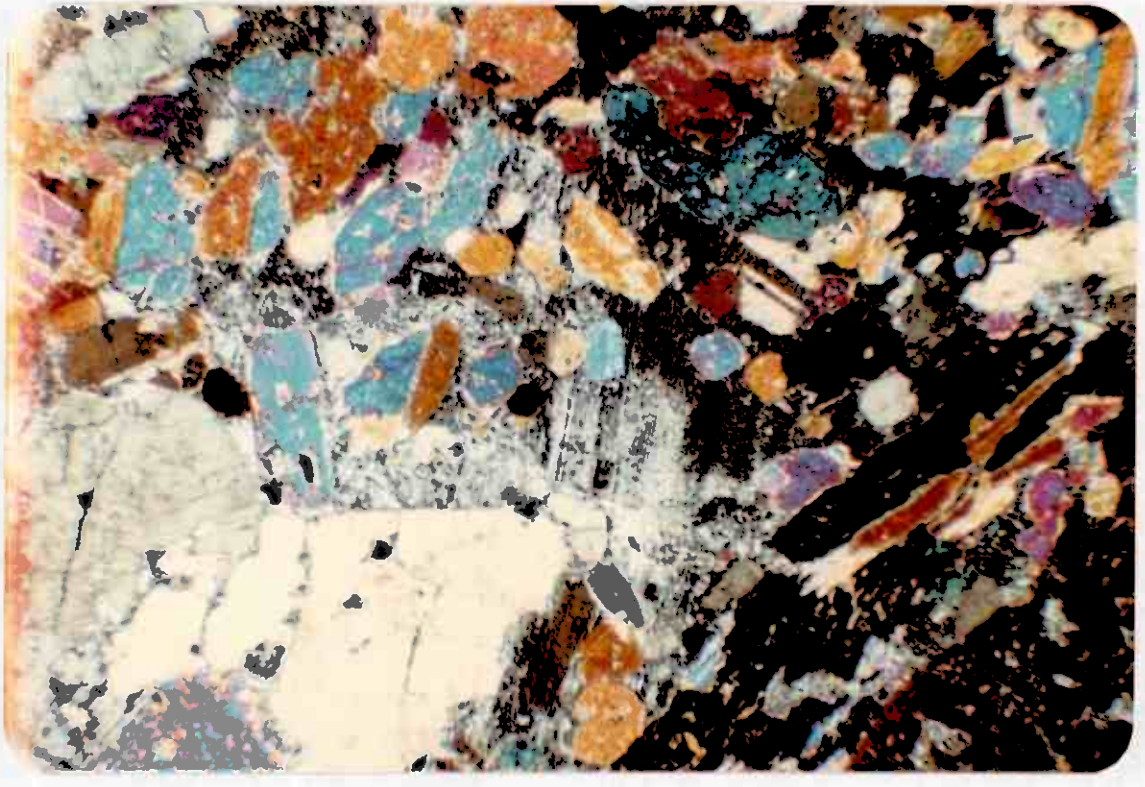

Plate (9): Clinopyroxene poikilitically enclosed in plagioclase. Gabbro. XPL x 10 (T.S. N4).

partially or completely replaced by hornblende, actinolite-tremolite or chlorite. The clinopyroxenes are sometimes poikilitically enclosed by plagioclase (plate 9).

Brown hornblende is the common mafic mineral in hornblendite (T.S. B7), hornblende gabbro (T.S. B7/a) and is subordinate in the pyroxenite and cumulate gabbro. It occurs either as well developed primary phase crystals or after clinopyroxenes. A few probe analyses (appendix 2) suggest that the amphiboles are aluminous with low Fe^{2+} and with Fe^{3+} in their formula and they occur in the field of tschermakitic hornblende to actinolitic hornblende (Leake, 1978).

Altered calcic plagioclase ranges from modal 10% in the pyroxenite and hornblendite to 60% in the massive gabbro. In the first two it occurs as an intercumulus phase (plate 10) and in the latter as large interlocked grains showing ophitic to subophitic relationships with pyroxenes and hornblende (plate 11) and sometimes poikilitically enclosing pyroxenes (plate 9). In most cases the plagioclase is either saussuritised giving rise to epidote minerals or sericitized and full of phyllosilicate minerals. However, relics of lamellar twinning and grain boundaries are commonly observed.

Opaque minerals (magnetite, titanomagnetite) are the most common accessories and may sometimes exceed modal 5% (T.S. N6). Generally the grains are euhedral but very often they are rimmed by hematite or secondary sphene (plate 12). Apatite, biotite and sphene are the next most abundant accessory phases

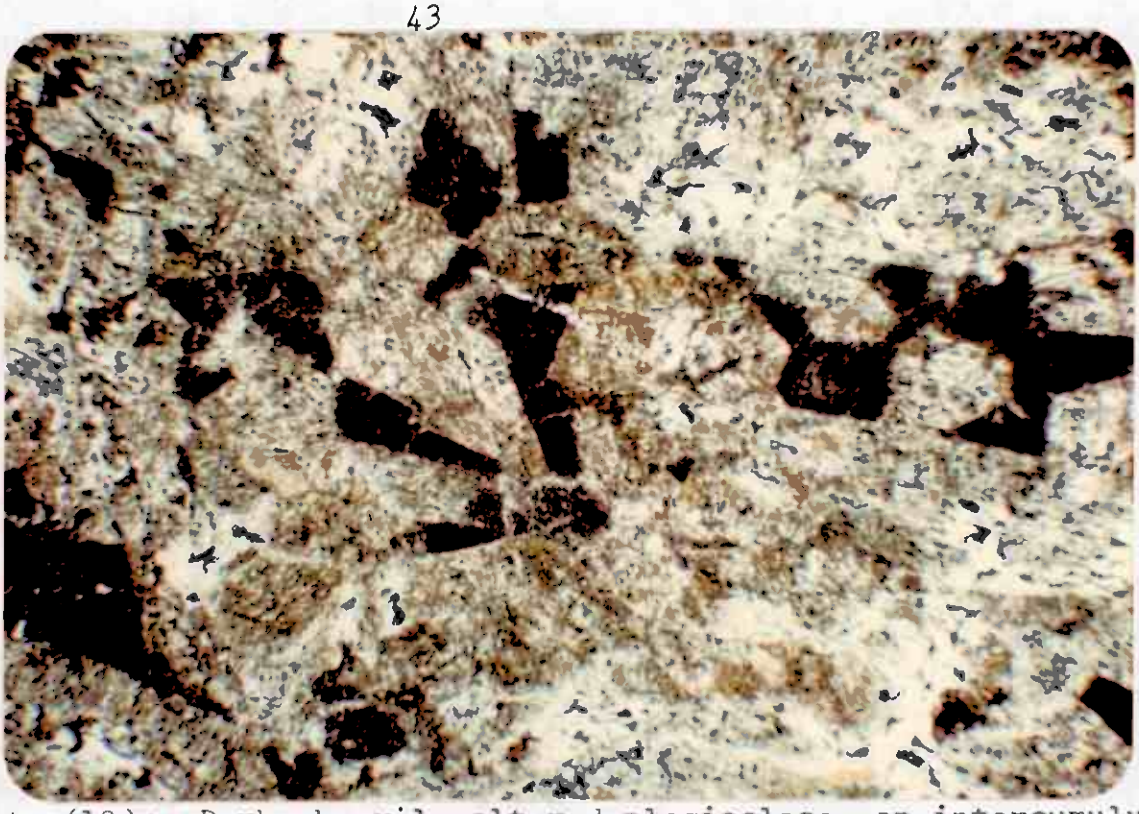

Plate (10): Dark, heavily altered plagioclase, an intercumulus interstitial phase to green, uralitised pyroxene. Altered gabbro. XPL x 28 (T.S. B7/b).

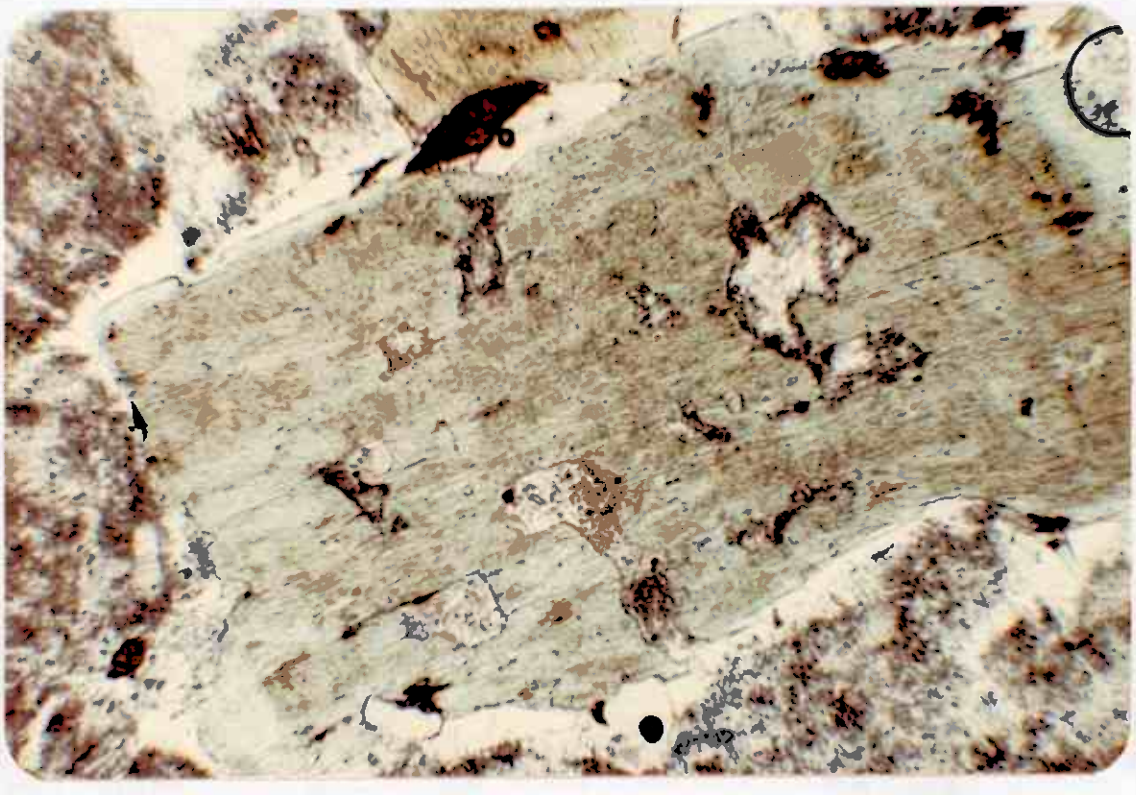

Plate (11): Euhedral pale green amphibole containing altered plagioclase, surrounded by altered plagioclase, amphibole and well developed sphene. Metagabbro. XPL x 70 (T.S. B7/a).

with occasional quartz. Chlorite, sericite, epidote and green amphiboles are the common secondary alteration products. They are generally dispersed and show no distinct fabric. The epidote is Fe epidote (appendix 2).

3.4.2 Diorite

Diorite is an important component of the plutonic suite that intrudes the Gjersvik Nappe (Halls et al., 1977) but in terms of outcrop these rocks are rare in the Fremstfjell area. Their occurrence is restricted to the greenstone-trondhjemite boundary north of Cyprustjern where they occur as pockets and pegmatitic veins (map 1) and to within the gabbro/trondhjemite north of Korttjern. However, elsewhere in the region diorites have been found in Grøndalsfjell and Nesåpiggen in considerable volume (Halls et al., op. cit.).

The diorites are dark green, speckled with milky plagioclase and are porphyritic in texture. Plagioclase forms phenocrysts (1-5 mm) while the dark minerals constitute the groundmass. Plagioclase (An_{0-15}) forms modal 60% of the rock and is entensively altered giving rise to a core of spongey epidote suggesting compositional zoning. Amphiboles ranging in composition from hornblende (T.S. C5, appendix 1) to green actinolite-tremolite are abundant with minor flakes of biotite. Quartz, calcite with sphene, opaques and apatite are the common accessory minerals. The secondary phases that formed after the plagioclase and amphiboles are epidote, sericite and chlorite. These rocks are interveined mainly by epidote-quartz veins.

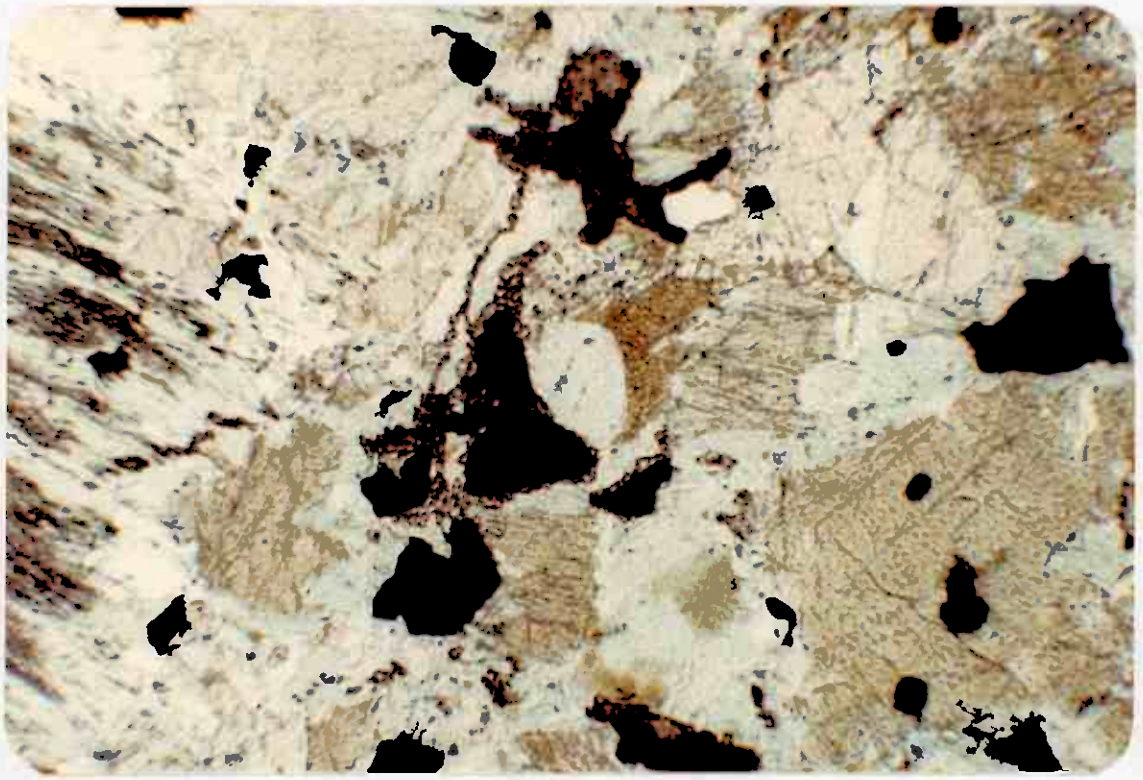

Plate (12): Ilmenite/titanomagnetite rimmed by sphene in altered gabbro with pale green actinolite and olive green hornblende. XPL x 65 (T.S. B7).

3.4.3 Trondhjemite

Trondhjemite is a leucocratic plutonic rock, composed essentially of sodic plagioclase (especially oligoclase), quartz, sparse biotite and little or no alkali feldspar (Goldschmidt, 1954). Trondhjemites have their type locality in Norway (Goldschmidt, 1916; Size, 1979). They are abundant in continental Archaean rocks (Arth and Hanson, 1975) and in Proterozoic-Phanerozoic orogenic belts (ref to Barker, 1979). According to Goldschmidt (1916) these rocks are formed by fractional crystallization, but Size (1979) suggested anatexis of granitic crust or partial melting for their origin.

Trondhjemites intrude the greenstone in the Fremstfjell area and elsewhere in the region, and are usually concordant with the structural elements of the country rocks. They occupy the centre and northern part of the area (map 1) and throughout they occur as extensive sheets, stocks and veins. They often carry lenses of gabbro and rafts of greenstones which are roof pendants of the intrusion. They weather to massive rounded outcrops but they are usually well jointed.

Southeast of Amoebtjern the trondhjemites are sheared and brittle. Here they lie close to the southern-most intrusive cover boundary with calcareous sediment (map 1). They are in direct contact with unconformably overlying oligmict conglomerate west of Langtjern (Gale, 1975) and east of Fremsttjern the contact is tectonic against keratophyres (plate 4). In most parts the contact with greenstone is sharp (plate 2). The contact between the trondhjemite and the greenstone window in the northwestern part of the area appears to be tectonic but in the north and northeastern part of the area although the contacts are sharp the concentration of greenstone rafts and xenoliths indicates the proximity of the roof of the intrusion.

Trondhjemite intrudes, veins and breaks up the earlier gabbros. However, the contact relationships between trondhjemite and the granite are more difficult. They are often gradational but in some places granites clearly vein into trondhjemite. Near the contact foliation is clear and it diminishes towards the centre of the intrusion. All of these rocks are traversed by a variety of shear planes.

3.4.3.1 Petrography

In hand specimen, these rocks are uniform greyish-white, but some are speckled with milky feldspar. They are homogenous, coarse-grained and massif, but often have a weak foliation that increases in intensity towards the margin of the intrusion.

Under the microscope these rocks are coarse to medium-grained, xenomorphic granular in texture (plate 13), the texture becomes less obviously granular with increase in alteration as the feldspars become sericitised and grain boundaries become more diffuse. The rocks are often sheared and quartz forms elongated aggregates and with white mica displays a submylonitic fabric (Hobbs et al., 1976). However, relics of primary textures can be easily observed. Mineralogically the trondjhemites are dominated by plagioclase feldspar which forms 60-65% of the mode and quartz which forms 30% of the mode. Plagioclase (An_{0-25}) forms 95% of the feldspar in these rocks and is mainly calcic oligoclase although albite is abundant and andesine sometimes occurs. The grains

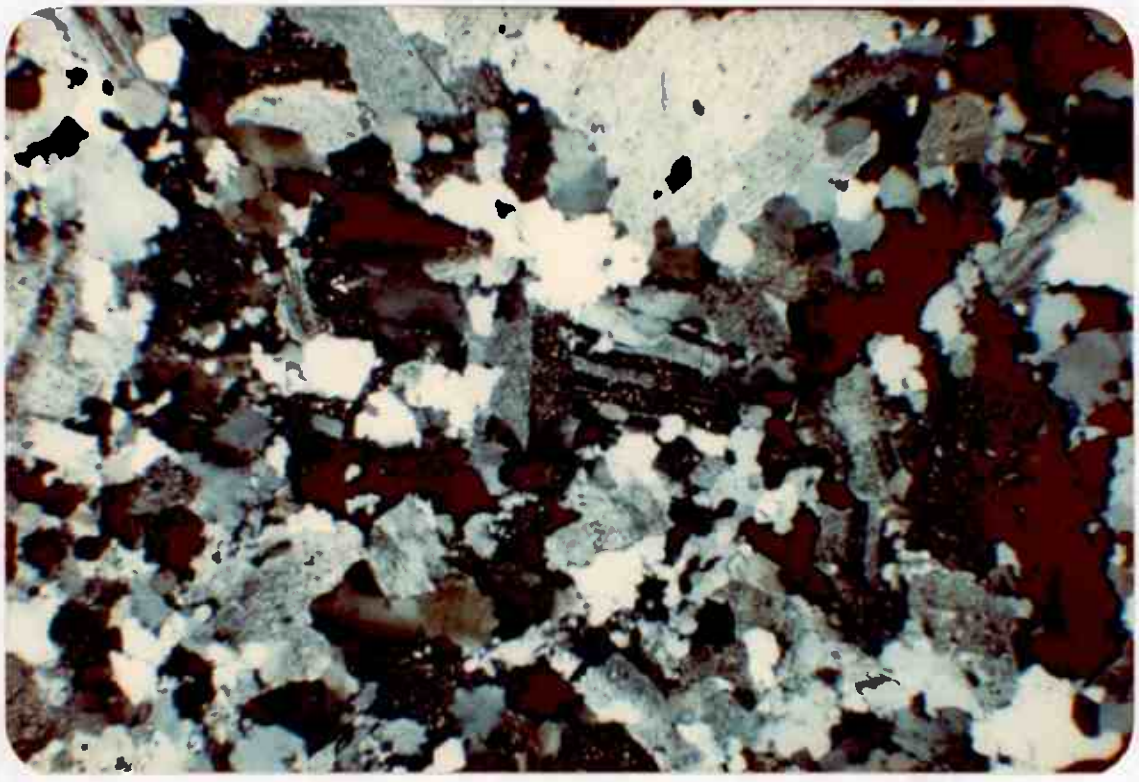

Plate (13): Xenomorphic granular texture in trondhjemite, with albite quartz and sphene. XPL x 17 (T.S. B2/a).

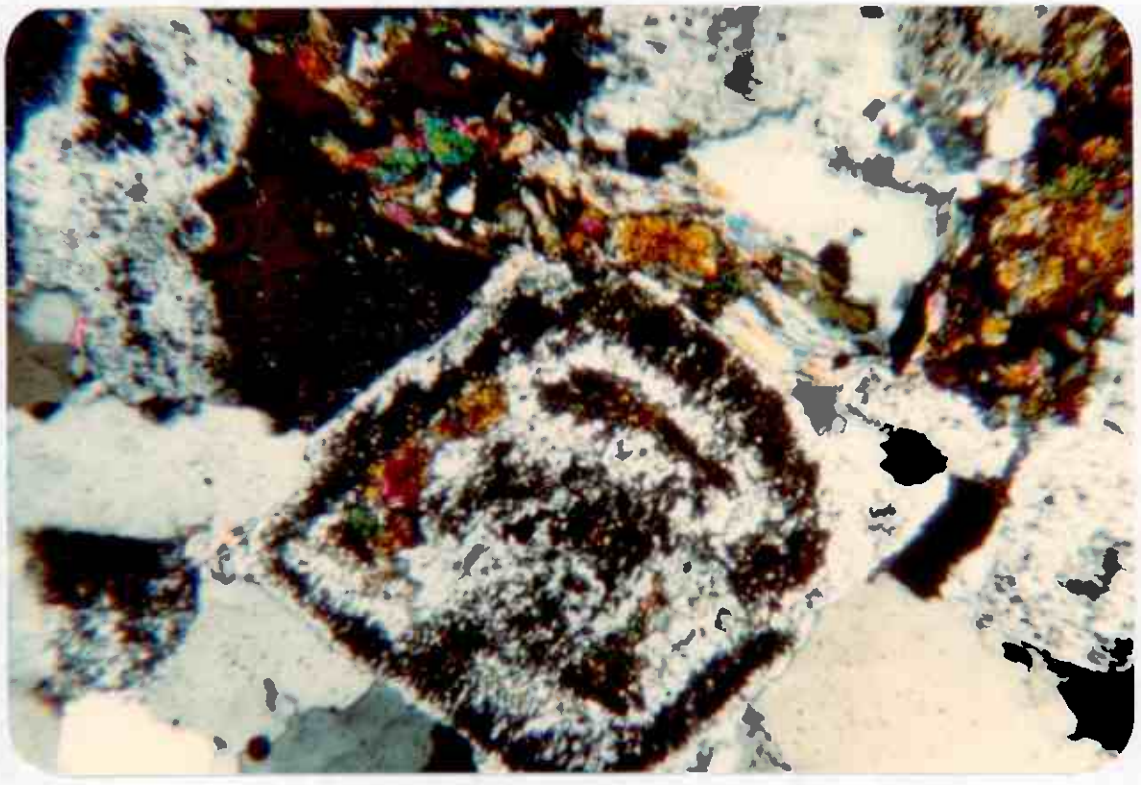

Plate (14): Zoned plagioclase in trondhjemite, with quartz, sericite and epidote. XPL x 45 (T.S. B5).

are subhedral to anhedral ranging from 0.5-3 mm in diameter. The core of this plagioclase is commonly replaced by spongy epidote (plate 14) suggesting compositional zoning and microprobe analyses (appendix 2) suggest the same phenomenon showing zoning from An_{35} in the core to An_5 at the margin. Perthite and microcline are rare, occurring as interlocked grains. Quartz occurs extensively throughout the rock. It often shows a granoblastic texture and undulatory extinction. The grain boundaries are sutured and locally the quartz and plagioclase have been microsheared into a mortar texture (plate 15) Spry, 1969).

Biotite, often replaced by chlorite and muscovite forms < 5% of the rock while sphene, opaques(mainly pyrite, magnetite ± molybdenite), apatite, zoned allanite and zircon are the common accessory minerals. Allanite analyses (appendix 2) show low totals and this may indicate the concentration of trace elements (chapter 4) in these minerals (Deer et al., 1966). Sericite, epidote, chlorite and carbonate form the secondary phases. Sericite is well developed along shear zones; epidote and carbonate are common in veins and chlorite is often associated with opaques. Epidote analyses (appendix 2) show that the epidote is Fe epidote with Mn, Ti and sometimes traces of Cr and Co. Petrographically they are similar to the trondhjemite in Finland (Arth et al., 1978).

3.4.4 Granite

Potassic granite occurs rarely within the Norwegian Caledonian terrain (Kollung, 1979; Wolf, 1980) and the largest intrusion is the Bindal granite north of Grong. Most

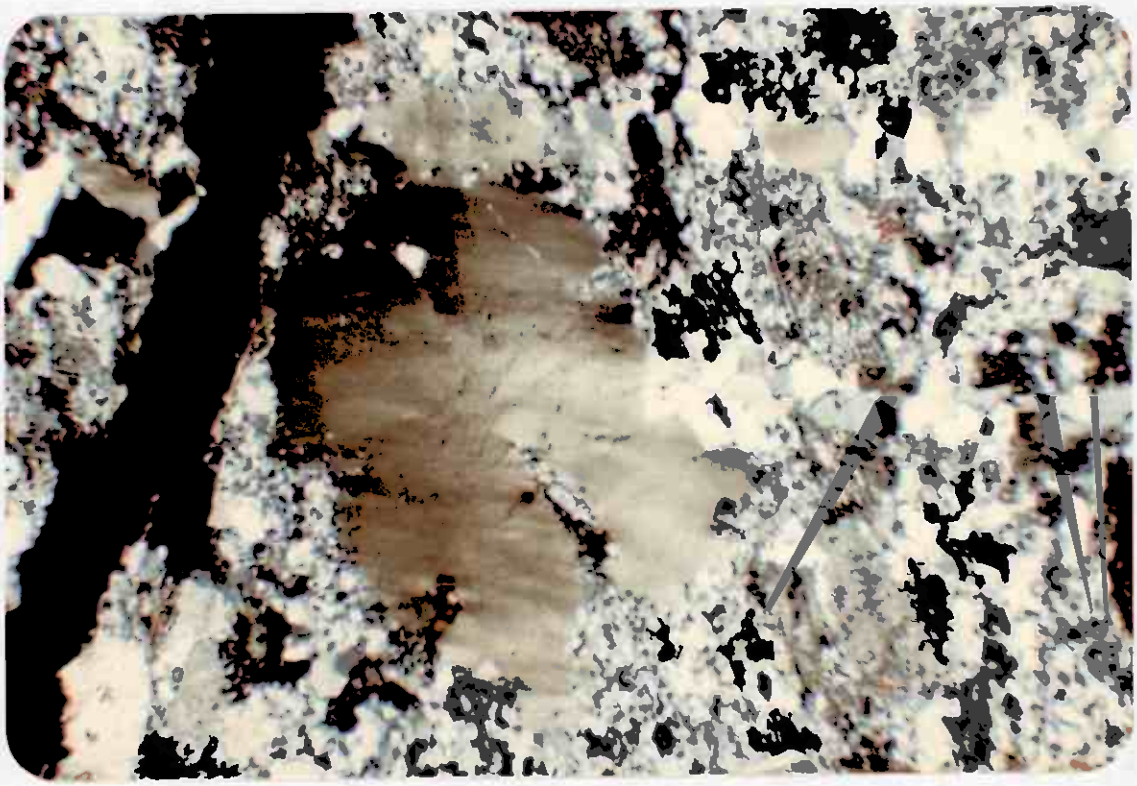

Plate (15): Crushed and recrystallized quartz showing mortar structure with plagioclase, sericite and epidote. Trondhjemite. XPL x 28 (T.S. A5).

of these granites are of Silurian age (Oftedhal, 1980).

In the Fremstjfell area (project area) potassic granite (the main host rock of molybdenum mineralization - see chapter 5) occurs as sheet-like bodies. This potassic granite was previously considered to be part of a larger trondhjemite complex (Fosile, 1927). However, the Fremstjfell granite differs both geochemically and petrographically from typical trondhjemite defined by Goldschmidt (1916) in having K-feldspar and Na_2O/K_2O ratio < 1 (chapter 4).

The granite occupies the centre of the area and is almost concordant with structural elements of the adjacent trondhjemite host rock with which it does not have a sharp contact or chilled margin. The outcrop is linear, extending for about 1400 m and pinching in the west to 100 m across and swelling to the east to 500 m across. Within the general form of this intrusion there is complex interfingering with trondhjemite (plate16), with gabbro blocks and greenstone lenses. The gabbro is clearly older and has been broken up by the emplacement of the granite which has a sharp contacts and chilled margins against the blocks of gabbro (plate 7). The outcrops are jointed with a prominent trend of ENE/WSW parallel to the pervasive cleavage and the main shear planes. They are also cut by a series of veins often parallel to the joints and containing the molybdenum mineralization.

3.4.4.1 Petrography

The Fremstfjell granite is potassium rich (chapter 4). Typical Fremstfjell granites from the centre of the intrusion are

Plate (16): Epidotised trondhjemite (grey in colour) veined by granite (pinkish white) south of Smalltjern.

pink whereas those from the margin of the body are sheared and grey. The pink varieties are massive with discrete veins of quartz, quartz-pyrite, quartz-pyrite-chalcopyrite and quartz-pyrite-molybdenite. Sheared varieties show schistosity produced by orientation of micaceous material.

Under the microscope the pink variety is generally coarse- to medium-grained, xenomorphic, and is dominated by microshears along which flaky minerals and aggregates of quartz are oriented giving rise to a weak non-penetrative fabric. The grain boundaries are mostly sutured but relics of primary structures are locally encountered including feldspar zoning (plate 17) and micrographic intergrowth (plate 18). Graphic intergrowths between quartz and K-feldspars are probably produced by replacement of one mineral by the other during late magmatic crystallization (Hatch et al., 1972). The sheared varieties display a submylonitic fabric in which white micas are preferentially orientated along distinct sheared zones with quartz and feldspars (plate 21).

Mineralogically the massive pink granite is dominated by feldspar which forms more than 60% of the mode and quartz which comprises about 30%. Muscovite and biotite constitute < 5% of the rock and sphene, opaques, apatite and zircon are the most common accessory minerals. Secondary minerals, including sericite and epidote, are frequent and are abundant along shear planes and in veins. Carbonate, actinolite-tremolite and chlorite also occur as secondary minerals.

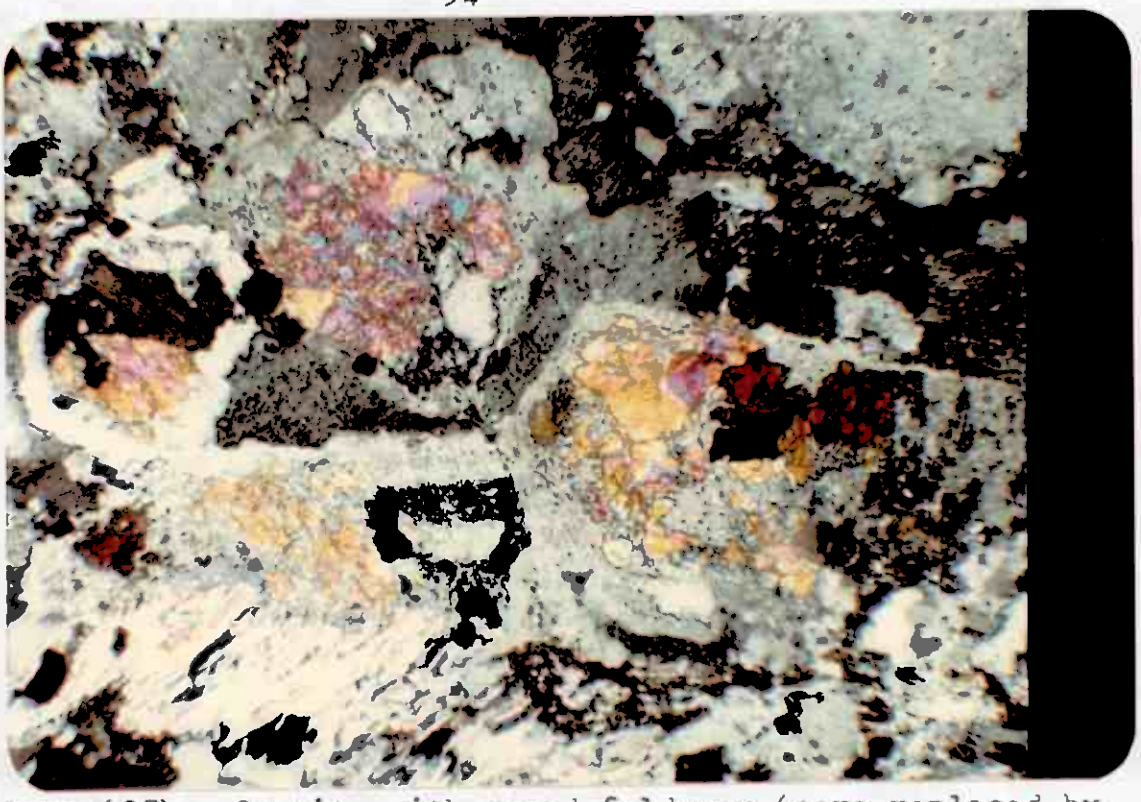

Plate (17): Granite with zoned feldspar (core replaced by epidote) quartz, sericite and pyrite. XPL x 60 (T.S. T5/c).

Plate (18): Feldspar (grey white) and quartz (black) showing coarse graphic intergrowth. Granite. XPL x (T.S. 6/30).

Perthite is the dominant feldspar. The crystals are generally irregularly shaped, slightly deformed and altered to sericite. Microcline forms large, marginally granulated crystals showing typical cross-hatch twinning (plate 19). Rare orthoclase forms irregularly shaped grains. Staining of these rocks indicates that 40-60% of the feldspar is alkali feldspar (plate 20). Albite-oligoclase (An_{5-15}) generally occurs as larger grains than the perthite and is altered. These Na-feldspars display various patternsof twin lamellae that in most cases are bent and discontinuous indicating a deformation event. Preserved primary structures are obliterated either by microshears or by local recrystallization.

Quartz occurs extensively in the rock. Two generations can be observed, an earlier phase showing undulatory extinction and sutured grain boundaries and a later recrystallised phase as interlocked minute grains and thin veins. Micas, mainly muscovite,form only a very minor proportion of the rock, biotite is rare and is the only coloured silicate mineral in the rock. Muscovite, epidote (appendix 1), sphene and ore minerals are well developed in veins and along the line of shears.

In the sheared varieties of granite, recrystallization, alteration and mylonitization fabrics dominate the rocks. Quartz occurs as recrystallized ribbon-shaped grains, and also as polygonized aggregates. Alkali feldspars occur as augen. Clinozosite, sphene, opaques and apatite are more frequent than in the less deformed varieties. All of the granites

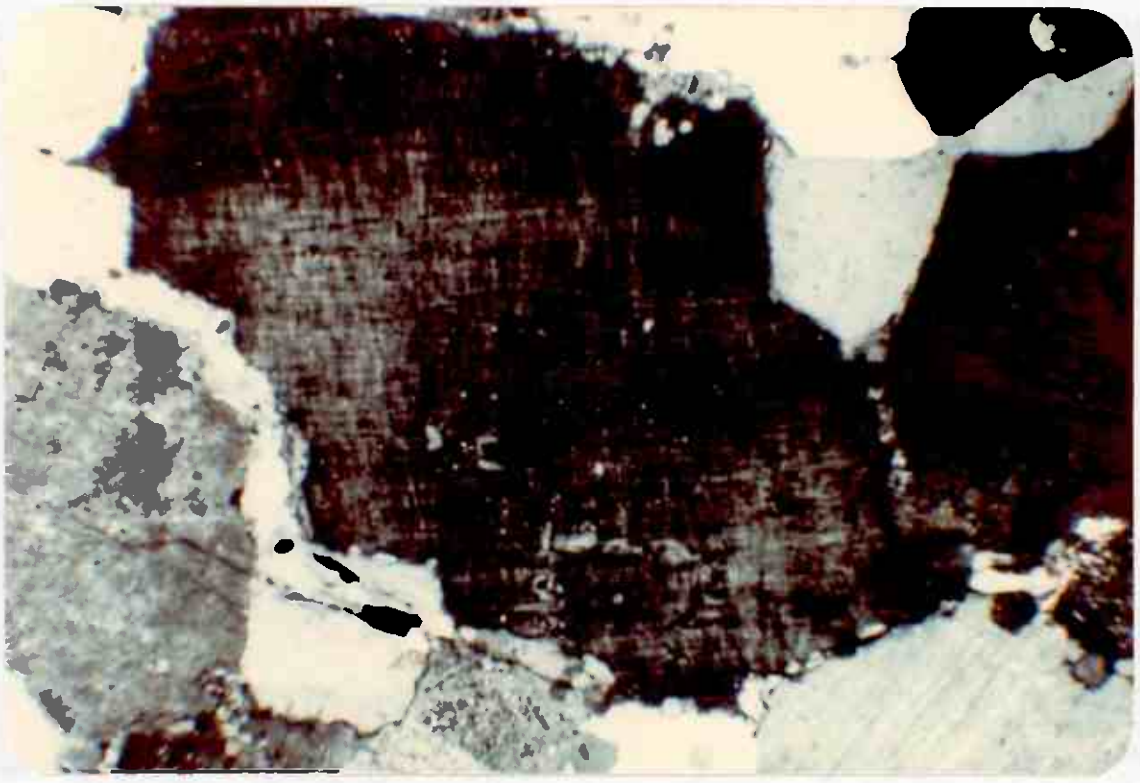

Plate (19): Microcline (cross-hatched and marginally granular) with quartz in the granite. XPL x 50 (T.S. T5/b).

Plate (20): K-feldspar (yellow), quartz (dark grey), pyrite (dark orange) and plagioclase (pale grey/brown) in stained granite. x 3.3 (T.S. T5/c).

have been subjected to greenschist facies metamorphism and (plate 22) show its characteristic assemblages (Winkler, 1974).

3.4.5 Dykes

The area is traversed by numerous narrow dykes which vary in lithology and structural control. Aplite dykes are associated with the granite and rarely cut through the trondhjemite. Quartz veins are mainly controlled by schistosity and are generally associated with the mineralizing events but sometimes they occur in the form of ore-free veins.

Dolerite dykes are younger than the mineralization because they are never cut by molybdenite-bearing veins. Their orientation and occurrence is controlled to some extent by pre-existing structures and fractures. They are dark green, fine-grained and in some parts they are porphyritic. They are highly altered so their primary compositions cannot be determined. The secondary minerals consist largely of epidote, sericite, green amphiboles and chlorite. Relics of altered albitic plagioclase occur with very rare quartz and sphene and opaques form the accessory phases.

3.5 Conglomerate

Conglomerate occurs as a band that extends more than 2 km northeast and southwest of Langtjern (map 1) and averages 150 m in outcrop width. This rock unconformably overlies trondhjemite to the north and is in a fault contact relationship with greenstone to the south. The clasts of this

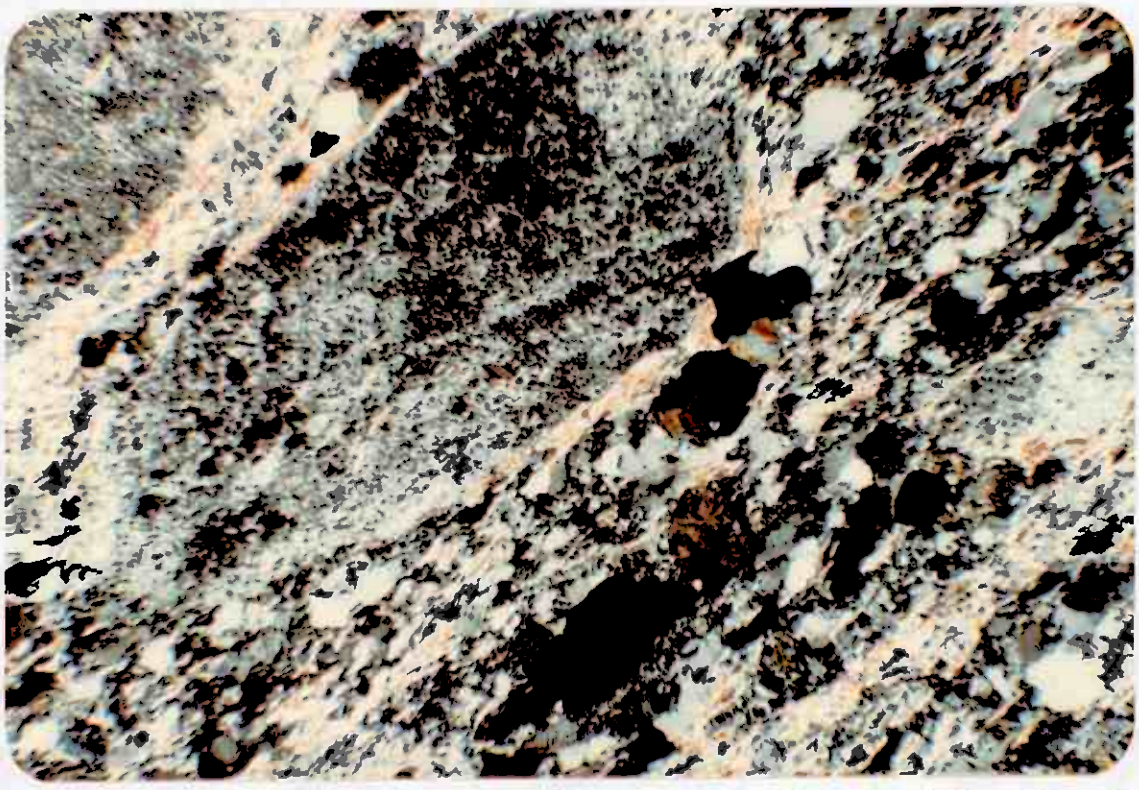

Plate (21): Sheared granite from trench 6 (map 1), composed of granoblastic feldspar, crushed recrystallised quartz, sericite, opaque and sphene. XPL x 60 (T.S. T6/e).

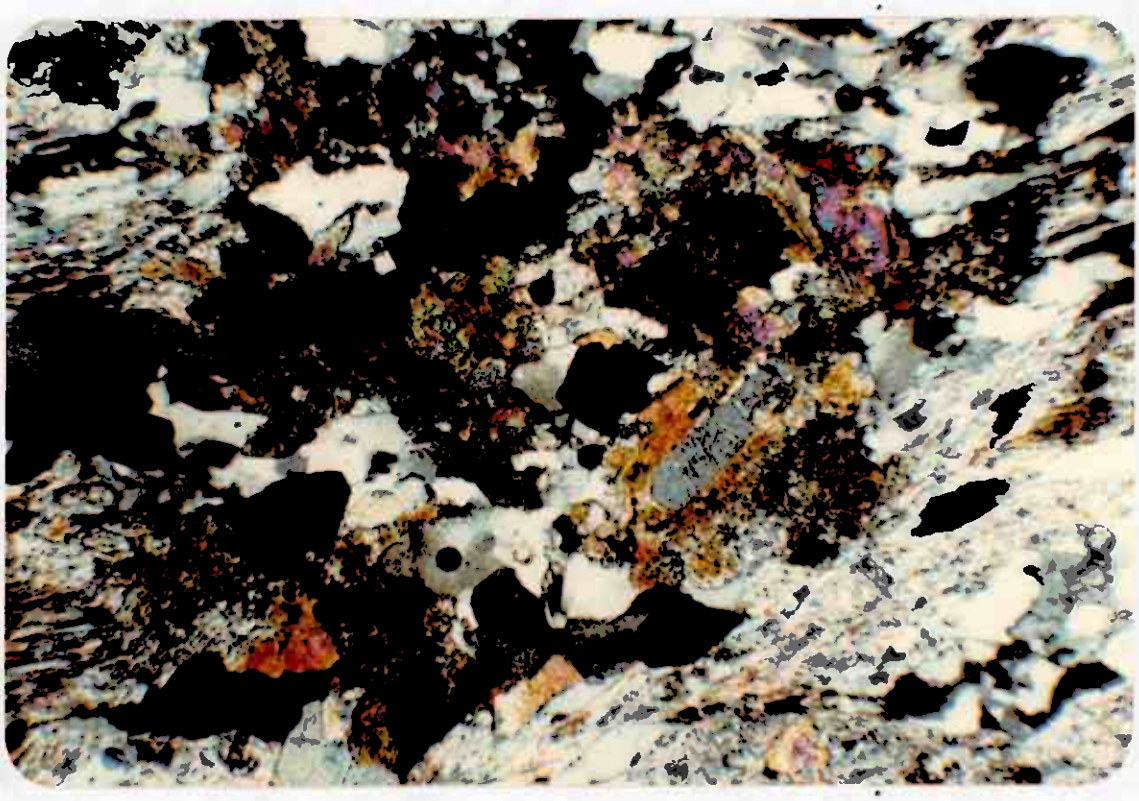

Plate (22): Deformed granite from trench 1 (map 1) consisting of sericite, epidote, quartz, opaque, sphene and apatite. XPL x 10 (T.S. T1/a).

predominantly oligomict conglomerate are mainly unmineralized trondhjemite.

The conglomerate is poorly sorted. It comprises clasts that vary from sand size to 3 m boulders near to the trondhjemite body in the north. The clasts are rounded and elongated with their long axes parallel to the foliation trend (plate 23). The intensity of deformation varies from one place to another within the conglomerate and increases along the shear planes (plate 24).

The matrix comprises mainly plagioclase, chlorite, opaques, quartz, sphene, epidote, sericite and carbonate, a typical assemblage of greenschist facies (Winkler, 1974).

3.6 Structure and metamorphism

The Grong district of central Norway is a part of the Gjersvik Nappe. It contains two distinctly different structural units namely: Precambrian basement and Lower Palaeozoic allochthonous metavolcanics, metasediments and associated igneous intrusives. The former occupies the southeast corner of the mapped area (map 1) and during the course of the present study it has not been investigated. The area under consideration is a part of a nappe of greenstone metavolcanics and metasediments intruded by a trondhjemite complex, the latter phases of which have associated mineralization.

The area is traversed by a number of high-angle faults and thrusts accompanied by mylonite and shear zones. The major thrust is the one that separates the basement from the Palaeozoic cover and the Sanddøla river runs along the thrust

Plate (23): Poorly sorted conglomerate south of Storfisktjern. The deformed clasts of trondhjemite are rounded and are embedded in a semi-pelitic matrix.

Plate (24): Highly deformed conglomerate near the greenstone contact to the west of plate (23).

plane (Halls et al., 1977) (map 1). The faults have NE/SW trends with minor ones trending NW/SE. The intensity of mylonitisation and shearing increases towards the south. The jointing patterns in the area have a prominent ENE/WSW direction parallel to the pervasive cleavage and the main thrust, and a less common one trending NW/SE.

Throughout the area the general foliation trend is E/W to NE/SW with dips towards the north (50^{o}-80^{o}N). Isoclinal folding predominates in the area (Halls et al., op. cit.) but no closures were observed in the field although microfolds are well developed in the metasediments east of Kortdjern.

The volcanics and sediments were deformed and metamorphosed into greenschist assemblages (section 3.3) before the intrusion of the trondhjemite complex. The trondhjemite is weakly regionally metamorphosed and foliated. It is intruded by a number of dolerite dykes. These dykes are younger than the mineralization because they have never been mineralized by molybdenite-bearing veins. The trondhjemite complex, together with its mineralized portion, has been metamorphosed to the same grade as the dolerite dykes. Whether there are two episodes of metamorphism, one before and one after the mineralization, is not clear. Whereas the trondhjemite is always weakly foliated, certain parts of the granite are apparently unmetamorphosed, especially the pink variety, although this may simply reflect the lack of phyllosilicate minerals.

Thus the sequence of events in the area is assumed to be:

i) Deformation and metamorphism of volcanic and sedimentary rocks to produce schistose and lineated greenstone, presumably synchronous with nappe formation on the regional scale (Halls et al., 1977).

ii) Refolding of the earlier structures into open cross-cutting folds, well seen in the metasediments east and north-east of Korttjern.

iii) Intrusion of trondhjemite complex (with possibly a metamorphic event separating early trondhjemite from a late granite/hydrothermal alteration and mineralization).

iv) Dolerite dyke emplacement.

v) Conglomerate.

vi) Metamorphism and deformation to develop schistosity in the conglomerate, dolerite, the trondhjemite complex and deformed mineral veins.

vii) Brittle shear zones and silicified schistosity zones cross-cutting all earlier rocks and mineralization. NNE-SSE dextral shear zones break up the mineralized area into a number of segments.

CHAPTER 4

Geochemistry

4.1 Introduction

Sixty five samples that represent the greenstones and intrusive rocks of the Fremstfjell area have been selected for the geochemical study. All of the samples were analysed for 10 major elements (Si, Al, Fe, Mg, Ca, Na, K, Ti, Mn, P) and a number of trace elements (V, Cr, Ni, Rb, Sr, Y, Zr, Nb, Ba, La, Ce and Nd) using the X-ray fluorescence (X.R.F.) spectrography method (Jenkins and De Vries, 1967). The samples were crushed in a mechanical jaw crusher and a random selection of fragments was powdered for 3 minutes in a Tema tungsten carbide disc mill. A sample of powder was removed after 30 seconds for FeO determination by the titration method of Wilson (1955). The powders were pressed into pellets according to the method of Norrish and Chapel (1967) and were analysed on a Philips PW 1410 X.R.F. spectrometer in the Geology Department at Portsmouth Polytechnic. The data were then reduced using techniques and programs described by Brown et al. (1973). All the data obtained from the analysed samples, including C.I.P.W. norms, are given in the tables 1, 2,3,4 and 5 and the petrography of a selection of the analysed rocks is given in appendix 1.

4.2 Major elements

4.2.1 Basalt, basaltic andesite, andesite and rhyolite

The volcanic rocks of Fremstfjell and elsewhere in the Grong area are regionally metamorphosed with greenschist facies mineral assemblages (Chapter 3). A limited number of

analyses of these rocks is presented in Table 1 in order of increasing wt.% SiO_2. The rocks are classified arbitrarily in terms of increasing SiO_2 content within the calc-alkaline suite of igneous rocks as follows:

	wt.% SiO_2
Basalt	< 53
Basaltic andesite	53-58
Andesite	58-64
Dacite	64-70 (None present)
Rhyolite	> 70

Analyses 1-5 are of basic volcanic rocks (basalts and basaltic andesite), and according to Yoder and Tilley's (1962) nomenclature, both tholeiitic and alkaline types are present as olivine, hypersthene and nepheline are represented in the norms. However, Na/K ratios are very high and together with the obvious petrographic evidence of metamorphism, suggest that alkali contents must have been disturbed and that apparent basalt affinities must be treated with caution. Further, as the area has obviously been subjected to metamorphism, the Fe^{3+}/Fe^{2+} ratios were probably altered because Fe^{3+} contents are higher than the TiO_2 + 1.5 limit for unaltered basalts set by Irvine and Barager (1971). The rocks have relatively high Na_2O contents (Fig. 4,f) which may be a secondary feature due to sea-floor metamorphism (Miyashiro, 1973) or due to sea-water metasomatism during the low grade metamorphism (Cann, 1969; Hughes, 1973; Coleman, 1977).

Table 1: Geochemical analyses of Basalt, basaltic andesite, andesite and rhyolite

Analysis Number	1	2	3	4	5	6	7	8	9
	Basalt				Basaltic andesite	Andesite *		Rhyolite	
Sample Number	N5	N16	N17	N1	N15	Y3	Y4	Y1	Y2
SiO_2	41.89	45.10	48.14	51.92	56.52	62.83	70.95	75.46	77.65
Al_2O_3	15.87	14.54	17.02	13.96	13.78	14.35	13.37	12.49	12.11
Fe_2O_3	5.17	3.86	4.47	5.80	3.46	2.71	1.95	1.09	1.02
FeO	8.48	7.46	10.96	3.40	3.70	6.28	4.02	2.16	1.01
MgO	14.02	13.28	10.16	9.97	8.45	6.48	3.02	2.37	1.36
CaO	8.80	11.81	2.78	9.66	7.01	1.17	0.69	0.52	0.55
Na_2O	2.30	2.29	3.67	3.16	4.00	4.65	4.71	4.96	5.31
K_2O	0.03	0.02	0.16	0.32	1.71	0.11	0.41	0.40	0.51
TiO_2	1.03	0.43	1.52	0.53	0.80	0.51	0.41	0.21	0.15
MnO	0.24	0.29	0.20	0.20	0.16	0.26	0.16	0.07	0.02
P_2O_5	0.16	0.14	0.25	0.19	0.32	0.14	0.10	0.01	0.03
Total	98.99	99.22	99.33	99.73	99.91	99.49	99.79	99.74	99.72
C.I.P.W. Norms Wt. %									
Q	-	-	-	0.05	2.58	19.52	33.83	39.16	41.33
C	-	-	6.40	-	-	4.79	4.16	2.98	1.89
Or	0.18	0.12	0.95	5.45	10.11	0.65	2.42	2.36	3.01
Ab	15.00	14.31	31.26	26.81	33.88	39.35	39.85	41.97	44.93
An	33.23	29.59	12.24	21.25	14.61	4.89	2.77	2.51	2.53
Ne	2.52	2.84	-	-	-	-	-	-	-
Di	7.87	22.87	-	20.06	14.29	-	-	-	-
Hy	-	-	37.20	16.51	17.25	25.07	12.91	8.75	4.19
Ol	31.28	23.52	1.94	-	-	-	-	-	-
Mt	7.57	5.60	6.53	8.43	5.02	3.93	2.83	1.58	1.48
Il	1.98	0.82	2.91	1.01	1.52	0.97	0.78	0.40	0.28
Ap	0.37	0.33	0.58	0.44	0.74	0.32	0.23	0.02	0.07
ppm									
V	321	262	395	258	169	134	22	26	24
Cr	317	28	19	313	345	7	2	3	4
Ni	120	28	6	76	108	n.d.	n.d.	n.d.	2
Rb	n.d.	n.d.	n.d.	n.a.	25	n.d.	n.d.	2	1
Sr	379	604	230	586	918	28	56	71	63
Y	15	12	26	n.a.	14	24	54	38	34
Zr	40	24	83	48	134	113	248	145	98
Nb	4	5	7	6	10	10	23	12	11
Ba	22	n.d.	49	252	1074	n.d.	55	41	48
La	1	5	3	16	38	2	16	4	13
Ce	6	2	15	35	80	9	36	13	25
Nd	4	1	10	13	34	1	21	5	10

n.d. = not detected

n.a. = not analysed

* = included with rhyolite in all variation diagrams

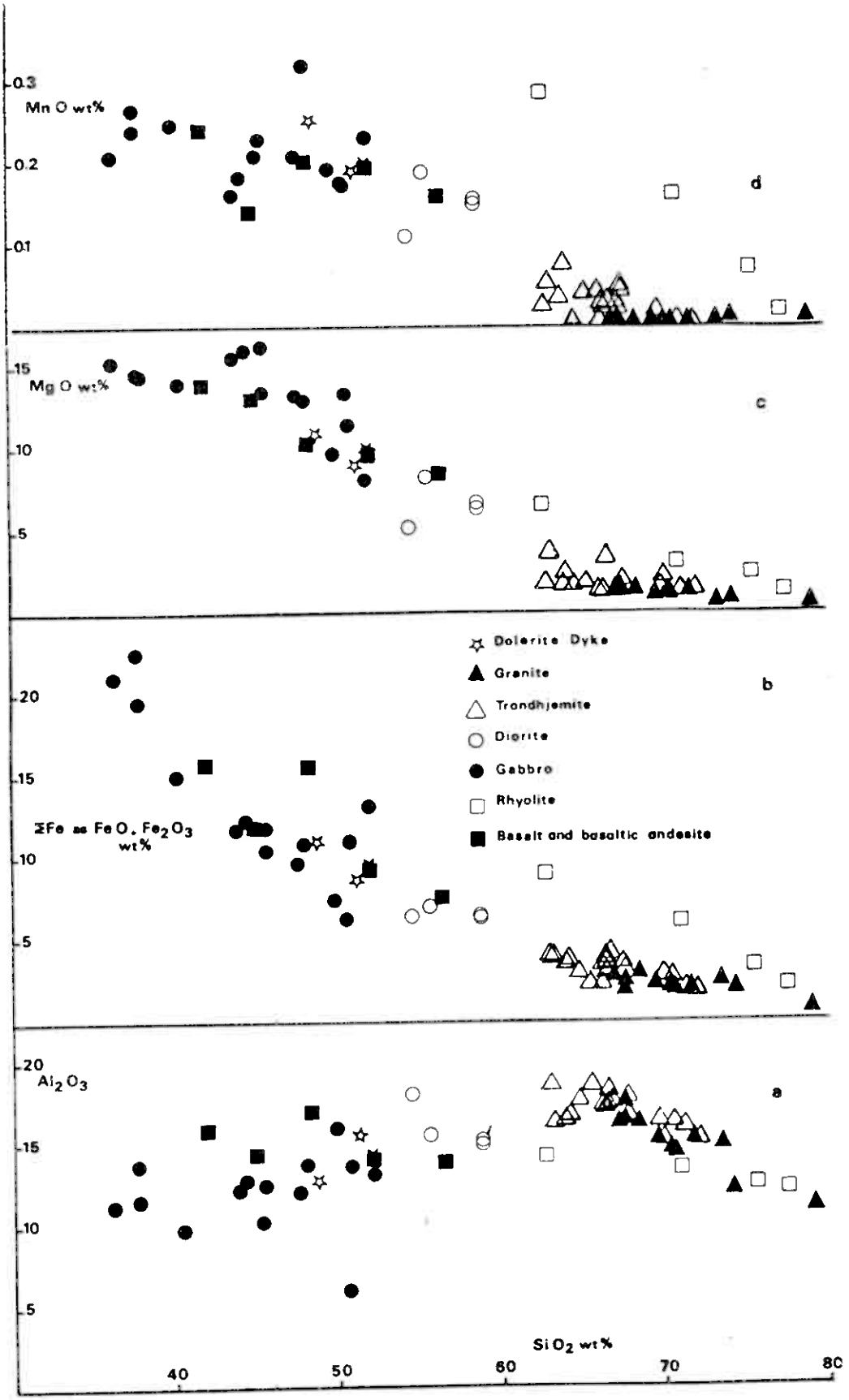

Fig. 4: Harker variation diagram for all analysed rocks.

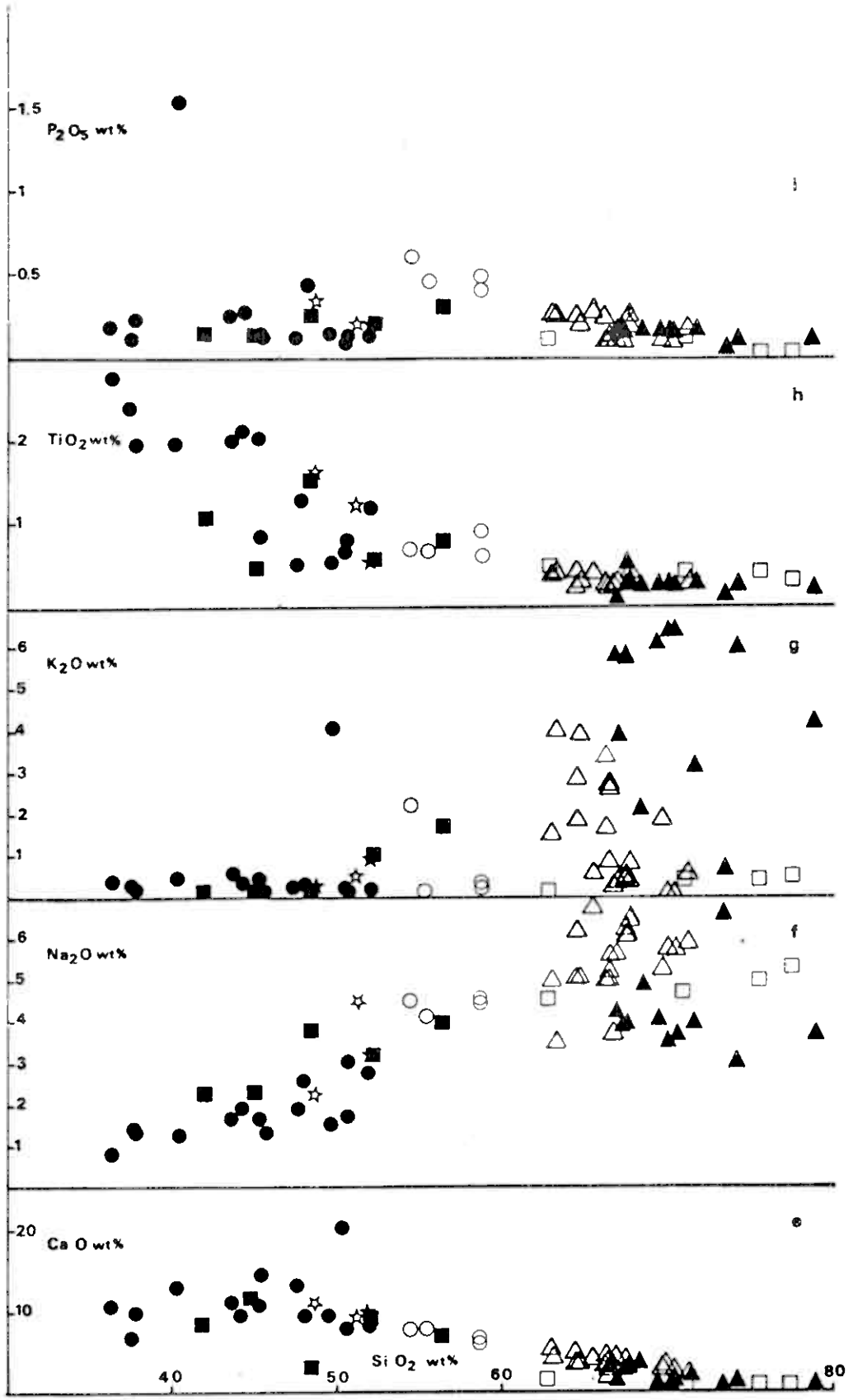

Fig. 4: continued.

Using a variety of discrimination diagrams it is difficult to clearly ascribe these rocks to any of the major igneous rock series. On a total alkalis versus SiO_2 diagram (Fig. 5), samples N5, N16 (analyses 1, 2) plot in tholeiitic field and samples N17, N1, N15 (analyses 3,4,5) occur in the high-alumina field. Analyses (1,2,3) follow a tholeiite trend and the others (anslyes 4,5) occur in the calc-alkaline field on the AFM diagram (Fig. 7). On a K_2O versus SiO_2 diagram (Fig. 13) the analyses are widely spread but sample N17 (analysis 3) occurs in the field of subalkaline oceanic basalts and gabbros and sample N1 (analysis 4) plots in the field of continental tholeiitic basalt. All the samples plot in the calc-alkalic field on SiO_2 versus FeO^t/MgO diagram (FeO^t is total iron, Fig. 9) but they follow the abyssal tholeiite trend on diagrams of TiO_2 and FeO^t versus FeO^t/MgO (Figs. 10 and 11 respectively). Also, they plot in the basalt and andesite fields on a diagram Na_2O versus CaO (Fig. 8).

Elsewhere in the region previous workers (Gale and Roberts, 1974; Lutro, 1979; Gale and Pearce, 1982) concluded that these rocks are of tholeiitic affinity while Halls et al. (1977) suggest they are tholeiites with a distinct trend towards calc-alkaline affinities and this seems to be the case for the rocks under discussion.

The andesites and rhyolites (analyses 6-9) are altered felsic rocks which are probably of pyroclastic origin. They usually occur as fine-grained thin sequences between individual basic units.

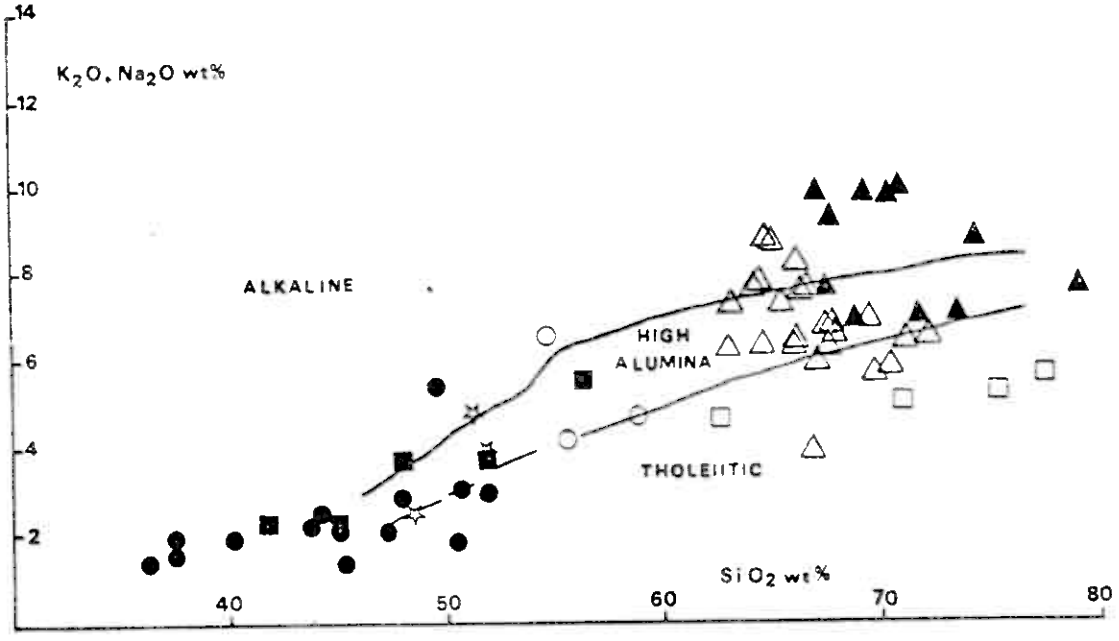

Fig. 5: Total alkalis versus silica diagram for all analysed rocks. Fields are those of Kuno (1969). Symbols as for Fig. 4.

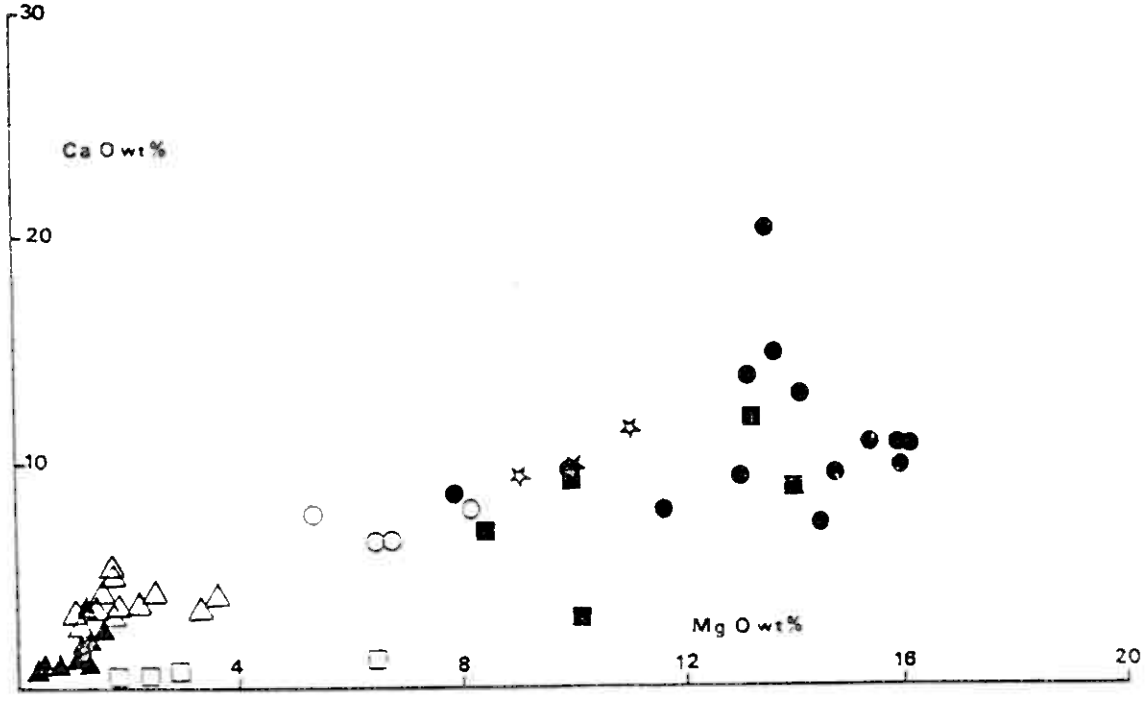

Fig. 6: CaO-MgO variation diagram, all analysed rocks. (Symbols as for Fig. 4).

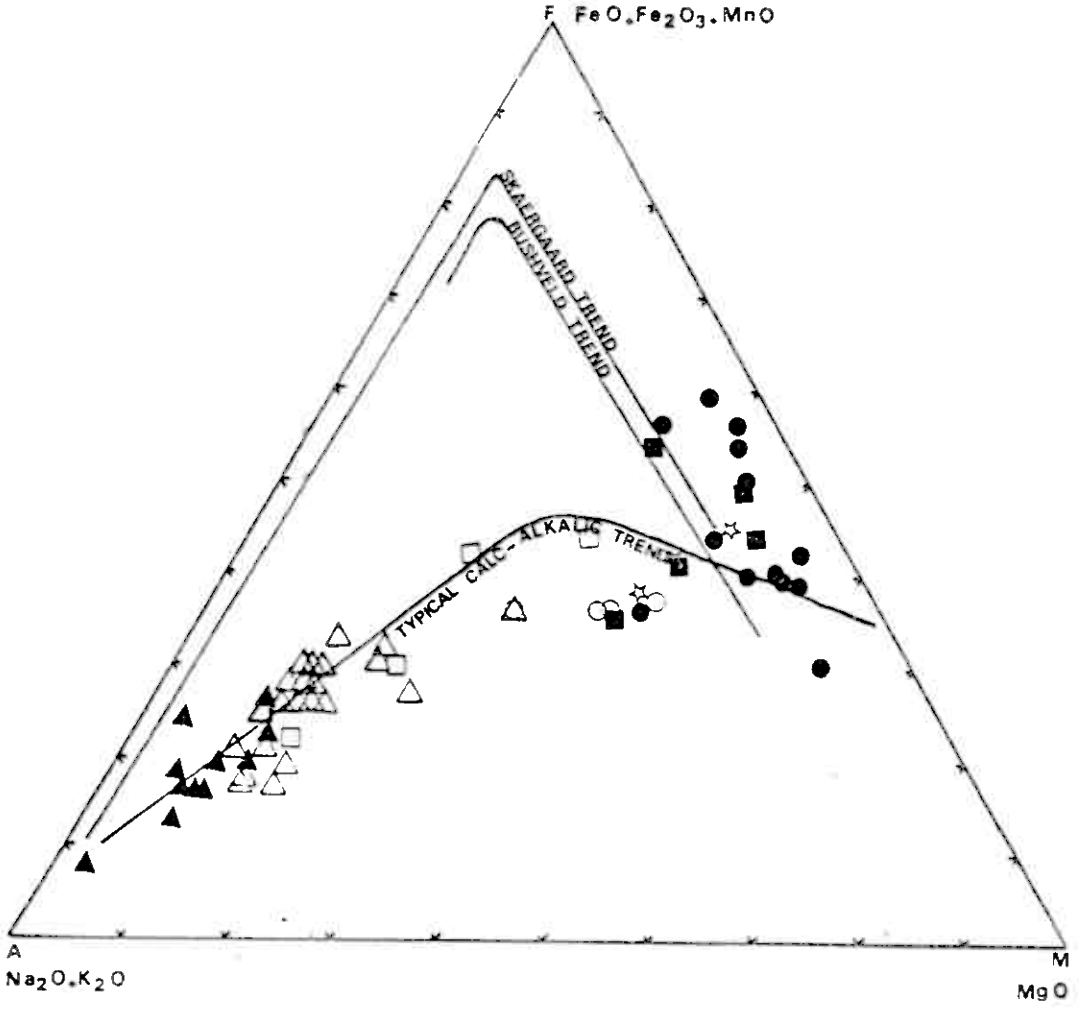

Fig. 7: AFM diagram for all analysed rocks (after Hess, 1960). Symbols as for Fig. 4.

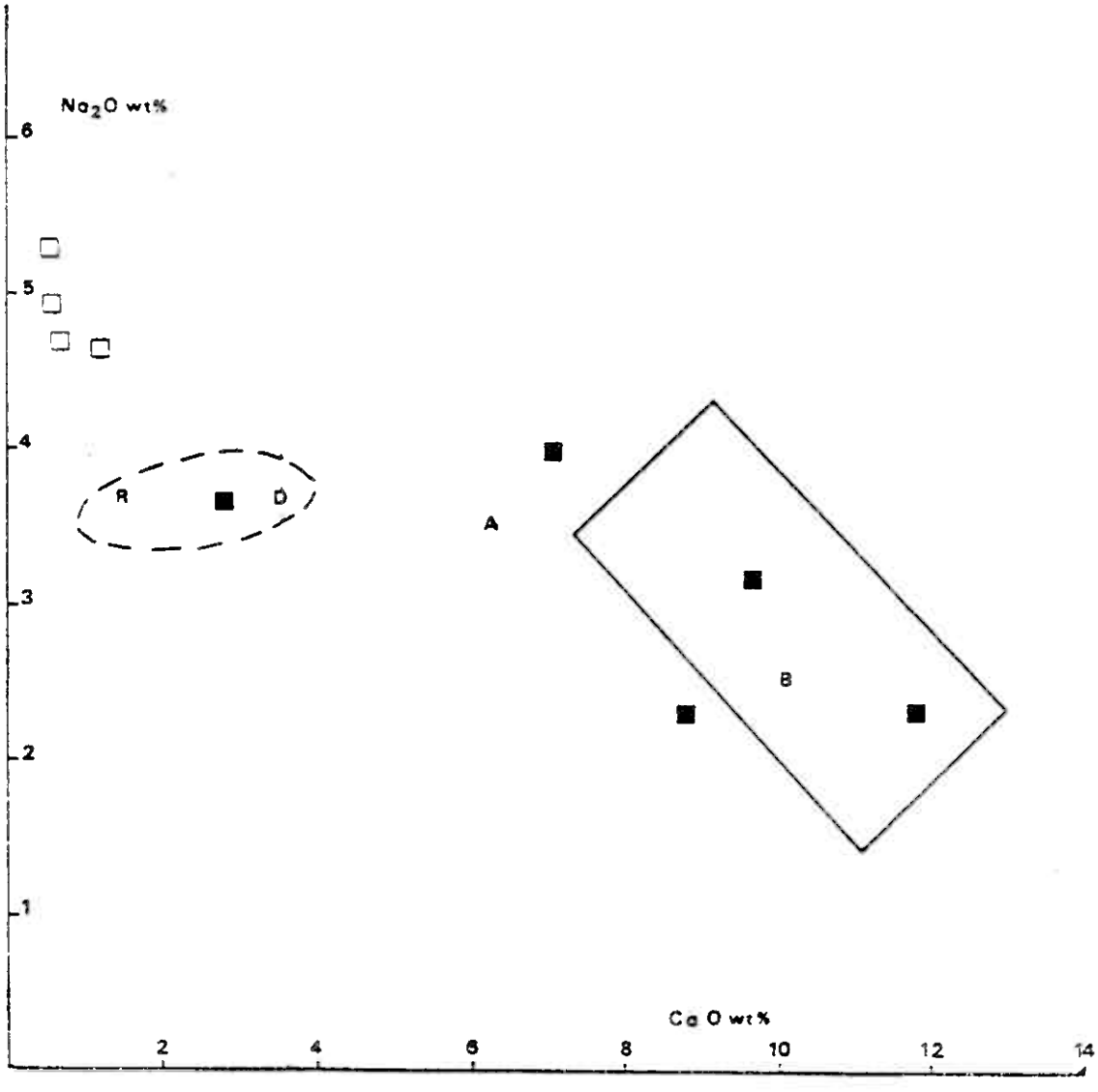

Fig. 8: Na_2O/CaO diagram. Symbols as in Fig.4. Fields after Stephens (1980), A - andesite, B - basalts, R - rhyolites and D - dacites.

They are relatively high in Na_2O and low K_2O (Fig. 4, f, g) which makes the rhyolites quartz keratophyres in terms of the classification of Schermerhorn (1974), although the high Na/K is almost certainly a function of metamorphism. They have low CaO and MgO (Fig. 6) and on the total alkalis versus SiO_2 diagram (Fig. 5) they plot in the tholeiitic field while on the AFM diagram (Fig. 7) they follow the calc-alkalic trend. They cluster around the rhyolite-dacite field on the Na_2O versus CaO diagram (Fig. 8).

4.2.2 Gabbro and diorite

Fourteen samples of the gabbro and four from the diorite were analysed and the data are presented in (Table 2) and shown graphically in the subsequent variation diagrams (Fig. 4-23).

The gabbros show both tholeiitic and alkaline characteristics (Yoder and Tilley, 1962) in having olivine, hypersthene and nepheline in the norm, iron enrichment without increasing silica (Fig. 4, b), low K_2O contents (Fig. 4, g) and moderate to high Na_2O/K_2O ratio (2.5-6). The rocks are apparently enriched in CaO which may be due to epidotization that occurs all through the area and which is clearly illustrated in the CaO versus MgO diagram (Fig. 6). For example, sample N4 (analysis 21) has > 20% wt. CaO. This rock is mainly composed of diopsidic augite and has 73% diopside in its norm. Some of these gabbros are over-saturated with respect to SiO_2, having up to 6% Q in the norm (Table 2).

Table 2 : Geochemical analyses of the Gabbro and the Diorite

Analysis Number	10	11	12	13	14	15	16	17	18	19	20	21
Sample Number	B7	N6	B7/c	N7	B7/d	B7/a	B7/b	4/8/8	4/8/9	E2	4/8/14	N4
SiO_2	36.25	37.62	37.69	40.26	43.93	44.27	45.27	45.45	47.44	48.06	49.67	50.44
Al_2O_3	11.33	11.58	13.73	9.89	12.22	12.57	11.15	12.17	12.05	13.60	15.96	6.05
Fe_2O_3	10.47	10.28	10.63	5.66	6.21	5.59	5.79	5.22	3.83	5.89	1.49	1.92
FeO	10.46	12.04	9.02	9.30	5.67	6.43	5.99	5.04	5.63	4.89	6.02	4.23
MgO	15.37	14.46	14.65	14.17	15.89	16.00	16.03	13.77	13.27	13.08	9.89	13.57
CaO	10.84	7.17	9.62	13.03	10.83	9.72	10.70	14.79	13.82	9.41	9.48	20.22
Na_2O	0.94	1.50	1.45	1.33	1.76	1.95	1.63	1.36	1.92	2.61	1.50	1.75
K_2O	0.43	0.38	0.24	0.53	0.53	0.42	0.47	0.09	0.26	0.30	4.10	0.15
TiO_2	2.55	2.38	1.99	1.97	2.02	2.11	2.03	0.85	0.50	1.32	0.51	0.63
MnO	0.21	0.27	0.24	0.25	0.16	0.18	0.21	0.23	0.21	0.22	0.19	0.17
P_2O_5	0.18	0.13	0.23	1.53	0.26	0.28	0.15	0.12	0.12	0.44	0.14	0.13
Total	99.11	99.16	99.49	99.01	99.48	99.53	99.42	99.65	99.69	99.80	100.22	99.71
C.I.P.W. Norms Wt. %												
Q	-	-	-	-	-	-	-	-	-	-	-	-
Or	2.42	2.29	1.42	3.20	3.13	2.48	2.78	0.54	1.55	1.77	24.49	0.89
Ab	-	12.97	8.02	6.73	14.63	16.50	13.79	10.77	14.99	22.09	8.75	4.42
An	25.42	24.27	30.25	19.85	23.88	24.31	21.72	27.08	23.72	24.51	24.97	8.27
Ne	4.31	-	2.30	2.58	0.14	-	-	0.46	0.76	-	2.21	5.69
Di	21.52	8.96	12.61	28.87	22.05	17.37	23.85	36.37	35.48	15.14	17.39	72.71
Hy	-	1.92	-	-	-	2.81	7.07	-	-	15.66	-	-
Ol	24.90	29.40	25.17	22.97	22.21	23.29	17.61	15.25	16.65	8.59	18.71	3.72
Mt	15.18	15.24	15.41	8.37	9.00	8.11	8.39	7.63	5.61	8.54	2.18	2.80
Il	4.84	4.62	3.78	3.82	3.83	4.01	3.85	1.63	0.96	2.51	0.98	1.21
Ap	0.42	0.31	0.53	3.62	0.60	0.65	0.35	0.28	0.28	1.02	0.33	0.30
ppm												
V	682	602	581	424	321	365	292	313	251	245	184	154
Cr	83	n.d.	86	36	21	7	88	302	154	426	656	133
Ni	31	n.d.	26	52	80	42	113	86	98	108	117	34
Rb	n.d.	n.d.	n.d.	n.d.	n.d.	n.d.	n.d.	n.d.	n.d.	n.d.	84	n.d.
Sr	1171	529	1753	1232	1031	1210	882	318	349	1771	248	752
Y	18	35	18	41	8	19	13	9	8	15	9	15
Zr	103	50	104	106	86	163	88	9	10	183	17	63
Nb	8	10	7	11	10	12	10	4	4	16	5	5
Ba	186	154	78	275	232	132	185	14	71	134	642	45
La	29	7	14	82	20	22	21	n.d.	5	73	2	19
Ce	72	36	65	203	53	73	58	1	2	147	5	46
Nd	50	34	36	123	33	43	37	n.d.	1	57	1	30

Table 2 ctd.

Analysis Number	22	23	24	25	26	27
Sample Number	4/8/10	4/8/15	CS	N2	N8	CYP
SiO_2	50.75	51.93	54.60	55.63	58.80	58.85
Al_2O_3	13.75	13.24	18.09	15.65	15.43	15.10
Fe_2O_3	6.35	5.94	4.71	3.18	3.05	4.14
FeO	4.75	7.05	1.72	3.55	3.01	2.44
MgO	11.63	7.82	5.32	8.19	6.53	6.83
CaO	7.99	8.60	7.68	7.87	6.44	6.42
Na_2O	3.09	2.84	4.46	4.16	4.44	4.57
K_2O	0.06	0.23	2.19	0.03	0.35	0.23
TiO_2	0.81	1.14	0.72	0.68	0.90	0.62
MnO	0.17	0.23	0.11	0.19	0.13	0.15
P_2O_5	0.15	0.15	0.62	0.45	0.43	0.48
Total	100.02	99.97	100.22	99.58	99.51	99.83
C.I.P.W. Norms Wt. %						
Q	0.68	6.04	0.05	4.74	10.29	10.54
Or	0.36	1.37	12.95	0.18	2.08	1.36
Ab	26.28	24.23	37.74	35.35	37.75	38.67
An	23.59	22.89	22.87	24.04	21.24	20.01
Ne	-	-	-	-	-	-
Di	11.99	15.29	8.70	9.65	6.33	6.79
Hy	25.97	18.95	9.22	19.06	15.14	14.17
Ol	-	-	-	-	-	-
Mt	9.25	8.68	3.82	4.63	4.45	6.00
Il	1.55	2.18	1.37	1.30	1.72	1.18
Ap	0.35	0.37	1.44	1.05	1.00	1.11
ppm						
V	281	544	176	146	131	143
Cr	330	n.d.	24	193	155	181
Ni	116	2	12	61	57	58
Rb	n.d.	n.d.	34	n.d.	n.d.	n.d.
Sr	222	278	2236	1150	1974	1499
Y	18	21	9	14	14	7
Zr	42	52	139	146	142	187
Nb	6	6	5	11	9	10
Ba	25	43	1144	97	186	228
La	2	1	70	43	49	43
Ce	3	12	144	87	95	91
Nd	2	6	62	36	38	35

n.d. = not detected

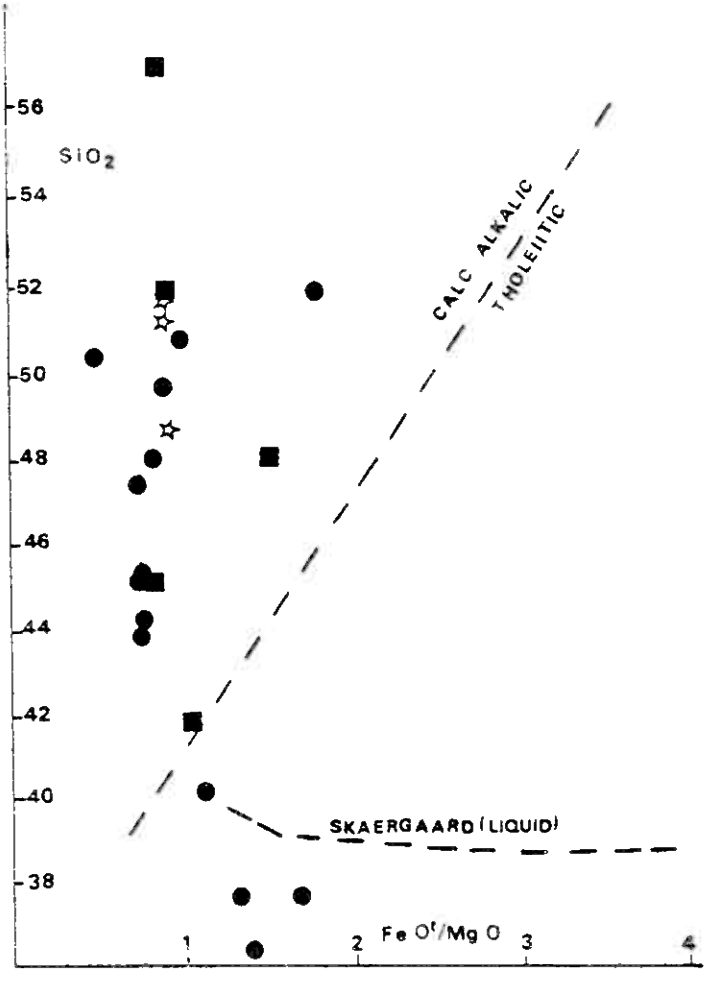

Fig. 9: SiO_2 versus FeO^t/MgO (FeO^t = total iron as FeO) diagram for basalt, basaltic andesite (solid squares), gabbro (solid circles) and dolerite dyke (stars). The calc-alkalic, tholeiitic fields and the Skaergaard trend from Miyashiro (1973).

On the total alkalis versus SiO_2 diagram (Fig. 5) the data plot in the tholeiitic and high alumina fields except sample 4/8/10 (analysis 22) that occurs in the alkaline field. This rock was taken from near an aplitic vein and that may be the reason for its 4.10 wt.% K_2O. The samples show the typical iron enrichment of tholeiites on the AFM diagram (Fig. 7) with only mild alkalinity. In the diagrams discussed by Miyashiro (1973) in which SiO_2, TiO_2 and FeO^t (total iron as FeO) are all plotted against the fractionation index FeO^t/MgO, most of the samples cluster in the calc-alkalic field (Fig. 9) in the SiO_2 diagram while in the others (Fig. 10 , Fig. 11) all of the samples follow the abyssal tholeiite trend. On the K_2O-SiO_2 diagram (Fig. 13) the samples cluster around the subalkaline oceanic basalts and gabbros.

Diorites are rare in the area and are found as scattered pockets at the contact between the trondhjemite and the greenstone or greenstone rafts. Four samples were analysed and contain between 55 and 59 wt.% SiO_2 and high alumina and consequently they are all corundum normative. They have high P_2O_5 contents (Fig. 4, i) and apatite is an abundant accessory mineral. On the total alkalis versus SiO_2 diagram (Fig. 5) they plot in the high-alumina field and follow the calc-alkalic trend on the AFM diagram (Fig. 7).

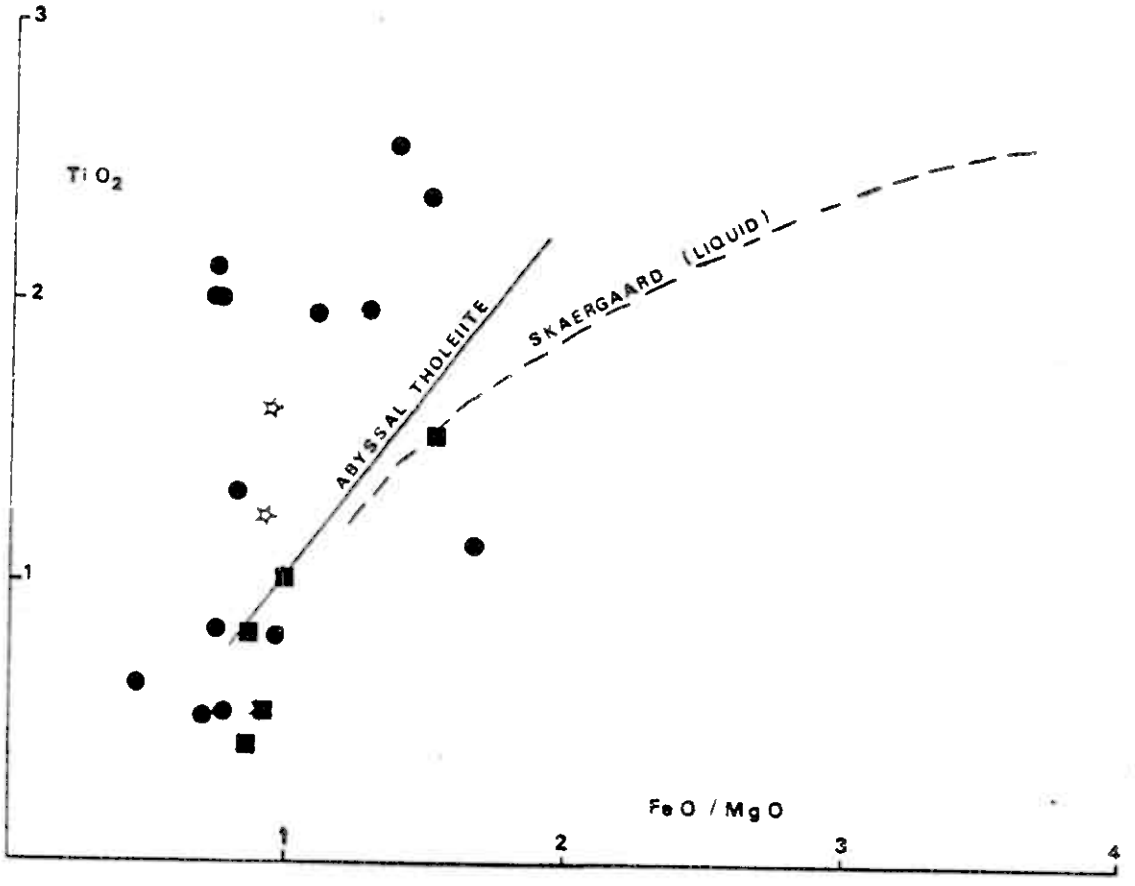

Fig. 10: TiO_2 versus FeO^t/MgO diagram, see Fig. 9.

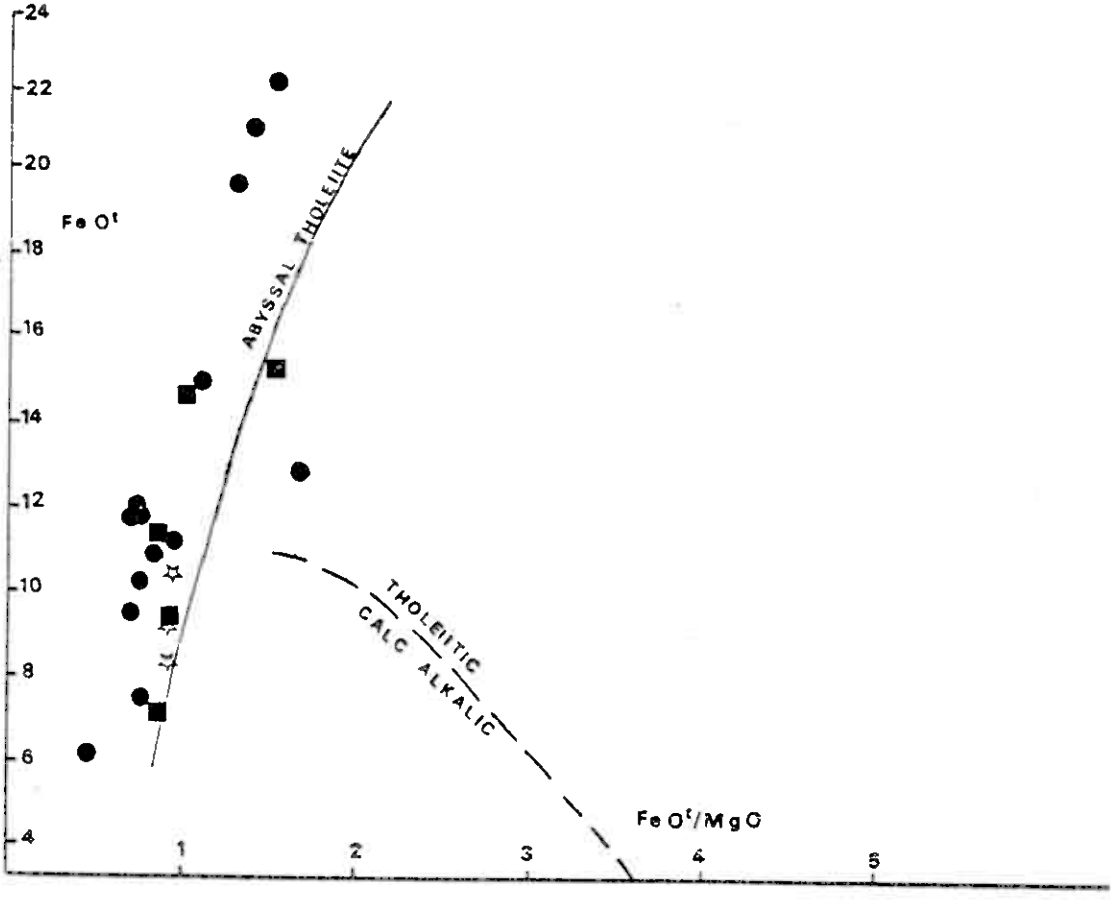

Fig. 11: FeO^t versus FeO^t/MgO diagram, see Fig. 9.

4.2.3 Trondhjemite

Twenty four samples were analysed from the trondhjemite suite which covers more than half of the mapped area and the data are presented in Table 3 and graphically shown in 4-23. They are moderate to high in silica (63-72%) and are high alumina types (> 15% wt. Al_2O_3) as defined by Barker and Arth (1976). Their total iron is moderate to high for granitic rocks and it does not show enrichment with increasing silica (average 3.1% wt.). FeO^t/MgO ratios are comparable to trondhjemite from other regions (Arth and Hanson, 1975; Barker, 1979). Their sodium contents are high (> 6% wt.) in contrast to low potassium, except for the samples F1, H1, H2, J1/a, J1/b, J2 (analyses nos. 31, 29, 38, 34, 30 and 36) which have relatively high K_2O (c. 3.2%)(Table 3). These K_2O rich samples were collected from southeast of the granite body where the granite interfingers with the trondhjemite which may be the reason for this enrichment.

The Na_2O/K_2O ratio is > 3 on average, except in the analyses mentioned above. The high Na_2O in the trondhjemite is probably in part due to alteration and metasomatism (sericitization and albitization) and consequently they are high albite normative. Most of the trondhjemites are peraluminous types, having corundum in their norm (Table 3) and this may be due to alteration or to late stage introduction of aluminium which resulted in newly grown muscovite rimming altered feldspars (Cawthorn et al., 1976).

Table 3: Geochemical analyses of the Trondhjemite

Analysis Number	28	29	30	31	32	33	34	35	36	37	38	39
Sample Number	A1	H1	J1/b	F1	D4	N13	J1/a	D5	J2	B3	H2	B1/b
SiO_2	63.05	63.31	63.38	64.14	64.36	64.60	64.74	65.54	66.24	66.27	66.37	66.51
Al_2O_3	18.30	16.06	16.99	16.58	16.67	17.02	17.49	18.43	17.07	17.33	17.41	18.12
Fe_2O_3	3.23	3.45	3.74	3.12	1.86	3.29	2.04	1.66	1.63	2.74	2.83	2.06
FeO	0.72	0.58	0.29	0.29	1.72	0.89	0.86	0.28	0.43	0.72	0.72	1.29
MgO	1.76	3.66	2.05	1.76	2.19	2.52	1.72	1.77	1.53	1.57	1.57	1.51
CaO	5.32	4.19	4.58	4.91	3.62	4.15	3.53	3.93	3.34	3.86	2.62	3.29
Na_2O	4.90	3.46	4.74	5.05	6.20	4.61	4.94	6.81	5.06	4.99	4.98	5.72
K_2O	1.48	3.91	2.90	2.77	1.77	1.92	3.89	0.62	3.41	1.72	2.80	0.78
TiO_2	0.37	0.41	0.19	0.26	0.38	0.39	0.36	0.39	0.35	0.35	0.32	0.31
MnO	0.03	0.06	0.04	0.04	0.08	0.08	0.01	0.04	0.01	0.04	0.03	0.01
P_2O_5	0.25	0.26	0.22	0.27	0.27	0.29	0.23	0.32	0.19	0.26	0.18	0.23
Total	99.41	99.35	99.12	99.19	99.12	99.79	99.85	99.79	99.80	99.85	99.83	99.83
C.I.P.W. Norms Wt. %												
Q	15.82	15.03	13.49	13.55	11.56	18.53	12.06	13.40	15.19	20.78	19.24	21.52
C	-	-	-	-	-	0.48	-	0.18	-	0.86	1.85	2.44
Or	8.75	23.11	17.14	16.37	10.46	11.55	22.99	3.66	20.15	10.16	16.55	4.61
Ab	41.46	29.28	40.11	42.73	52.46	39.09	41.80	57.62	42.82	42.22	42.14	48.40
An	23.57	16.74	16.52	14.39	12.43	18.73	14.06	17.41	13.79	17.45	11.82	14.82
Di	0.93	1.83	3.71	0.39	2.99	-	1.52	-	1.20	-	-	-
Hy	3.95	8.27	3.38	1.42	5.18	6.29	3.58	4.41	3.26	3.91	3.91	3.93
Mt	1.35	0.88	0.48	0.28	2.70	2.00	1.76	-	0.40	1.44	1.49	2.99
Il	0.70	0.78	0.36	0.49	0.72	0.74	0.68	0.68	0.66	0.66	0.61	0.59
Ap	0.58	0.60	0.51	0.63	0.63	0.67	0.53	0.74	0.44	0.60	0.42	0.53
ppm												
V	67	100	84	68	67	59	78	64	59	59	59	62
Cr	6	10	5	6	7	8	6	6	6	7	4	5
Ni	3	3	2	3	2	5	2	2	1	3	1	1
Rb	15	71	79	65	20	29	89	n.d.	35	18	43	4
Sr	2799	1720	1743	2183	1386	1576	1608	1123	1223	1641	1198	1661
Y	n.d.	2	7	5	5	17	2	8	2	5	6	5
Zr	214	202	190	215	184	171	209	210	173	178	173	191
Nb	8	8	9	11	11	11	9	14	9	9	11	8
Ba	930	1517	1237	926	3214	1273	1751	411	1107	909	1069	222
La	14	45	37	52	50	49	28	63	22	52	46	38
Ce	60	84	77	101	104	84	72	120	57	84	88	87
Nd	21	29	28	35	40	32	27	44	23	23	28	27

Table 3 ctd.

Analysis Number	40	41	42	43	44	45	46	47	48	49	50	51
Sample Number	D2	A2	A3	B5	B6/a	D6	B4	A0	A4	A5	B2/d	D3
SiO_2	66.51	66.84	67.02	67.59	67.62	67.76	67.84	69.63	69.99	70.43	71.25	72.29
Al_2O_3	17.00	17.62	17.26	17.23	16.72	17.51	16.87	16.14	15.60	16.11	15.85	15.28
Fe_2O_3	2.78	2.48	2.38	1.79	2.28	1.84	1.56	1.95	2.21	1.94	1.59	1.43
FeO	0.29	1.72	0.86	1.49	0.86	0.14	1.49	0.29	0.86	0.58	0.28	0.29
MgO	1.39	3.35	1.49	1.43	1.56	1.75	1.71	1.05	1.25	1.19	1.13	1.28
CaO	3.43	3.34	4.19	2.74	3.75	3.03	2.95	3.24	3.47	2.95	2.66	2.00
Na_2O	5.26	3.67	5.61	6.29	5.93	6.55	5.95	5.29	5.68	5.87	5.87	5.42
K_2O	2.61	0.33	0.40	0.63	0.44	0.50	0.81	1.87	0.20	0.18	0.62	0.23
TiO_2	0.32	0.31	0.36	0.33	0.34	0.38	0.33	0.28	0.30	0.30	0.32	0.31
MnO	0.03	0.02	0.03	0.03	0.05	0.02	0.04	0.00	0.02	0.01	0.00	0.01
P_2O_5	0.19	0.16	0.20	0.22	0.22	0.30	0.24	0.14	0.16	0.18	0.19	0.17
Total	99.81	99.84	99.81	99.77	99.77	99.78	99.79	99.78	99.74	99.74	99.76	99.71
C.I.P.W. Norms Wt. %												
Q	17.19	32.24	22.22	20.86	21.70	19.49	21.48	23.67	27.34	28.01	27.88	28.35
C	-	5.54	0.46	1.75	0.20	1.40	1.42	-	0.11	1.33	1.14	1.24
Or	15.42	1.95	2.36	3.72	2.60	2.95	4.79	11.05	1.18	1.06	3.66	1.36
Ab	44.51	31.06	47.47	53.22	50.18	55.42	50.35	44.76	48.06	49.67	49.67	54.32
An	15.07	15.52	19.48	12.16	17.17	13.07	13.07	14.77	16.17	13.46	11.95	8.81
Di	0.55	-	-	-	-	-	-	0.30	-	-	-	-
Hy	3.21	8.98	3.71	4.33	3.88	4.36	5.26	2.47	3.11	2.96	2.81	3.19
Mt	0.11	3.60	1.83	2.60	1.95	-	2.25	0.12	1.97	1.03	-	1.00
Il	0.61	0.59	0.68	0.63	0.65	0.34	0.63	0.53	0.57	0.57	0.59	0.59
Ap	0.44	0.37	0.46	0.51	0.51	0.69	0.56	0.32	0.37	0.42	0.44	0.39
ppm												
V	58	61	62	58	60	70	57	45	46	40	41	738
Cr	6	6	5	5	5	7	6	5	7	5	6	n.d.
Ni	2	n.d.	2	1	1	1	2	1	n.d.	n.d.	1	3
Rb	42	n.d.	n.d.	3	n.d.	n.d.	3	30	n.d.	n.d.	1	n.d.
Sr	1175	1713	1893	1343	1342	1180	953	1541	1502	1292	1117	725
Y	4	n.d.	n.d.	4	4	4	5	n.d.	n.d.	2	1	1
Zr	186	160	176	170	175	195	182	165	154	154	160	159
Nb	9	8	9	8	10	10		9	7	9	10	10
Ba	1104	291	1409	332	210	390	354	858	237	234	281	107
La	25	17	23	61	41	40	40	29	36	31	40	31
Ce	61	74	59	81	87	81	71	62	55	70	81	67
Nd	23	17	21	27	26	29	23	22	19	22	29	24

n.d. = not detected

These rocks can be classified as high-alumina on the total alkalis versus SiO_2 diagram (Fig. 5) and follow the calc-alkaline trend on the AFM diagram (Fig. 7). On the normative feldspar diagram (Fig. 12) the samples tend to cluster in the fields of tonalite and trondhjemite within the low pressure (< 5kb) feldspar stability field (Coleman and Peterman, 1975). Exceptions to this are all contact rocks. The analyses plot as a scatter from the oceanic plagiogranitic field to the continental granophyre field defined by Coleman and Peterman (1975) in a K_2O versus SiO_2 variation diagram (Fig. 13). This strongly suggests a continuum from true trondhjemitic plagiogranites through to more typical continental potassic granites.

4.2.4 Granite

Granites occur in the centre of the mapped area and they are the chief host rocks for the molybdenum mineralization. Previous workers (Fosile, 1927; Gale, 1975) consider these bodies as a part of a major trondhjemite intrusion but they are different from the trondhjemite in their petrography (Chapter 3) and in their chemistry.

Eleven samples were analysed from the granites and the data are presented in Table 4 and shown graphically on variation diagrams (Fig. 4-23). Significant chemical variation occurs between the granites depending on their degree of shearing. This is also clear in their petrography (Chapter 3).

Table 4 : Geochemical analyses of the Granite

Analysis Number	52	53	54	55	56	57	58	59	60	61	62
Sample Number	T5/j	T1/a	B15	T1/d	T5/c	T5/b	T5/f	T6/e	T2/g	T5/o	T3/b
SiO_2	67.01	67.41	67.57	68.58	69.43	70.17	70.67	71.77	73.54	74.20	79.10
Al_2O_3	16.12	17.39	16.31	16.13	15.36	14.80	14.41	15.12	15.17	12.04	11.01
Fe_2O_3	2.30	2.45	1.86	2.42	1.72	1.77	1.46	1.42	2.24	2.07	0.53
FeO	0.43	0.14	0.28	0.43	0.43	0.28	0.28	0.60	0.14	0.14	0.14
MgO	1.42	1.51	1.34	1.25	1.10	1.25	1.09	1.37	0.43	0.81	0.24
CaO	1.79	2.74	2.30	3.52	1.13	1.02	1.18	2.98	0.75	1.00	0.49
Na_2O	4.30	3.88	3.89	4.96	3.95	3.49	3.73	3.97	6.55	2.96	3.68
K_2O	5.78	3.86	5.70	2.10	6.12	6.40	6.41	3.13	0.75	5.02	4.21
TiO_2	0.33	0.28	0.28	0.27	0.26	0.27	0.25	0.29	0.12	0.25	0.11
MnO	0.00	0.00	0.01	0.00	0.00	0.00	0.00	0.00	0.00	0.01	0.01
P_2O_5	0.19	0.17	0.14	0.16	0.13	0.14	0.13	0.17	0.01	0.10	0.02
Total	99.67	99.83	99.68	99.82	99.63	99.59	99.51	99.82	99.69	99.62	99.78
C.I.P.W. Norms Wt. %											
Q	14.47	22.43	16.66	22.93	19.34	21.72	20.95	30.89	30.35	31.42	40.49
C	-	2.25	-	-	0.50	0.61	-	2.01	2.24	-	-
Or	34.16	22.81	33.68	12.41	36.16	37.82	37.88	18.50	4.43	35.57	24.89
Ab	36.38	32.83	32.92	41.97	33.42	29.53	31.56	33.59	55.42	25.05	31.14
An	7.61	12.48	10.21	15.55	4.78	4.15	3.65	8.71	3.66	1.79	1.09
Di	0.02	-	0.22	0.68	-	-	1.06	-	-	1.74	0.94
Hy	3.53	3.76	3.23	2.80	2.74	3.11	2.22	3.41	1.07	1.21	0.16
Mt	0.43	-	0.12	0.60	0.63	0.12	0.18	0.77	0.10	-	0.17
Il	0.63	0.30	0.53	0.51	0.50	0.51	0.48	0.55	0.23	0.32	0.21
Ap	0.44	0.40	0.32	0.37	0.30	0.32	0.30	0.39	0.02	0.23	0.05
ppm											
V	58	51	53	48	44	43	43	46	28	40	29
Cr	5	5	4	5	4	5	4	5	5	4	5
Ni	1	n.d.	1	n.d.	1	2	1	1	6	1	1
Rb	58	52	79	23	65	69	63	24	n.d.	44	23
Sr	591	1326	1007	1230	356	328	507	848	498	392	243
Y	5	3	3	1	1	3	n.d.	n.d.	n.d.	n.d.	n.d.
Zr	155	158	138	141	118	118	121	139	77	107	71
Nb	8	8	7	9	9	7	7	8	6	4	5
Ba	2590	797	2025	1070	1986	1912	2218	1758	212	4502	1550
La	57	36	39	31	40	45	31	19	3	27	16
Ce	104	67	69	68	69	72	59	45	20	53	22
Nd	35	23	23	23	25	26	21	19	4	24	4

n.d. = not detected

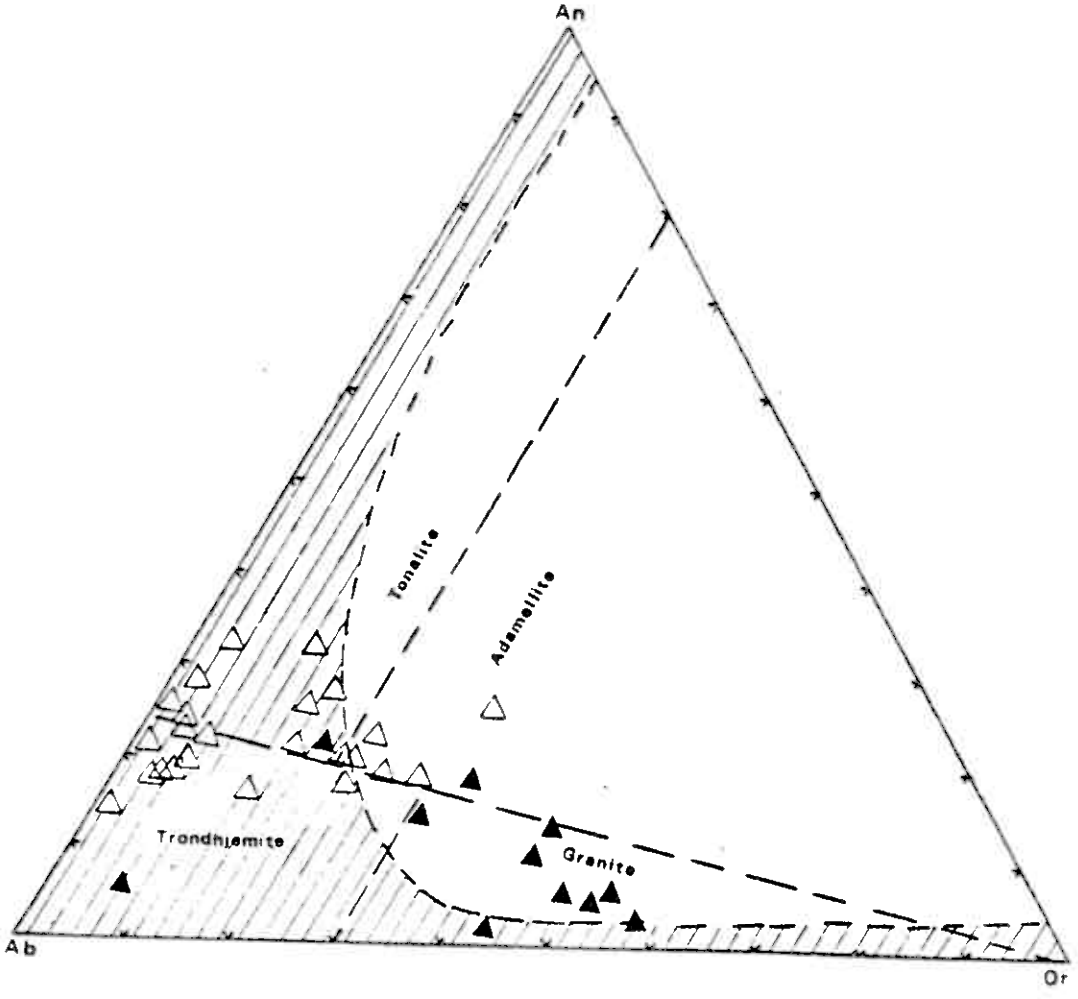

Fig. 12: Normative feldspar diagram for trondhjemite and granite.

Fields: Trondhjemite, granite, adamellite and tonalite after O'Connor (1965) and the shaded area is the low pressure feldspar stability field (< 5 kb) after Coleman and Peterman (1975). Symbols as in Fig. 4.

The sheared granites (samples T1/a, T1/d, T6/e, T2/g; analyses 53, 55, 59, 60) are high in Al_2O_3 and low in K_2O and have normative corundum. The remainder of the granite samples have high K_2O contents (> 5.8% wt.) and consequently have higher normative orthoclase contents. In these rocks the Na_2O/K_2O ratio is < 1 while in the trondhjemites this ratio is > 1.

On the total alkalis versus SiO_2 diagram (Fig. 5) the sheared granites plot in the high-alumina field and the rest occur in the alkaline field while the trondhjemites plot in the high-alumina field. The samples follow the calc-alkaline trend on the AFM diagram (Fig. 7). On the normative feldspar diagram (Fig. 12) all of the samples cluster in the granite field, except sample T1/d and T2/g which occur in the tonalite and trondhjemite fields respectively. All the samples plot around the granophyre field on a K_2O versus SiO_2 diagram (Fig. 13), except analysis T2/g that occurs in the continental trondhjemite field. This sample probably has a low K_2O content because it comes from close to the contact of the granite with a gabbro lens.

4.2.5 Dolerite dykes

Dolerite dykes probably represent the latest magmatic activity in the Fremstfjell area. Three samples were analysed and they show a range of 49-52% wt. SiO_2 (Table 5), they are enriched in Na_2O (Fig. 4, f) compared to low K_2O (Fig.4, g).

Table 5 : Geochemical analyses of the Dolerite Dyke

Analysis Number	63	64	65
Sample Number	N20	Md	N3
SiO_2	48.86	51.28	51.92
Al_2O_3	12.66	15.57	13.96
Fe_2O_3	5.98	5.50	5.13
FeO	4.44	2.81	4.00
MgO	11.10	9.04	9.97
CaO	11.48	9.33	9.68
Na_2O	2.21	4.50	3.16
K_2O	0.27	0.42	0.92
TiO_2	1.62	1.23	0.53
MnO	0.25	0.19	0.20
P_2O_5	0.34	0.22	0.19
Total	99.21	100.09	99.66
C.I.P.W. Norms Wt. %			
Q	1.01	-	-
Or	1.61	2.48	5.45
Ab	18.85	37.96	26.83
An	24.02	21.03	21.26
Ne	-	0.05	-
Di	24.34	18.51	20.20
Hy	17.54	-	15.62
Ol	-	9.75	1.72
Mt	8.74	6.11	7.47
Il	3.10	2.33	1.01
Ap	0.79	0.51	0.44
ppm			
V	249	188	184
Cr	279	11	27
Ni	57	6	8
Rb	n.d.	n.d.	33
Sr	2109	2223	1000
Y	23	16	16
Zr	109	88	105
Nb	10	5	8
Ba	96	146	504
La	29	10	11
Ce	63	28	23
Nd	39	15	12

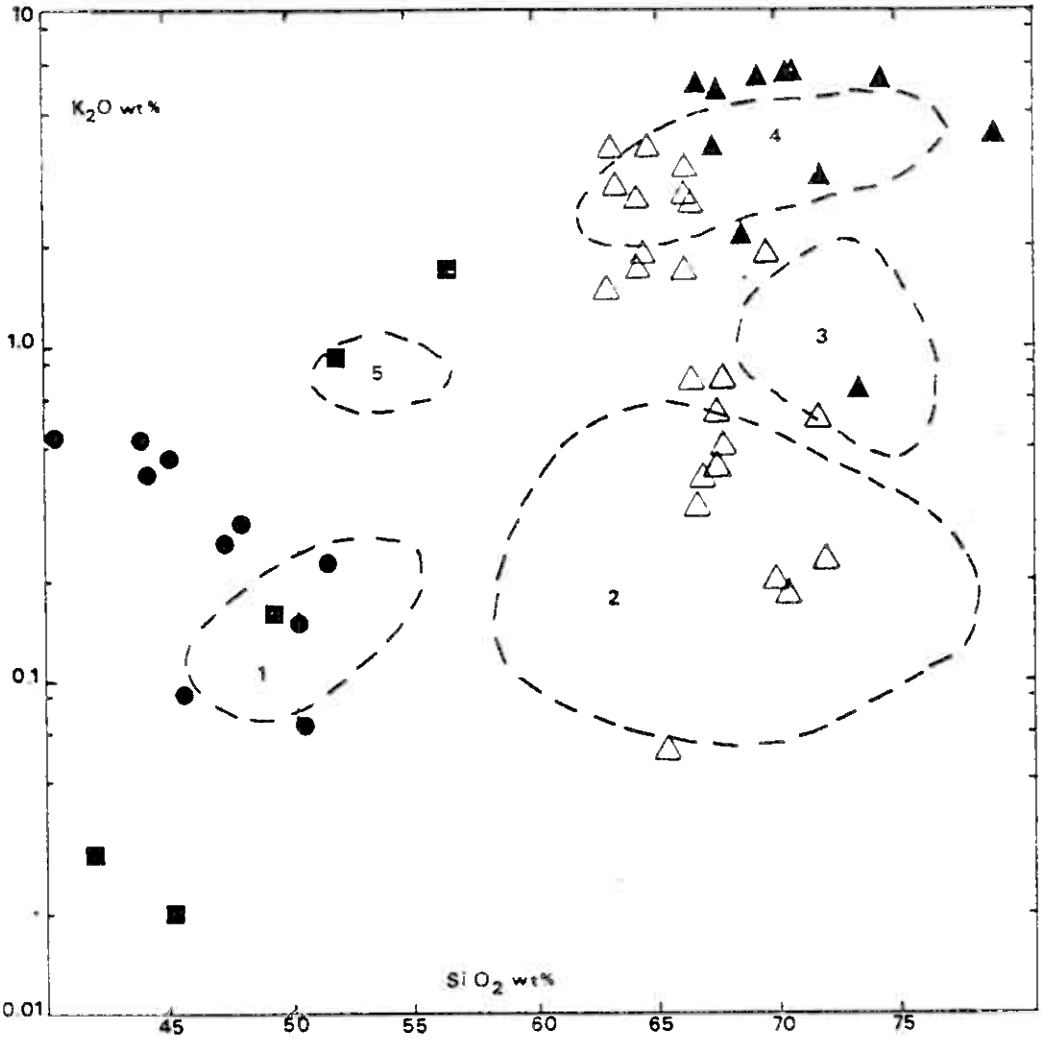

Fig. 13: K_2O versus SiO_2 diagram for basalt and basaltic andesite (solid squares), gabbro (solid circles), trondhjemite (open triangles) and granite (solid triangles).

Fields: 1) subalkaline oceanic gabbros and basalts, 2) oceanic plagiogranite, 3) continental trondhjemite, 4) continental granophyre, 5) continental tholeiitic basalts all from Coleman and Peterman (1975).

On a total alkalis versus SiO_2 diagram (Fig. 5) they plot in the high-alumina field and follow the calc-alkalic trend on the AFM diagram as well as on the SiO_2 against FeO^t/MgO diagram (Fig. 9). They follow the abyssal tholeiite trend on TiO_2 and FeO^t both versus FeO^t/MgO (Figs. 10, 11 respectively) However, the CIPW Norm shows that they range from just quartz tholeiite, through olivine tholeiite to just alkali olivine basalt, suggesting that they have an overall transitional basalt character.

4.3 Trace element geochemistry

4.3.1 Vanadium

The V content is high in the mafic rocks (basalt, basaltic andesite, gabbro and dolerite) and drops as silica increases (Tables 1-5). The V versus SiO_2 diagram (Fig. 14) tends to follow the trends of TiO_2 and FeO (as total iron) versus SiO_2 diagrams (Fig. 4, h,b). As V tends to be absorbed into magnetite this relationship may suggest a fractional crystallization effect, although there is no evidence of significant magnetite removal to deplete Vanadium.

Shervais (1982) investigated the Ti/V ratio from many modern volcanic rock associations that are diagnostic of tectonic environments. In the present work, this ratio (Ti/V) ranges between 10-26 for basalt and basaltic andesite which is comparable with island arc rocks. According to that ratio, the gabbros are tholeiitic to calc-alkaline. The dykes, ratio ($> 20 < 50$) strongly suggests they are calc-alkaline.

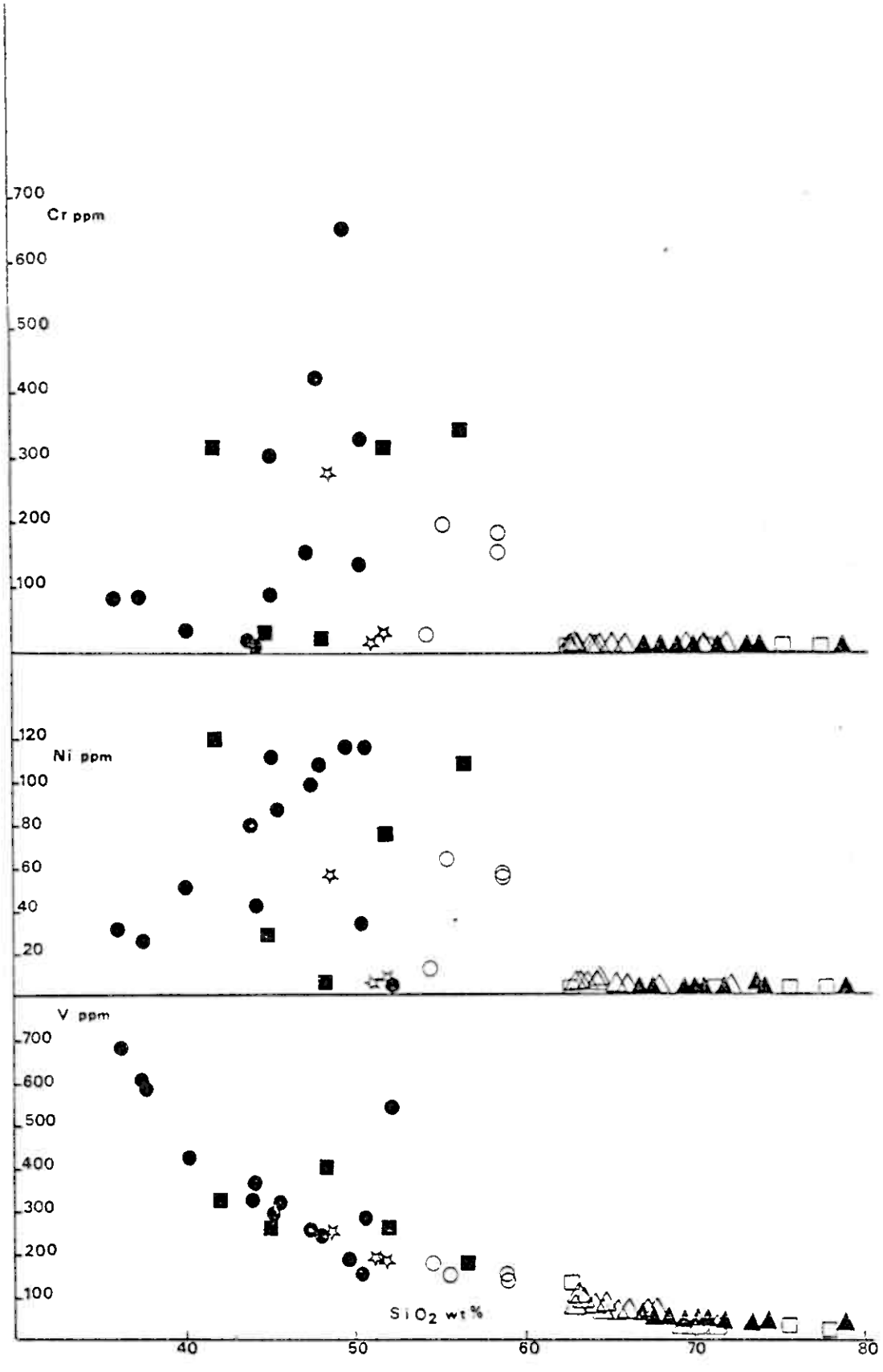

Fig. 14: Variation diagram of Cr, Ni and V versus SiO_2 for all analysed samples. Symbols as for Fig. 4.

Generally these rocks, with Ti/V ratios ranging between 10-50, overlap both the arc-tholeiite and MORB fields which provides evidence of their tholeiitic character and oceanic affinity.

4.3.2 Nickel and chromium

The transition metals Ni, Cr and V are relatively insensitive to secondary mobilization (Pearce, 1975; Shervais, 1982). Ni and Cr are compatible elements that are extracted into solidus phases during crystallization and retained in residual phases by partial melting.

The concentration of Ni and Cr in the analysed samples is generally low (Table 1-5). The two elements are strongly depleted in the trondhjemite, granite and rhyolite (Fig. 14). In the mafic rocks, the two elements are scattered and Ni increases with SiO_2 increase in the gabbro (Fig. 14). In the mafic rocks Cr varies between < 10-656 ppm and Ni varies between 2-120 ppm. The latter is comparable to the average Ni content both in island-arc tholeiites (30 ppm, Jakes and Gill, 1977) and MORB (110 ppm, Hart et al., 1972).

Becealuva et al. (1979) plotted the Ti/Cr ratio against Ni to discriminate between ocean floor basalts and low K-island arc tholeiites. In Fig. 15 the data show the transitional character between ocean floor basalts and low K-island arc tholeiites. Some samples plot outside the range of the diagram because they are depleted in both Ni and Cr, or one of them (Table 1-2).

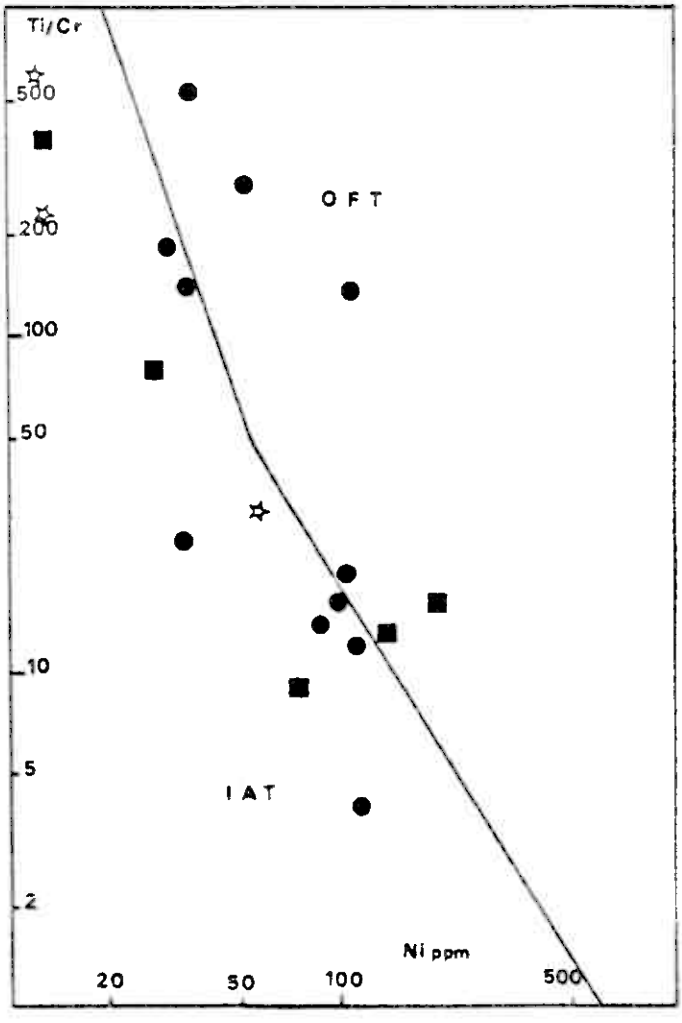

Fig. 15: Ti/Cr versus Ni diagram for mafic rocks. (Symbols as for Fig. 4). IAT (island arc tholeiite), OFT (ocean floor tholeiite). Fields after Beccaluva et al. (1979).

4.3.3 Rubidium

Rb and K are coherent lithophile elements that can substitute for each other and concentrate in magmas by fractional crystallization processes (Taylor, 1969). In the mafic rocks and rhyolites Rb is below the detection limit (Tables, 1,2,5). but it increases irregularly in the trondhjemites and granites relative to SiO_2 and K_2O (Fig. 16). Rb in the trondhjemite varies between 10-40 ppm and this range overlaps with the Rb range for the Follostad trondhjemite (Size, 1979). Granites have relatively high Rb values (30-80 ppm) compared to the trondhjemite. The depletion of these elements in these rocks could possibly be inherited from the magma source regions (Saunders et al., 1979) or perhaps due to the elements being highly mobile during the low grade metamorphism.

In most of the mafic rocks the K/Rb ratio is infinity except samples N15, 4/8/14, N3 (analyses 5, 20, 65) which possess K_2O (Tables 1,2,5). In the trondhjemites this ratio varies between < 1-3999. However, the low concentration of Rb in these rocks must throw some doubt on the precision of the high ratio. In the granite the K/Rb ratio varies between 600-1524. Thus the K/Rb ratios do not seem to confirm the behaviour of V which suggests the presence of fractionation trends.

4.3.4 Strontium

Sr is an alkaline earth element and like Rb and K it is often strongly affected by alteration and metamorphism. In general the analysed rocks are enriched in Strontium (Tables, 1-5).

Sr in the basalts and basaltic andesites ranges from 230 to 918 ppm. It is depleted in the rhyolites and granites with an inverse relationship to SiO_2 (Fig. 16). In the gabbros Sr values are scattered, decreasing with SiO_2 increase (from 222 to 1771 ppm). This also applies to the dykes and diorites. In the trondhjemite (Table 3 and Fig. 16) Sr is high with an inverse relationship to SiO_2. In the trondhjemites it is possibly accommodated in the epidote minerals and veins. In the mafic rocks the Sr values are higher than the average values of MORB (899 ppm compared with 120 ppm, Pearce, 1980). Elsewhere in the region the enrichment of Sr is said to be due to secondary alteration processes (Gustavson, 1978).

4.3.5 Zirconium

Zirconium is an incompatible element in igneous systems and it therefore tends to concentrate within the liquid fraction towards the pegmatitic stage of granite crystallisation (Smith, 1963). The mafic rocks have relatively low concentrations of zirconium (Fig. 16) varying between 9-109 ppm (Table 1-2).

The trondhjemites and rhyolites have higher values of Zr (98-248 ppm, Table 2,3), rather more than the granite (71-158 ppm). Over the range of granitic rocks Zr has an inverse relationship with SiO_2 (Fig. 16). It is possible that zircon fractionation is responsible for this pattern. Zr is immobile with respect to weathering and metamorphism and so it is used with Ti and Y in variety of discriminant diagrams

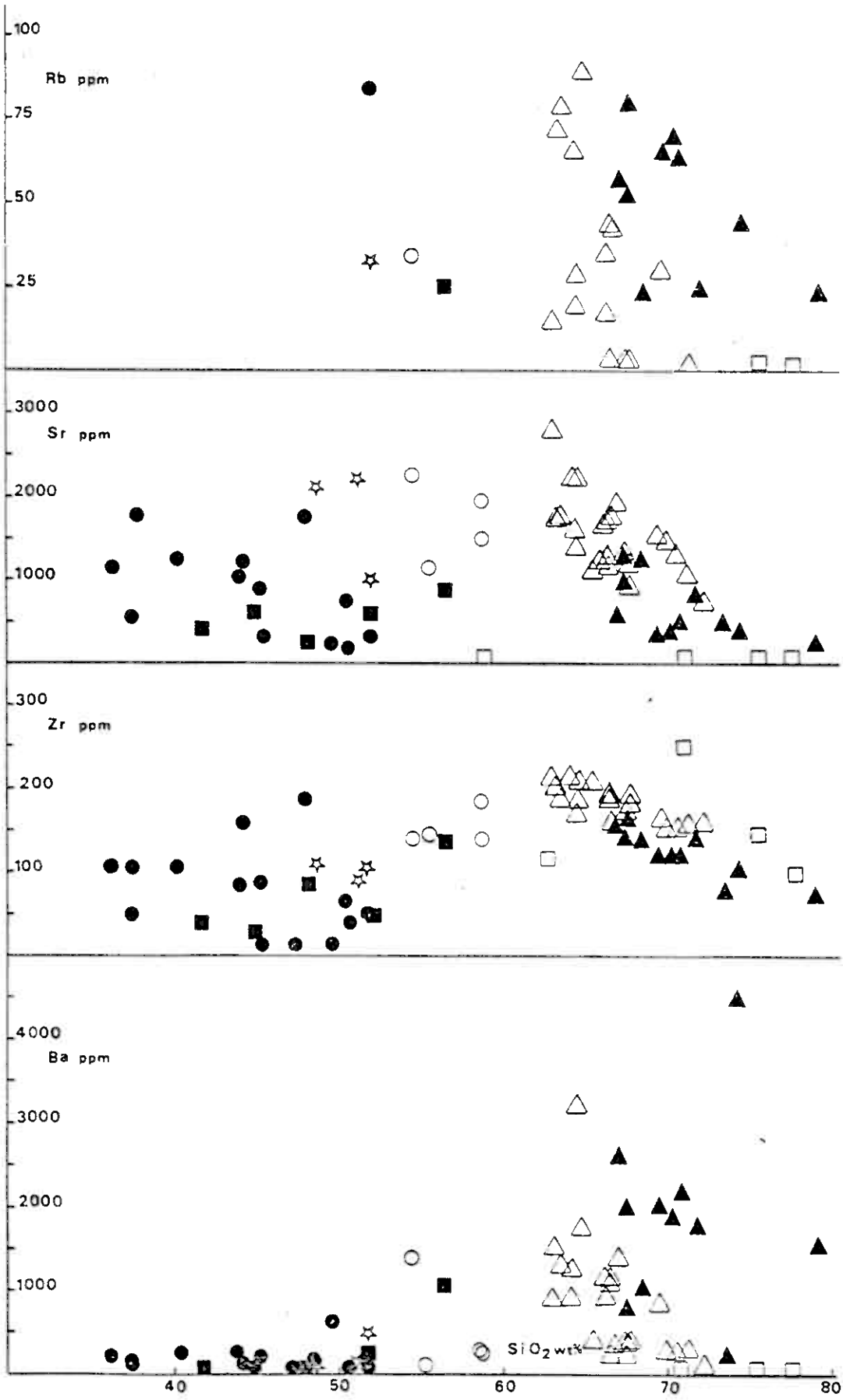

Fig. 16: Variation diagram of Rb, Sr, Zr and Ba for all analysed samples. Symbols as for Fig. 4.

to demonstrate igneous processes and relationships (Pearce and Cann, 1971, 1973; Pearce, 1980, 1982). In the TiO_2 versus Zr and Zr/Y versus Zr diagrams (Figs. 17, 18) respectively) the mafic rocks clearly show transitional characteristics between low-K arc tholeiites and mid-ocean ridge basalts (MORB). This conclusion is comparable to the results of Gale and Roberts (1974) and Gale and Pearce (1982).

4.3.6 Barium

Barium is a large ion lithophile element which concentrates in biotite and potash feldspar replacing K (Mason, 1966) and which is sensitive to alteration and metamorphism (Philpotts et al., 1969). Ba is generally low in the mafic rocks and rhyolites (Fig. 16). The trondhjemites and granites are relatively enriched in this element. The K/Ba ratio varies between < 20-50 for most of the mafic rocks which may suggest that they are low-K arc tholeiites (Hart et al., 1972).

4.3.7 Rare earth elements (R.E.E.)

La, Ce, Nd and Y are a member of a coherent group of elements known as R.E.E. (Y is not a R.E.E. but chemically proxies for a heavy member ∿ Ho, Er) which resist low-grade metamorphism (Ferrara et al., 1976). The R.E.E. may be accommodated in Ca-bearing minerals such as apatite or allanite (for example the allanite with low major oxide totals, described in Chapter 3 and Appendix 2 probably has a high R.E.E.

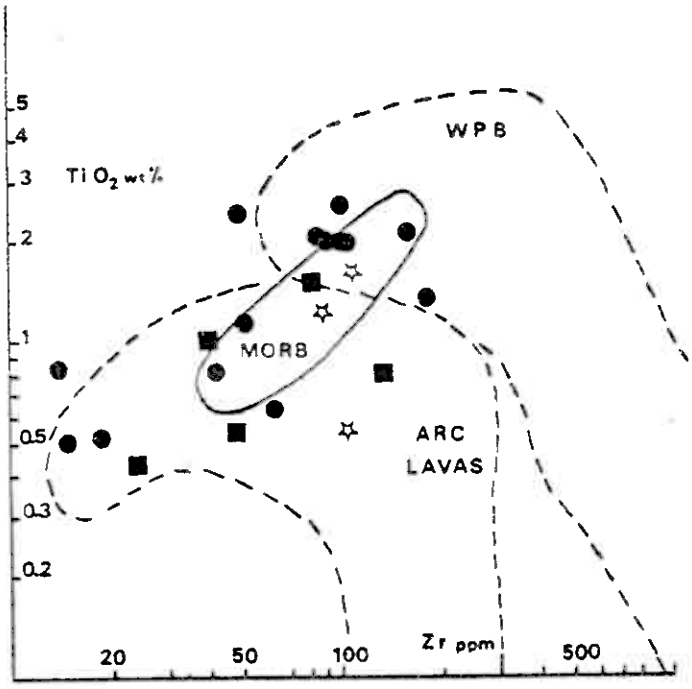

Fig. 17: Diagram of TiO_2 versus Zr for the mafic rocks. (Symbols as for Fig. 4). ARC LAVAS (island arc tholeiitic basalt), MORB (mid-ocean ridge basalt), WPB (within plate basalt). Fields from Pearce (1980, 1982).

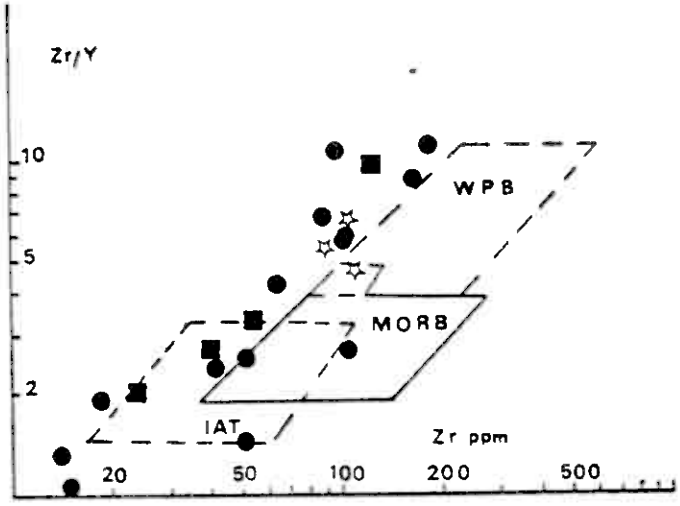

Fig. 18: Zr/Y versus Zr diagram for the mafic rocks. (Symbols as in Fig. 4). IAT (island arc tholeiite), MORB (mid-ocean ridge basalt), WPB (within plate basalt). Fields from Pearce (1980, 1982).

content) and the rhyolites are relatively enriched in Y (Fig. 19).

The abundances of these elements are presented in Tables 1 to 5 and they are plotted against SiO_2 (Fig. 19). La and Ce abundances in the trondhjemites and granites are relatively high with an inverse relation to SiO_2 which may reflect allanite fractionation, while Nd and Y show almost flat, low patterns (Fig. 19).

In Fig. 20 and 21 La, Ce, Nd and Y concentrations of averages of samples of diorite, trondhjemite, granite and rhyolite have been normalized against those of the average carbonaceous chondrite (data after Nakamura, 1974). There is clearly a marked increase in total R.E.E. content from basalt, basaltic andesite to granite. In Fig. 20 the trondhjemites and granites show similar patterns which may suggest that they are derived from similar source regions or it may be a function of the contamination of the trondhjemite by the granite complex. Probably for this reason the trondhjemites described here have higher R.E.E. concentrations compared to trondhjemites from other regions (Barker and Millard, 1979). In the diorites the concentration of R.E.E. is the highest.

4.3.8 Niobium

Niobium seems not to form any silicate phase because it occurs in the form of pentavalent ions. It has been established that minerals which contain essential titanium or which accept some titanium in their structure, will also accept

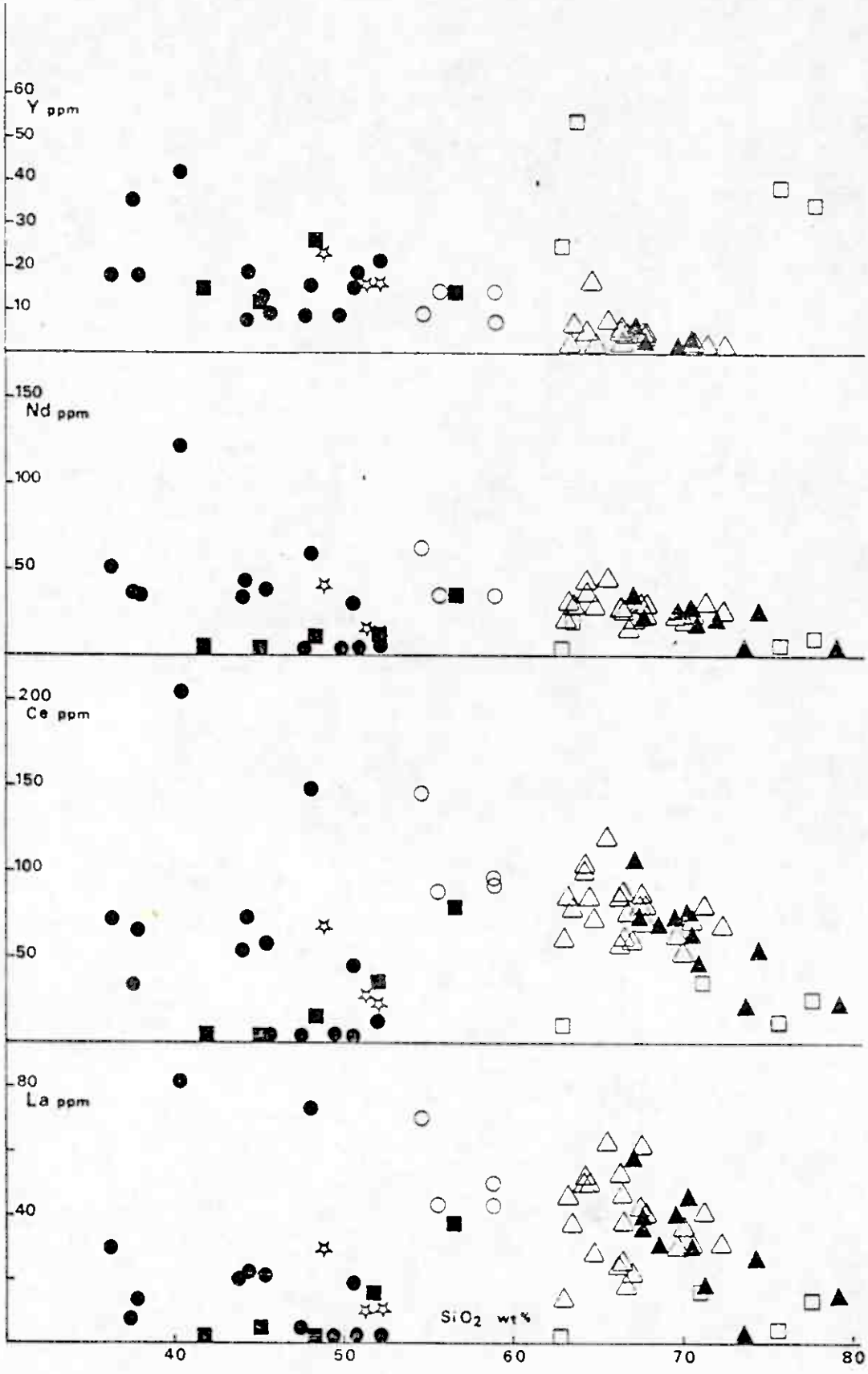

Fig. 19: Variation diagram of Y, Nd, Ce and La versus SiO_2 for all analysed samples. (Symbols as in Fig. 4).

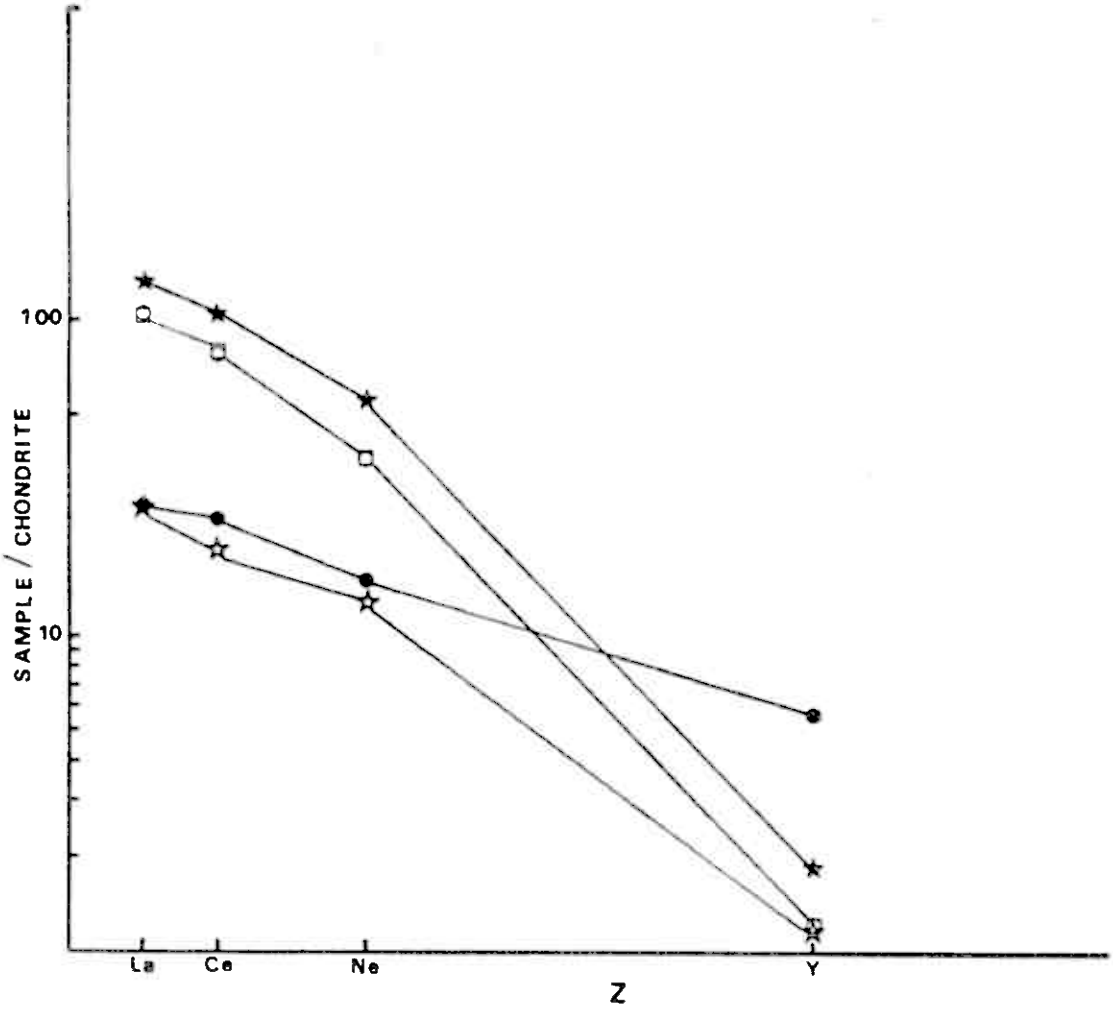

Fig. 20: Average chondrite-normalized R.E.E. plot for diorite (solid stars), trondhjemite (open circles), granite (open squares), rhyolite (solid circles), and trondhjemites described by Barker and Milland (1979)(open stars). Average chondrite values from Nakamura (1974).

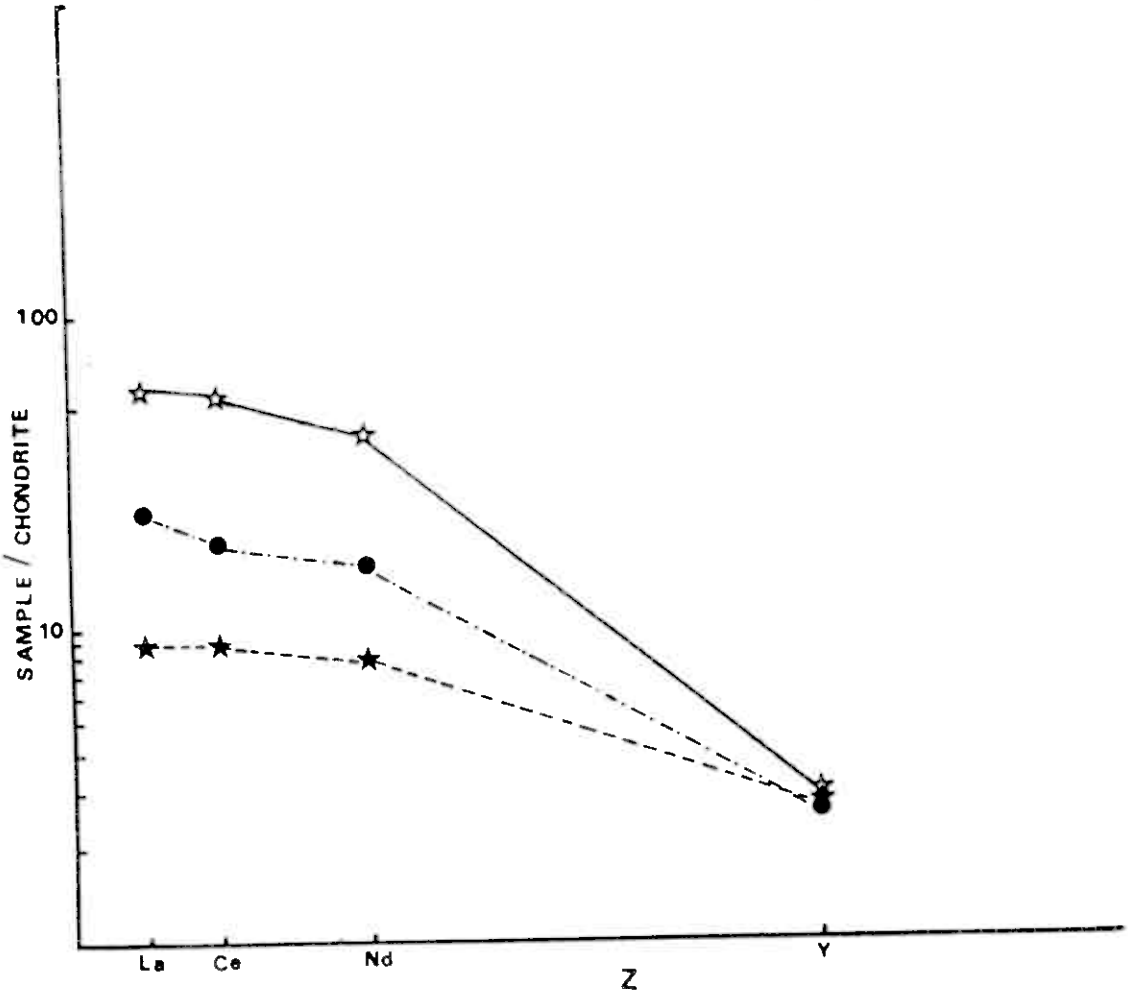

Fig. 21: Average chondrite-normalized R.E.E. plot for dolerite (open stars), gabbro (solid circles) and basalt and basaltic andesite (solid stars). Average chondrite values from Nakamura (1974).

niobium. Otherwise it concentrates in residual liquids, during crystal fractionation (Day, 1963).

It is generally low in all rock units in the present area (< 20 ppm, Tables 1-5). Because of its immobility in igneous systems niobium is used in discrimination diagrams with other immobile elements (Zr, Y, Ti, Pearce and Cann, 1973). It has been used with silica to deduce the environment of acid-intermediate intrusive rocks (Pearce and Gale, 1977). Fig. 22 shows that all of the analysed rocks plot in the field of volcanic arc magmas which is further evidence to suggest that these rocks were generated in an island-arc environment.

4.3.9 MORB normalized element abundances

For further comparison some minor and trace elements in the basalts, basaltic andesites, gabbros and dolerites have been normalized against a typical MORB composition (Pearce, 1980; Fig. 23). The rocks are low in K, Rb and Zr and high in Sr and Ba. The first three could possibly be inherited from the magma source (Saunders et al., 1979) and Sr and Ba may perhaps have been concentrated by alteration and metamorphism. The rocks show a transitional character between tholeiite and calc-alkaline affinities that is demonstrated clearly in their major element chemistry (section 4.2). This conclusion compares with the results of Gale and Pearce (1982) who stated that the Grong rocks are island-arc tholeiites that have calc-alkaline characteristics.

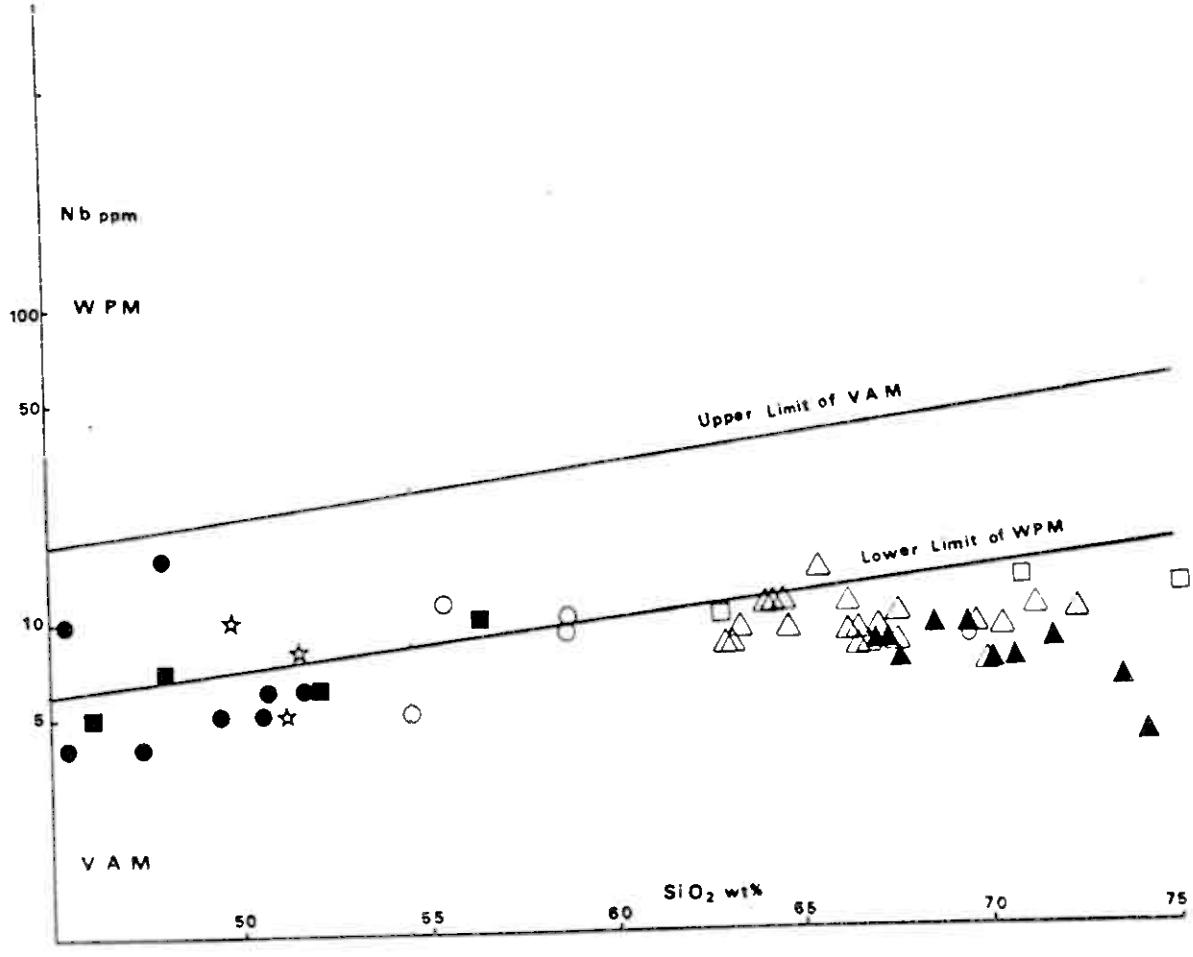

Fig. 22: Variation diagram of Nb versus SiO_2 for all analysed samples (Symbols as in Fig. 4). Field boundaries after Pearce and Gale (1977). WPM - Within plate magma; VAM - Volcanic arc magma.

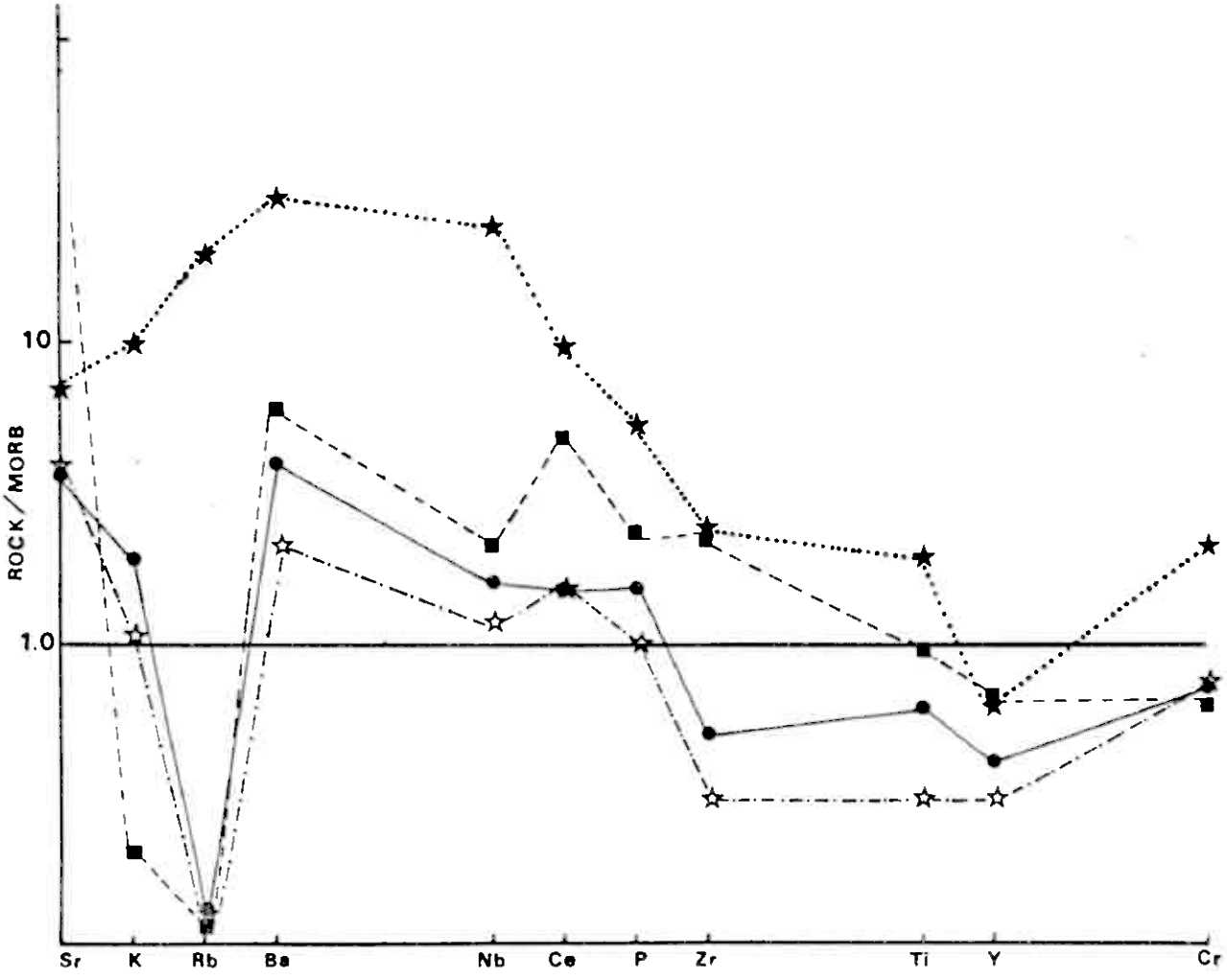

Fig. 23: Geochemical patterns for basalts and basaltic andesites (solid squares), dolerites (solid circles), gabbros (open stars) normalized against a typical MORB composition (after Pearce, 1980) and compared to a typical alkali basalt (solid star) (from Gale and Pearce, 1982).

CHAPTER 5

Mineralization

5.1 Introduction

Molybdenite (MoS_2) is the naturally occurring disulphide of molybdenum, an element which does not exist as a native metal (Read, 1970). Molybdenite was discovered two hundred years ago by Carl Wilhexim Scheele and the metal was extracted by Peter Jacob Hjelm (Sutulov, 1975). Molybdenum is an incompatible element with respect to the major rock-forming minerals and tends to concentrate in residual phases of magmatic systems (Krauskopf, 1979). Molybdenum deposits occur throughout the world, mainly in granitoid rocks ranging in age from Precambrian to late Tertiary (Vokes, 1978).

In the Fremstfjell area (the field area) the molybdenum occurrence was discovered by G. Gale in 1973/74 who was following regional geochemical anomalies determined from stream sediments (Gale, unpublished report, 1975). Gale (op. cit.) found very weak shows of molybdenum-copper mineralization close to Smalltjern (Map 2). Very limited local blasting was carried out by Grong Gruber in 1975, traces of which have now almost been destroyed by frost and vegetation. In 1979 Vokes (University of Trondheim) and Haugen (Grong Gruber) reported the possibility of porphyry-type mineralization (Grong Gruber, unpublished report). In 1980 detailed reconnaissance and sampling, including blasting six trenches was carried out by M. Ryan and M. Holman (Portsmouth Polytechnic). Further mapping of the area and the examination of the cores from nine boreholes, in which the present author and M. Ryan participated with a group of students from Portsmouth

Polytechnic, was done in 1981 and 1982 and a further deep borehole was drilled in 1984. The results of the latter are unavailable at the time of writing.

Norway was the world's first molybdenum producer and mining operations started at the end of the 18th century at the Knaben mine, which was recently closed down (Vokes, 1978). Knaben is situated in Precambrian granitic gneisses in southern Norway. As well as Knaben, molybdenum is also known in northern Norway in the Bodø area (Vokes, op. cit.) and it occurs in Permian rocks of the Oslo Graben where it is hosted by multistage intrusions of biotite granite (Olerud and Sandstad, 1983).

5.2 Geochemistry and mineralogy of molybdenum

Molybdenum is considered to have siderophile and chalcophile affinities in terms of its distribution in meteoritic minerals (Sutulov, 1975). It is generally uniformally distributed among igneous rocks because of its ability to replace a number of elements (Table 6 see next page) (Al^{+3}, Fe^{+3} and Ti^{+4}). Thus it is found in the lattice of feldspar, biotite, amphibole, pyroxene, magnetite and ilmenite but it does not closely follow any single major constituent (Kuroda and Sandell, 1954). Its concentration increases from ultrabasic through to acid rocks and reaches a maximum in the alkaline rocks where it concentrates in the last differentiates by crystal fractionation (Smith, 1963).

Table 6: Valence and Ionic Radius

(after Kuroda and Sandell, 1954)

element and valence	ionic radii in Å
Mo (+4, +6)	0.68, 0.65
W (+4, +6)	0.68, 0.65
Re (+4, +6)	0.72, 0.52
Al	0.75
Fe (+3)	0.67
Ti (+4)	0.64
Ge (+4)	0.52
Se (+4)	0.50

Molybdenum is highly mobile in oxidizing and alkaline environments and can migrate together with V but it is less mobile in acid conditions and may be precipitated (the reverse of the behaviour of Cu). Molybdenite weathers to give ferrimolybdite ($Fe_2O_3.3MoO_3.8H_2O$) or powellite ($Ca(Mo, W)O_4$) (if W is available) in soils (Rose et al., 1979). Biochemically Mo is essential in fixing atmospheric nitrogen by reducing nitrites and nitrates but excess Mo in forage is extremely toxic to livestock (Rose et al. op. cit.).

Re^{+4} and W^{+4} are the only two ions that totally satisfy the geometric conditions and electrical charges to substitute Mo^{+4} in molybdenite. However, the very high affinity of W^{+4} for oxygen tends to exclude it from sulphides and so only rhenium is present as a foreign element in molybdenite (Sutulov, 1975).

Mineralogically, molybdenum occurs in a number of species (molybdenite, ferrimolybdite and wulfenite) but molybdenite is the only commercial source of the metal (Sutulov, op. cit.). Molybdenite (MoS_2) is mainly Mo and S with traces of Re, Ge and Se. Molybdic acid forms salts (molybdates) that replace W in tungstates and, to a lesser extent, V in vanadates (Sutulov, op. cit.). Ferrimolybdite is the hydrated iron molybdate and wulfenite is lead molybdate ($Pb\ Mo\ O_4$). Wulfenite is formed in the oxidized zone of lead- and molybdenum bearing deposits (Read, 1970).

5.3 Types of molybdenum deposits

It is widely recognised that molybdenum is concentrated by hydrothermal systems associated with crystallizing magma to form stockwork and porphyry molybdenum deposits, very often with recoverable copper (Ganster, 1976; Wallace et al., 1978). Molybdenum deposits have been classified into many types depending on the ore geometry and their mode of occurrence in the host rocks, the often concentric patterns of alteration produced in the host rocks, their chemistry and their tectonic setting (Lowell and Guilbert, 1970).

Based on the goetectonic setting of molybdenum deposits, Sillitoe (1980) subdivided them into two categories - subduction-related deposits associated with quartz monzonite and rift-related deposits associated with alkali granite. On the basis of the geochemistry of the host plutons Mutschler et al. (1981) distinguished two types of molybdenum deposits,

those associated with granodiorite and those associated with true granite.

Westra and Keith (1981) classify stockwork molybdenum deposits according to magma series chemistry using the five magma series: i) calcic, ii) calc-alkaline, iii) high K calc-alkaline, iv) alkali-calcic, and v) alkalic. They distinguish two categories of deposit:

a) calc-alkaline molybdenum stockwork deposits associated with calc-alkaline and high K calc-alkaline magmas. These are characterized by having low F, < 20 ppm Nb, 100-800 Sr, 100-350 Rb, TiO_2 > 0.2% wt. Tin is absent but tungsten is possibly present. They are associated with volcano-plutonic arcs in plate collision zones.

b) alkali-calcic/alkalic deposits associated with alkali-calcic and alkalic magmas. These show strong F enrichment with fluorite and/or topaz, 25-250 ppm Nb, < 125 ppm Sr, 200-800 Rb. Enrichment in tin and tungsten is commonly present. They occur in a variety of tectono-magmatic settings: the Climax-type in areas of crustal relaxation and extension above the deepest parts of subduction zones; in back-arc spreading sites; intracratonic rifts and rifts associated with the opening of oceans.

The Fremstfjell data conform more or less to type (a) above. No fluorite or topaz have been seen in the field or under the microscope. Nb contents lie in the range 4-16 ppm. Rb values are all less than 90 ppm. TiO_2% averages 0.3% for

the trondhjemite and granite (Tables 3,4) and Sr averages 1198 ppm for the same rocks (see Chapter 4). No tin or tungsten minerals have been found. The low Rb and high Sr values are more typical of porphyry copper deposits (see Westra and Keith, 1981, Figure 7) and a continuum exists between calc-alkaline stockwork molybdenum deposits and porphyry copper.

5.4 Mineralization at Fremstfjell

5.4.1 Introduction

Mineralization occurs in an area of c. 600 x 400 m^2 and to a depth of c. 250 m, north of the contact between the Caledonides and the basement rocks (Fig. 24). Granite (section 3.4.4) is the main host rock for molybdenite but it may be found rarely in other rocks in the form of fine disseminations. The prominent marker for molybdenite mineralization is a vivid brown staining due to the widespread associated pyrite. The staining is not recognisable from any distance but is clearly discernible at close range (a few metres). It is not easy to define the metal zoning but pyritization picks out a pyrite halo enclosing the mineralized area around an intermediate zone of pyrite (Py) - molybdenite (Mb) with very little chalcopyrite (Cp), bornite (Bo) and magnetite (Mt) and an inner zone with pyrite, molybdenite, chalcopyrite and rare bornite (Fig. 24, Map 2).

The association of pyrite, molybdenite and chalcopyrite occurring in veins, veinlets or as disseminations with minor magnetite, bornite and traces of lead, zinc and silver is

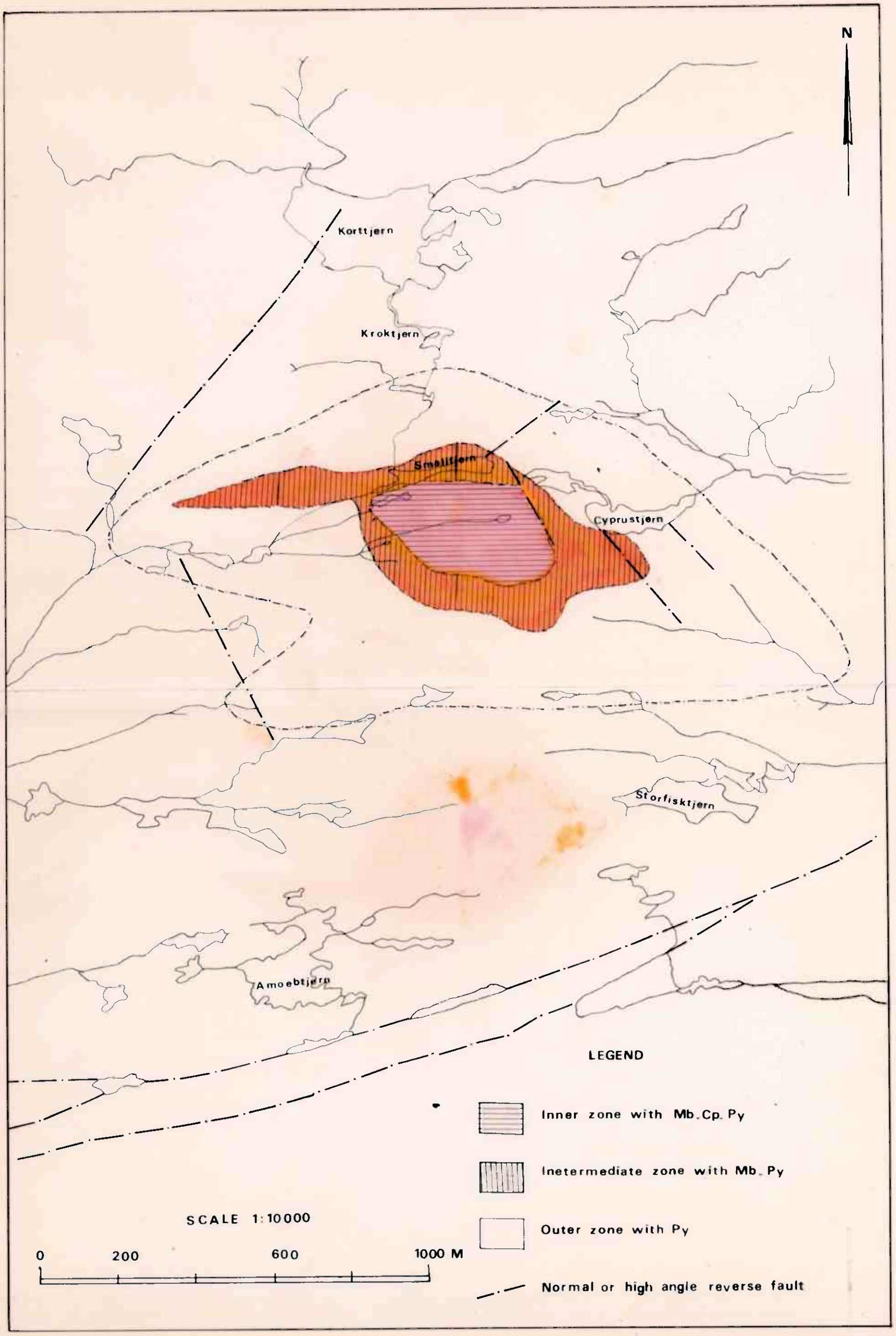

Fig.24 Mineral zoning in Fremstfjell Area

very similar to the mineralogy of the porphyry deposits described by Craig and Vaughan (1981).

5.4.2 Molybdenite

Molybdenite is encountered in the granite around Fremstfjell in the area that extends from south of borehole 3 (B.H.3) to B.H.1 (map 1). Generally, the granite here is potassium rich (Chapter 3, 4). The mineralization occurs in the following forms:

i) in veins that run parallel to or along the pervasive cleavage (plate 25) associated with quartz + pyrite ± chalcopyrite.

ii) microcrystalline/cryptocrystalline molybdenite indicated by a blue-grey coloration in quartz.

iii) isolated individual flakes or clots disseminated through the rocks, generally < 0.5 mm but occasionally 1-2 mm across (plate 26 , trench 1 and drill core B.H.6 (section 5.5).

iv) 'dry paint' (a thin oxidised blue-grey film) on joint and cleavage surfaces, well seen between B.H.5 and B.H.2 (map 1, plate 27).

v) cross cutting stockwork veins south of Smalltjern (plate 28).

vi) 'crackle-breccia' (spaced angular rock fragments in a quartz matrix), which is less frequent but seen in drill cores especially at the top of B.H.2 and at 68.49 m in the same borehole.

Plate (25): Quartz molybdenite ± pyrite veins mostly parallel with foliation in granite, trench 1.

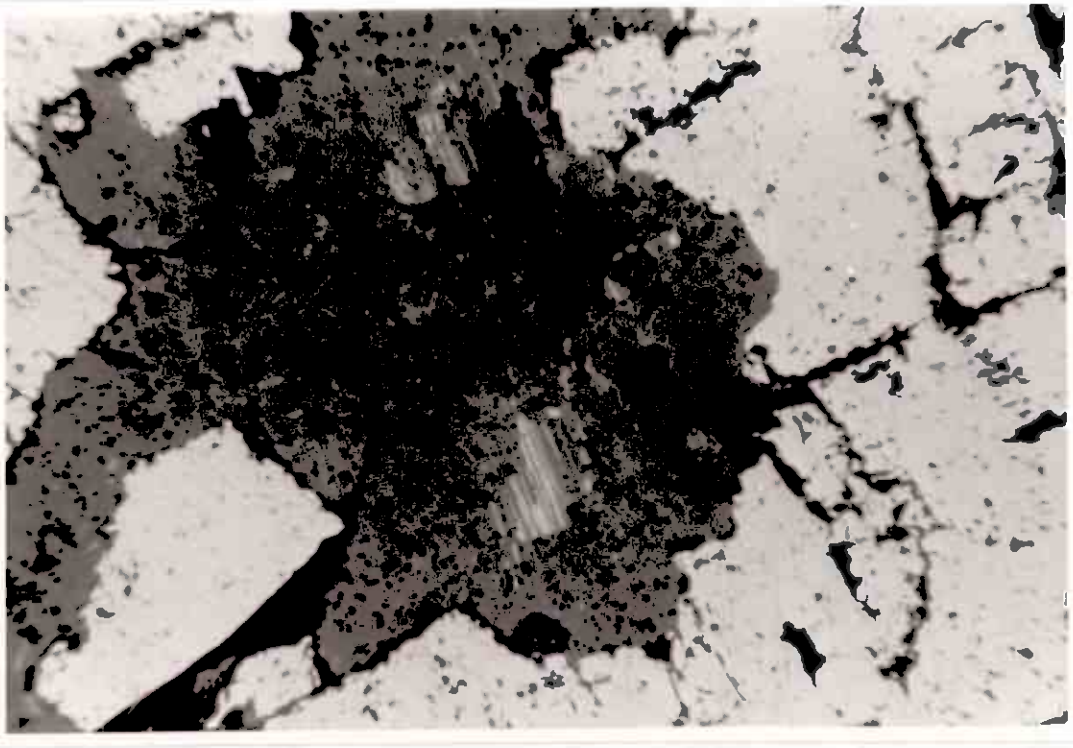

Plate (26): Isolated flakes of molybdenite (elongated white flakes) in quartz (dark-grey) surrounded by pyrite (white), reflected light, x 400. B.H. 5-24.

There seems to be more than one generation of molybdenite and this can be demonstrated clearly in the field in the area between trench 4 and Smalltjern (map 1). The molybdenite veins cut and displace ones with pyrite or vice-versa (plate 29). The general trends of the veins containing molybdenite are:

i) an oldest trend of 090° which is parallel with the cleavage; veins contain quartz + Mb + Py.

ii) an intermediate trend of 170°, containing quartz + Mb.

iii) the youngest trend of 040°, containing quartz + pyrite only. This may strengthen the suggestion in section 3.6 that there is more than one phase of deformation.

5.4.3 Copper minerals

The patchy and irregular appearance of copper minerals may possibly relate to the irregular occurrence of greenstone xenoliths and rafts within the trondhjemite/granite complex. Chalcopyrite dominates over rare bornite. Chalcopyrite occurs as anhedral interstitial grains up to 1 cm across around Smalltjern (map 2), often in association with epidote. It also occurs as fracture filling in pyrite in small veins of varied size. Massive veins of chalcopyrite, several centimetres wide, occur to the southeast of Amoebtjern (map 2) associated with secondary copper minerals and pyrite. Traces of Ag, Pb and Zn are associated with the Amoebtjern ore (analysis from Joma mine, 1981, pers. comm.).

Plate (27): Richly mineralized trench sample showing thick molybdenite smear (dry paint), trench 2.

Plate (28): Stockwork of quartz-molybdenite veins in schistose, highly sericitized granite with weak malachite, south of Smalltjern.

Bornite occurs from the top down to 29 m in B.H.5 (map 1). This could possibly be due to partial oxidation near surface effects or, more probably, it could be primary sulphide defining the centre of the mineralized area. Bornite is also observed west of Kroktjern, associated with magnetite and pyrite in a gabbroic block. Traces of malachite are widespread on the outcrop surfaces and along joints and cleavages well exposed in the trenches. Azurite is a common mineral in the Amoebtjern locality.

5.4.4 Pyrite and magnetite

Pyrite is ubiquitous in the whole area and this can be seen clearly from the induced polarization survey carried out by N.G.U. in 1980 (N.G.U. unpublished map, 1981). Its distribution is not governed by particular lithologies but the greenstones are slightly enriched in pyrite. Pyrite occurs as veins or veinlets of various sizes (0.5-5 cm) and as cubes with rough surfaces that are up to 5 cm across in a gabbro block west of Korttjern (map 1). There is clearly more than one generation of pyrite because sometimes pyrite-bearing veins are displaced by quartz-molybdenite veins, or they may displace the latter (plate 29). Pyrite also sometimes encloses molybdenite and chalcopyrite.

Magnetite is a common accessory mineral throughout (Chapter 3). It occurs as dispersed grains but it is rarely found in veins associated with pyrite. West of Kroktjern (map 1) magnetite occurs as massive veins in a gabbroic block associated with pyrite and bornite.

Plate (29): Quartz-molybdenite vein (grey) displaced sinistrally by pyrite-quartz veins (black). B.H.4-6. x 6.

5.5 Boreholes description

5.5.1 Introduction

Nine boreholes were drilled in the Fremstfjell occurrence by Grong Gruber in 1981 (map 1), totalling 1500 m of core. The I.P. survey that was carried out in 1980 showed that the mineralization dips to the north in the same direction as the dominant structures of the country rocks. All of the holes were drilled at an angle 58.5° to the south so as to intersect the northward dipping cleavage at a high angle.

5.5.2 Borehole 1

This hole, 99.4 m deep, is inclined towards Smalltjern near the northwestern boundary between the granite and trondhjemite. Trondhjemite is the dominant lithology in the hole and it changes gradationally into granite. The top 10 metres show molybdenite in the form of dry paint and disseminations in quartz veins and throughout the rest of the drill core mineralization is rare. Propylitic alteration (chlorite, epidote, carbonate and clay minerals) is seen between 39 m - 43 m.

5.5.3 Borehole 2

This hole is 100 m deep. The top 30 metres consist of granite containing pyrite + moly + chalcopyrite in the form of veins, disseminations and a stockwork or crackle breccia, especially between 8.6-9.5 and 20-26 m deep. The rest of the core is mainly greenstone with pyrite, molybdenite shows and rare chalcopyrite with intercalations of gabbro, granite, trondhjemite and occasional dolerite dykes. Pyrite predominates over the other ores while molybdenite decreases from top to

bottom. At the top K-feldspar is common with quartz but in the rest chlorite and epidote are dominant with patches of clay minerals.

5.5.4 Borehole 3

This 149.5 m hole, shows mainly 3 lithologies: granite, trondhjemite and greenstone. The top 10 m of the hole are made up of greenstone which also appears as lenses throughout the hole. The granite extends down to 112.5 m (Fig. 25) and contains lenses of trondhjemite and greenstone as well as shows of molybdenite. Between 10 and 40 m the molybdenite is rare, from 57 to 84 m the molybdenite concentrations are higher and below 84 m the hole is barren of molybdenite mineralization. From 112.5-149.5 m the core is trondhjemite with lenses of greenstone. Both the trondhjemite and greenstone are pyritized with a very weak dissemination of molybdenite.

5.5.5 Borehole 4

This 205 m deep hole contains granite and greenstone. The first 124 m (Fig. 25) are granite with minor greenstone rafts. In this section the intensity of molybdenite mineralization varies from moderate to high (the number of veins per metre) with associated pyrite. From 124-185.5 m greenstone predominates with granite veining. The greenstone is frequently mineralized by pyrite with less frequent chalcopyrite and little or no molybdenite. The rest of the hole comprises granite with molybdenite shows.

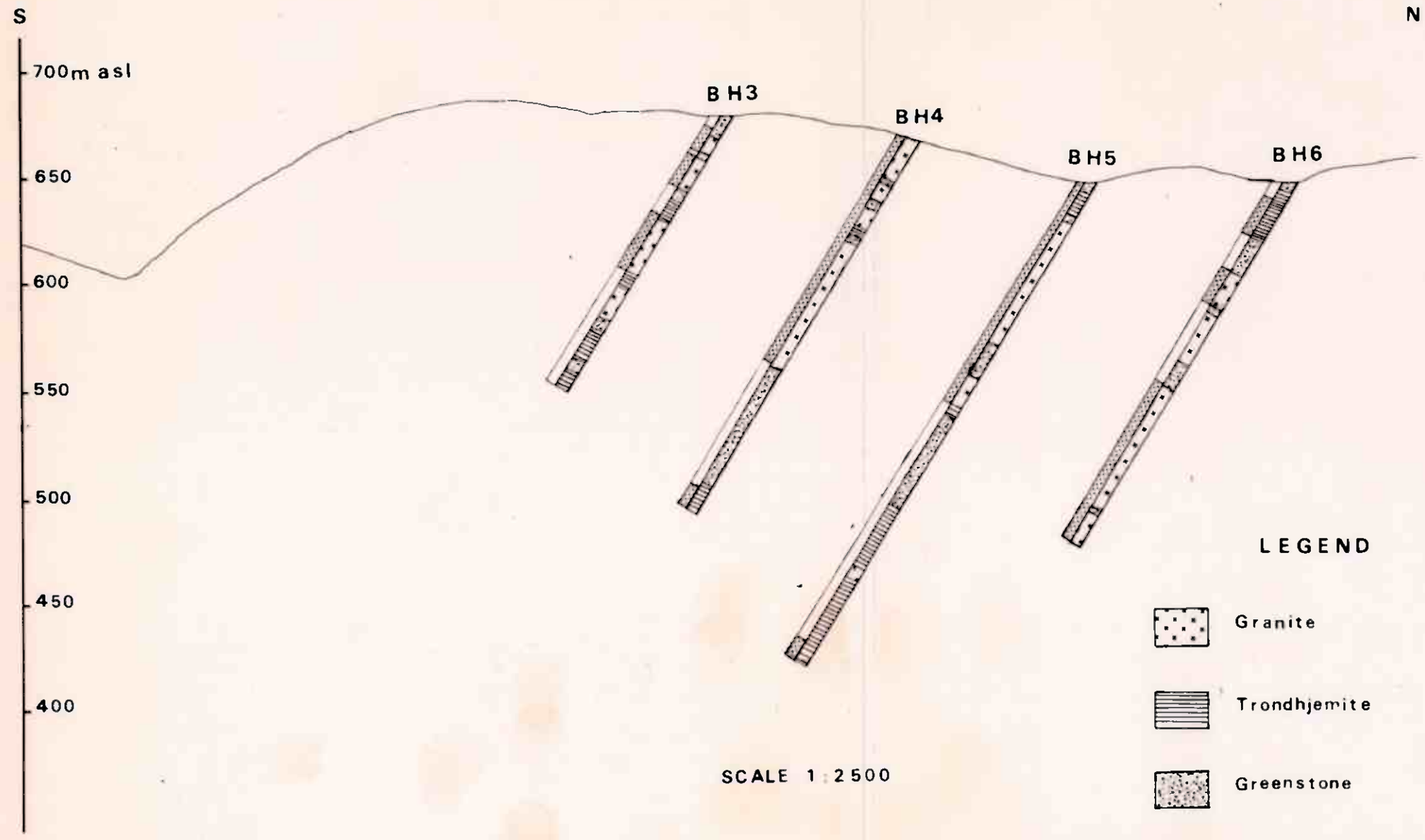

Fig Section from B.H.3 to B.H.6

5.5.6 Borehole 5

This hole attained a depth of 267 m. The top 5 m is through a greenstone lens which passes into trondhjemite, grading into granite which continues down to 150 m, with minor greenstone rafts and grading into trondhjemite from time to time (Fig. 25). From 150-190 m the rock is mainly greenstone and the remainder of the core is trondhjemite with minor greenstone and granite.

The hole contains bornite in the top 10 m and weak molybdenite shows in the greenstone and trondhjemite. The intensity of molybdenite mineralization increases in the granite in association with chalcopyrite. From 20 to 33 m there is propylitic alteration with fracturing and brecciation produced by ENE/WSW trending shear zones mapped on the surface.

5.5.7 Borehole 6

This is similar to borehole 5 in its lithologies but granite tends to be the dominant component. The core begins with a greenstone lens, passes into trondhjemite and a second greenstone and then has granite down to 200 m, the depth of the hole, with greenstone and trondhjemite rafts (Fig. 25). Molybdenite mineralization occurs through the first 197 m with variable intensity. Between 50-70 m and 130-170 the core is rich in molybdenite mineralization in a stockwork of quartz-molybdenite veins (plate 30) with associated pyrite and chalcopyrite.

Plate (30): Richly mineralized core from B.H.6, 164-170 m.

5.5.8 Borehole 7

The hole starts with greenstone (up to 5 m) and then passes into trondhjemite down to a depth of 62 m with interfingering of granite that demonstrates the nature of the contact (see map 1). Then a greenstone raft is followed by trondhjemite grading into granite, continuing to 140 m with intercalations of greenstone. The hole ends at 148 m in trondhjemite. Weak molybdenite mineralization is frequent but its intensity increases between 80-140 m depth in the granite. Pyrite common throughout and chalcopyrite less frequent.

5.5.9 Borehole 8

Greenstone interbanded with granite forms the bulk of the hole extending down to 120 m. From 120-150 m the core is mainly trondhjemite. Mineralization comprises pyrite-chalcopyrite in the greenstone with weak molybdenite in the granite bands. These rocks are altered, with chlorite, epidote and in some places clay minerals (suggesting propylitic and argillic associations).

5.5.10 Borehole 9

The 150 m of this hole are dominated by greenstone with bands of trondhjemite occurring at 50 m grading into bands of granite extending to 68 m. Pyrite is the main ore mineral in the greenstone with associated chalcopyrite and rare dry paint molybdenite along the joints. The borehole shows chlorite, epidote and clay minerals with occasional carbonate.

5.6 Alteration

Hydrothermal alteration may readjust the primary mineralogy and chemistry of a porphyry deposit host rock and this may take place during or after the ore mineralization (Westra and Keith, 1981). This activity can produce concentric zones of alteration such as those described by Lowell and Guilbert (1970) (inner potassic zone, phyllic zone, argillic zone, outer propyllitic zone), patterns similar to which have been reported in the Fremstfjell area by Vokes (1979) and which were broadly encountered during the current mapping.

The inner zone in the Fremstfjell occurrence (map 2) is potassium rich and coincides with the mineralised zone in which molybdenite-bearing veins occur more or less exclusively. Granite is the dominant rock type with minor lenses of trondhjemite, gabbro and greenstone (map 1 and section 3.4.4). In the granite, perthite is the dominant alkali feldspar, with albite and rare orthoclase (see section 3.4.4.1 and T.S. 6/30, T5/c, T1/a, appendix 1). Chemically, these rocks possess > 5.8% wt. K_2O and their norms show Ab+Or+Q > 80%. They are peraluminous (molecular Al_2O_3 > molecular Na_2O+K_2O, see table 4) and they are granites in terms of the classification of porphyry deposit hosts of Mutschler et al. (1981). The potassic alteration assemblage includes quartz, K-feldspar, sericite and traces of carbonate and apatite. The carbonates occur both in veinlets and as grains and shreds dispersed through the entire rock. Apatite occurs in veins and disseminated as anhedral grains (see appendix 1). In this potassic

zone pyrite and chalcopyrite are frequently encountered with molybdenite veinlets and rare bornite. The bornite occurs as discrete grains and intimate intergrowths with chalcopyrite at the top of B.H.5 and 25 m deep in the same borehole.

Sericitization and silicification are common phenomena in the Fremstfjell area and appear to be related to schistosity zones that trend east-west. The association: quartz-sericite-pyrite seen in these sericitized and silicified rocks comprises the phyllic zone which has a diffuse and indistinct boundary with the potassic zone. The low-grade metamorphism that has affected the area may have obliterated the zoning or imposed other mineral assemblages that are not characteristic of the phyllic zone, such as epidote and carbonate (Lowell and Guilbert, 1970). In this zone micas, especially fine-grained muscovite, are well developed (see appendix 1 , T.S. F1/a, H1, H2, J/1a, J1/b, Js). The mineralogy of these samples is reflected in their high values of K_2O (Chapter 4, table 3).

Primary quartz is overgrown by later quartz in the phyllic zone (section 3.4.3.1). Chlorite is very rare although the trondhjemites are pale in colour because they contain very few coloured minerals (see sections 3.4.3.1 and 3.4.4.1). Chlorite is a minor component of the phyllic zone found as dark greenish-black coloured patches (plate 31). As the intensity of alteration increases towards the potassic zone the degree of sericitization increases but away from the central zone sericitization occasionally becomes replaced by

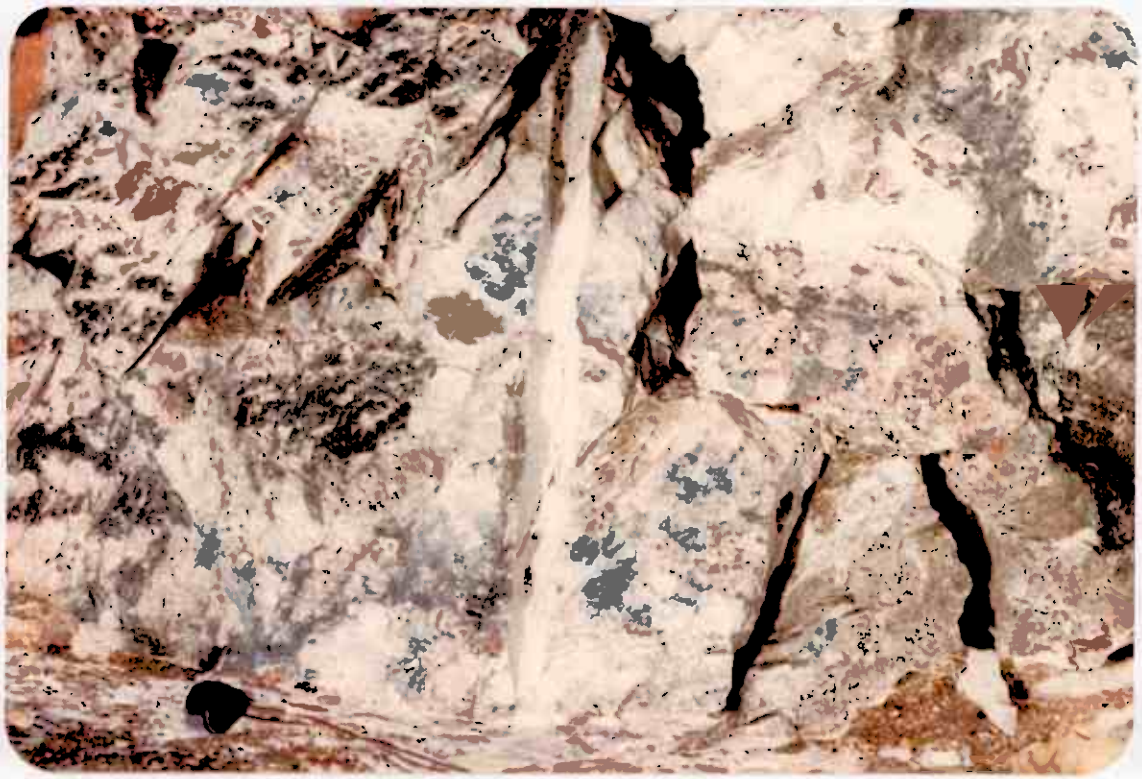

Plate (31): Patches of dark greenish-black chlorite with pink feldspar in altered granite, south of Smalltjern.

argillic alteration in which the primary feldspars are merely clouded with clay minerals. Clay minerals have been observed in the feldspars from the borehole cores B.H.3, 7 and 8. The ore mineral zones (Fig. 24) do not coincide with the boundary of the phyllic and argillic zones but the predominant minerals in this zone are pyrite, molybdenite and rare chalcopyrite.

Around the phyllic and poorly defined argillic zone a halo of pyrite-bearing rocks limits the mineralized area (Fig. 24). In this outer zone the typical alteration assemblage consists of altered plagioclase, epidote, chlorite, carbonate with prominent pyrite. These mineral assemblages constitute the propylitic alteration zone (Lowell and Guilbert, 1970) and this extends into the trondhjemite surrounding the granitic, molybdenum-bearing area. Plagioclase is altered to give rise to epidote which forms spongy cores to the grains (plate 14 page 48 and see Chapter 3) and sometimes the alteration extends further to give clay minerals indicating the onset of argillic type alteration (Chapter 3). Epidote fills veins and is associated with quartz and carbonate. Chlorite is associated with opaque minerals or after the rare biotite. In terms of ore minerals, pyrite is common in the forms of dispersed, coarse grained cubes or as veinlets and fine dissemination all through the area. Chalcopyrite occur in small amounts but molybdenite is rare in the form of fine dust in quartz.

5.7 Ore petrography

5.7.1 Introduction

Mineralization in the Fremstfjell area is restricted mainly to the granitic rocks and the trondhjemites around Amöebtjern and, except for disseminated pyrite, is chiefly of vein and veinlet type. The ore minerals include pyrite, chalcopyrite, molybdenite, bornite and magnetite.

5.7.2 Pyrite

Pyrite is the dominant opaque mineral throughout. It may be accompanied by combinations of chalcopyrite, molybdenite and magnetite. It occurs in a variety of forms, from euhedral cubes to ragged, amorphous grains varying in size from < 0.1 mm to > 10 mm. It frequently contains inclusions of other ores, principally chalcopyrite, less commonly molybdenite and rarely bornite. The chalcopyrite inclusions take the forms of: i) cleavage fracture fills (plate 32)
ii) en echelon tension fracture fills and irregular blebs (plate 33)
iii) tiny grains ± bornite (Plate 34)
There is obviously more than one generation of pyrite because it cuts and displaces quartz-molybdenite veins (plate 29) and vice versa, it is both embayed and enclosed by other minerals (plate 35) and it contains fracture fills (plate 32).

5.7.3 Chalcopyrite

Chalcopyrite occurs in several ways. It may be coarse-grained with equant grains up to 10 mm across or as a network

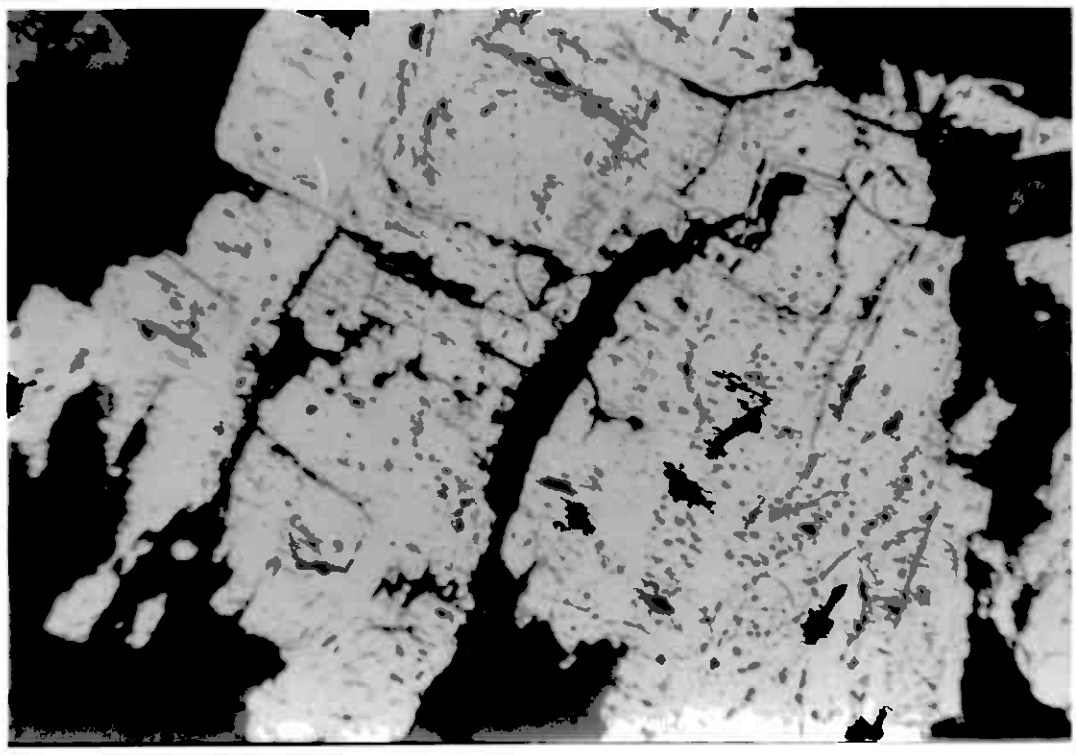

Plate (32): Cleavage fractures in pyrite (white) infilled by chalcopyrite (dark grey). x 400. B.H.3-3.

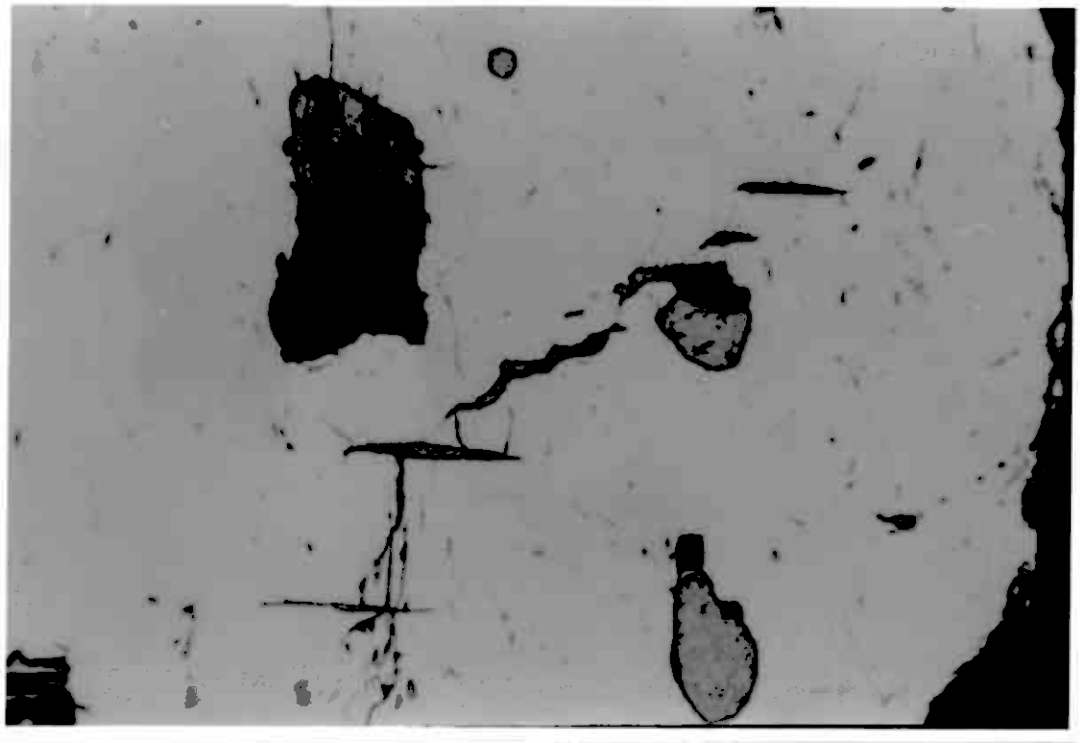

late (33): En echelon tension fractures fills and irregular blebs of chalcopyrite (dary grey) in pyrite (white). x 400. B.H.3-16.

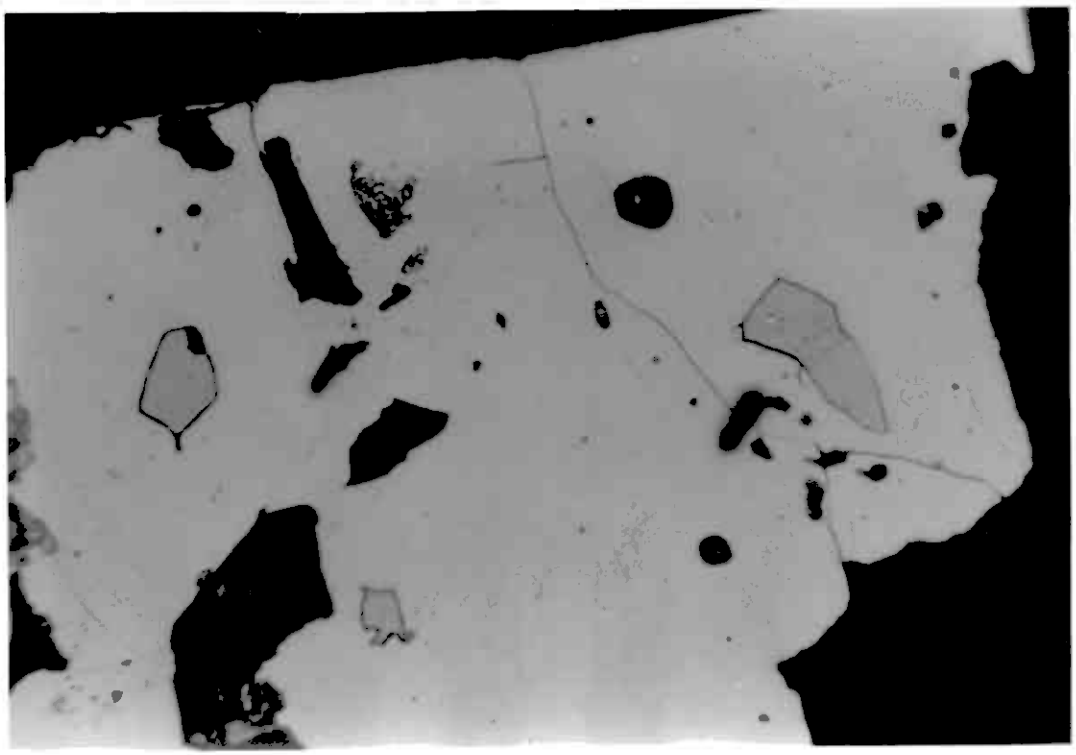

Plate (34): Tiny grains of chalcopyrite (medium grey) with bornite (pale grey) in pyrite (white), B.H.5-29, x 400.

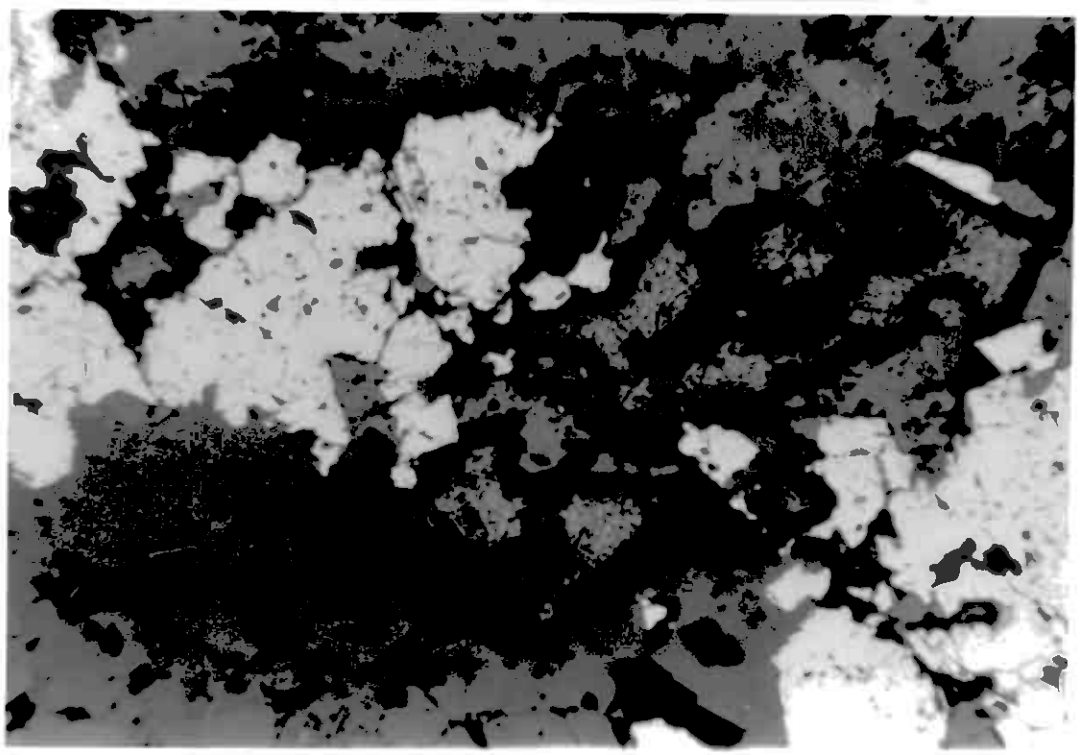

Plate (35): Anhedral pyrite (white) partly embayed and enclosed by chalcopyrite (medium grey, stippled high relief), B.H.3-3, x 100.

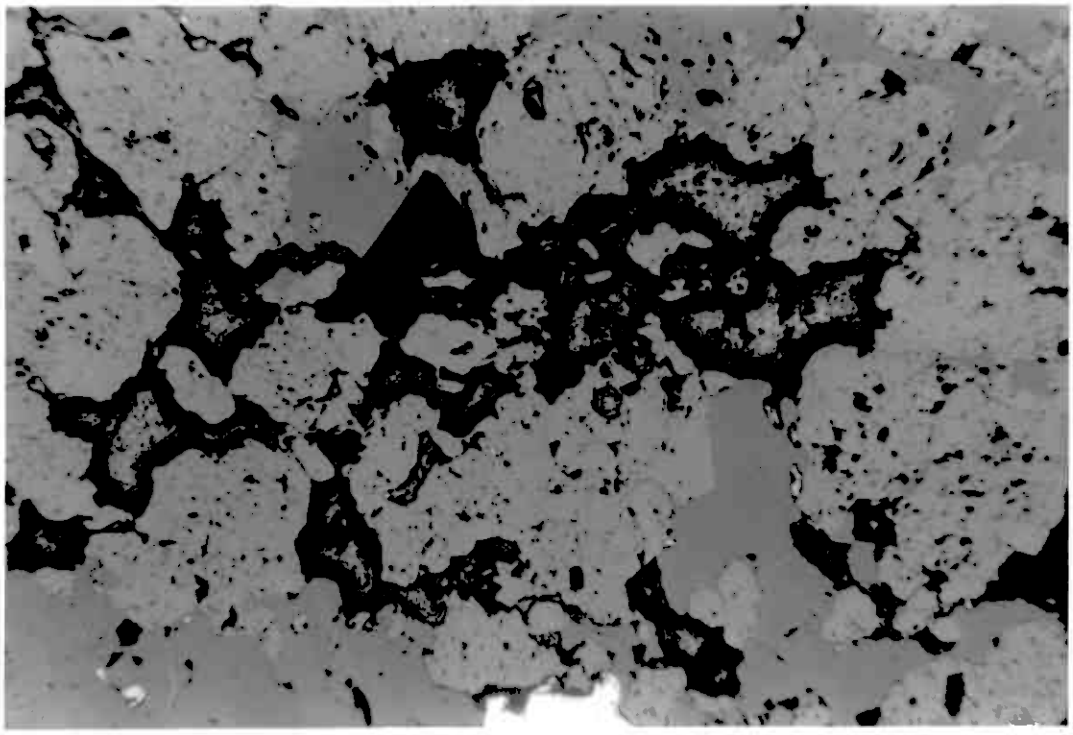

Plate (36): Network of skeletal grains of chalcopyrite (high relief) set in silicates, B.H.3-3, x 100.

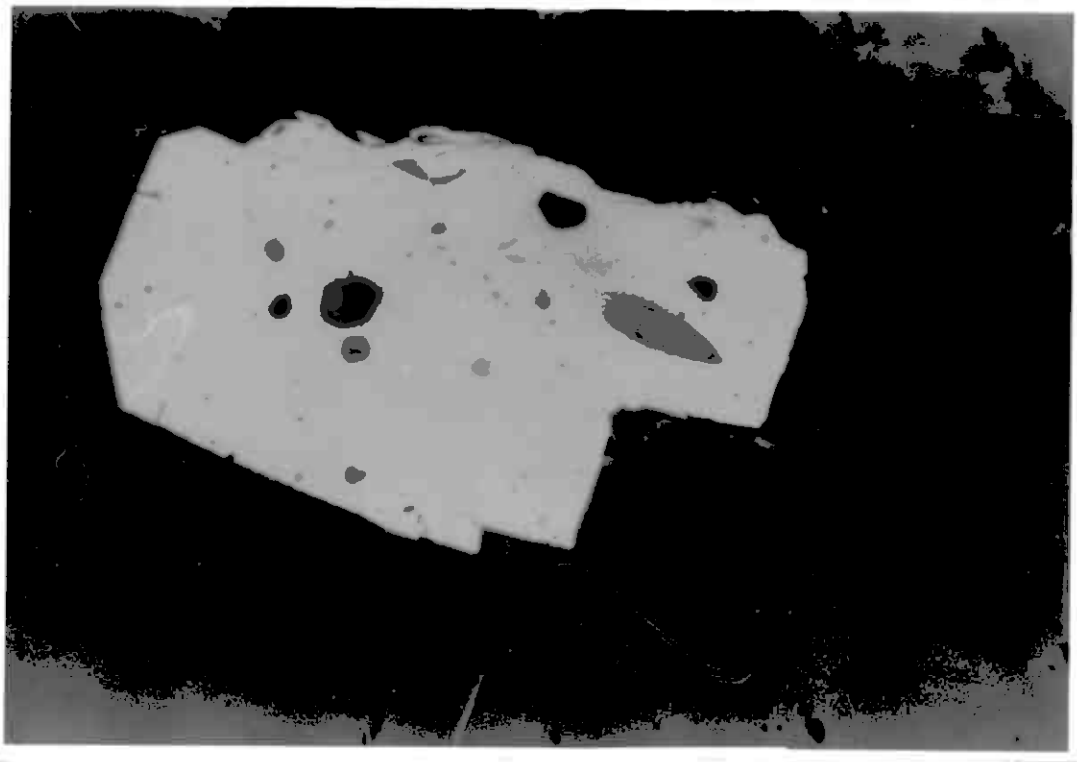

Plate (37): Lens of bornite (pale grey) with chalcopyrite (medium grey) in pyrite (white), B.H.5-20, x 400.

of skeletal grains (plate 36), or in distinct veins (30-40 mm wide) where it partially encloses ragged, subhedral pyrite grains (plate 35). Inclusions of chalcopyrite in pyrite are common in samples from boreholes 3 and 5 (plate 32,34) It is unclear whether they represent older included grains or younger exsolutions, although the presence of bornite and chalcopyrite as touching grains within pyrite (plate 34, 37) suggests that they are older primary included grains rather than exsolution material. In those cases where chalcopyrite infills fractures along pyrite cleavage, the chalcopyrite is clearly later than the pyrite.

5.7.4 Molybdenite

Molybdenite was easy to see in the field although it occurred only as very small grains in the several ways mentioned in section 5.4.2. In polished sections, it proved very difficult to observe. This was probably because of its extreme softness and fineness and it consequently did not survive the polishing techniques. Where it occurs it has a grain size of < 0.1 mm (plate 38). It is associated with quartz and embays pyrite (plate 39) and often shows weak bireflectance.

5.7.5 Bornite and magnetite

Bornite occurs in massive form in aggregates about 30 mm across, at the top of B.H.5. On the microscopic scale, bornite occurs as minute (< 0.05 mm) blebs or lenses (plate 34, 37).

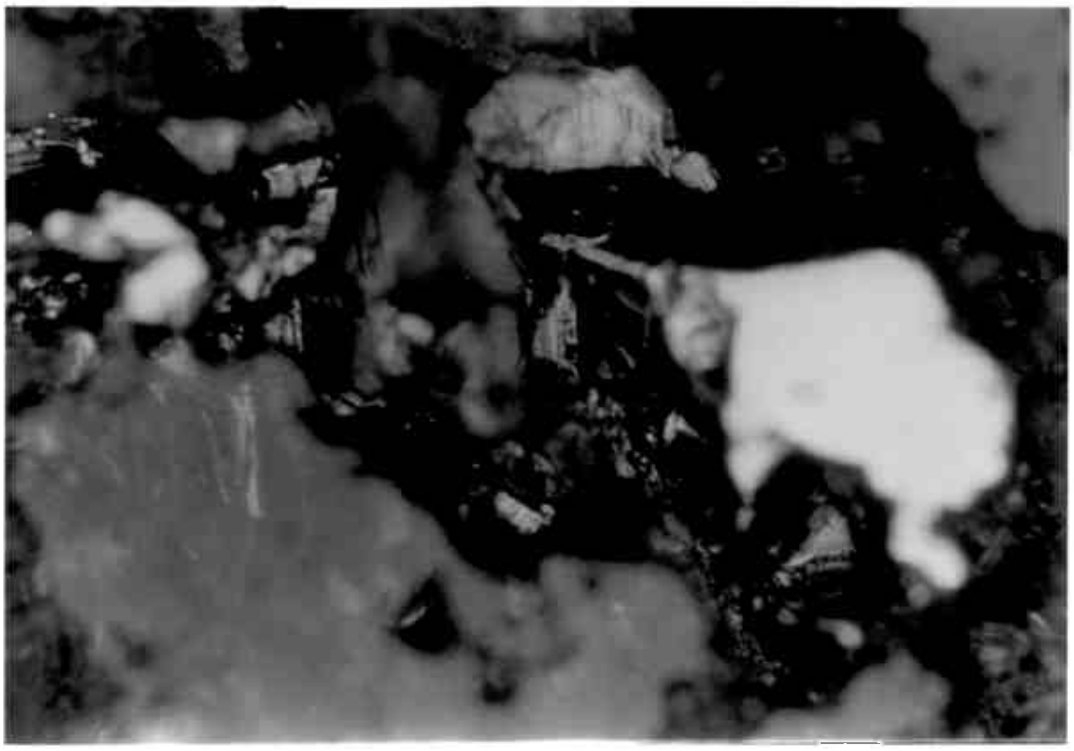

Plate (38): Cluster of molybdenite grains (dark grey) embaying pyrite (white), B.H.1-6. Relief contrast between pyrite and molybdenite makes focussing impossible at this magnification. x 400.

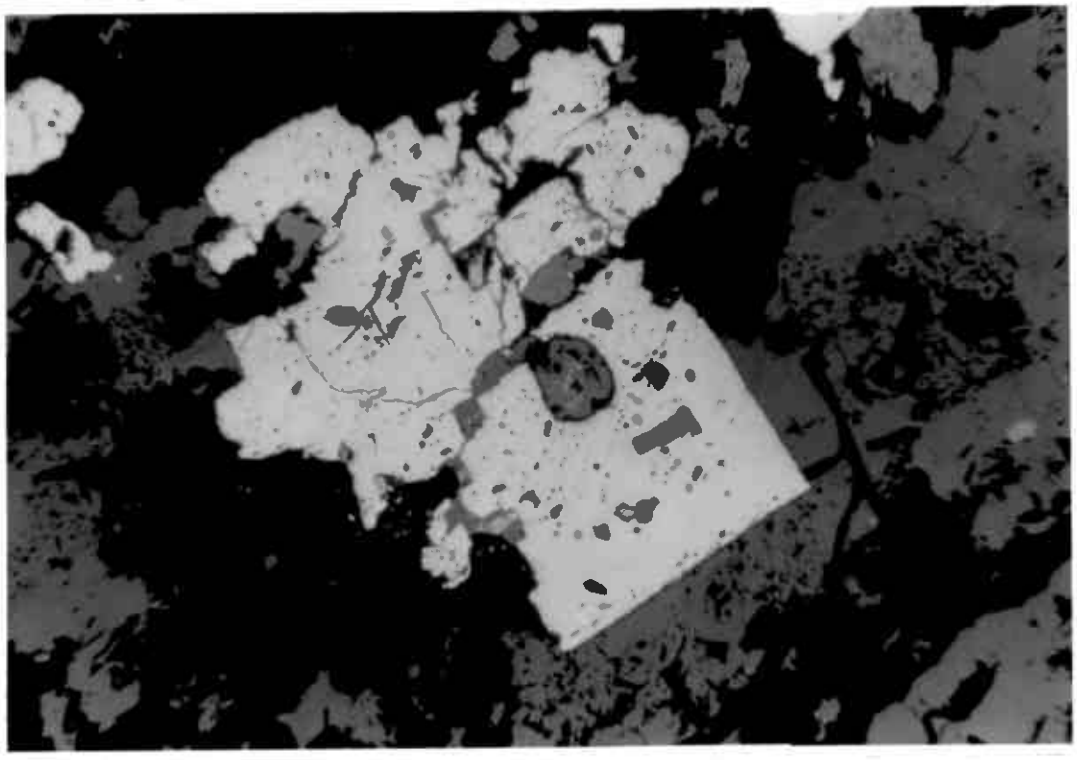

Plate (39): Subhedral pyrite (white) with bleb inclusions of chalcopyrite (pale grey) veined and embayed by quartz (medium grey) containing specks of molybdenite (pale grey), B.H.5-29, x 100.

included in pyrite and generally in contact with chalcopyrite. It seems to be significant that bornite has only been seen in the core from borehole 5 which is situated in the central part of the mineralized area.

Although magnetite is ubiquitous it is only found in massive form in a gabbro block west of Kroktjern (map 1) where it forms a complex radiating structure with silicate minerals (plate 40).

5.8 Grade and tonnage

Porphyry deposits are the world's major source of copper and molybdenum, and also a major source of silver and gold (Sheppard, 1977). Modern demands for molybdenum are being met by large tonnage and low-grade ores containing 0.2-0.5 per cent MoS_2 (Clark, 1972).

In the Fremstfjell area, the ore mineral assemblage consists of pyrite, chalcopyrite, molybdenite, magnetite, bornite with traces of lead, zinc and silver. The broad patterns of alteration and ore mineral assemblages suggests that area comprises a porphyry type occurrence. Molybdenite showings extend from west of B.H.1 to B.H.9 in the east (map 1), a distance of 1300 m, and the north-south extent of these showings is from B.H.6 to south of B.H.3, a distance of 400 m (map 1). However, if the mineralized zone is taken to measure only 500 x 300 m, from trench 5 to midway between B.H.7 and B.H.9 and north-south from B.H.6 to B.H.3, the surface area compares reasonably well with the average of the

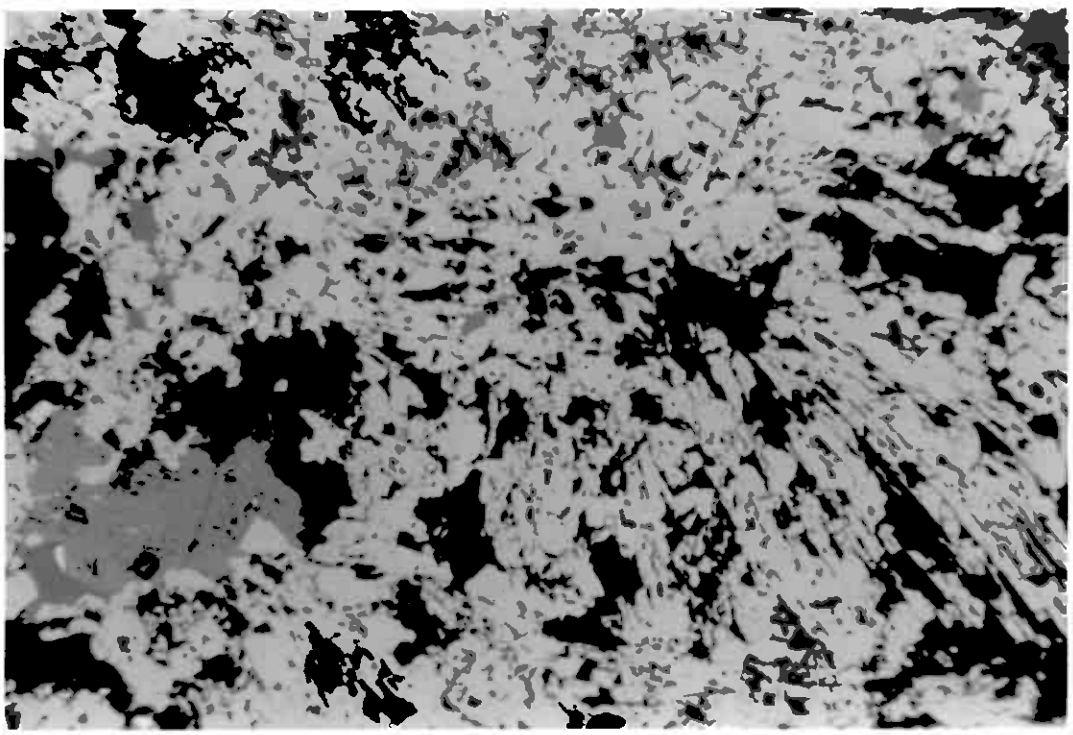

Plate (40): Radiating structure in magnetite from a gabbroic block, west of Kroktjern. Pistoltjer 1. x 100.

classic stockwork molybdenum deposits of North America (after Clark, 1972):

	Surface dimension (m^2)	Thickness m	Mo%
Alice	485 x 667	212	0.12
Endako	364 x 303	303	0.09
Urad	121 x 303	212	0.25
Henderson	667 x 909	303	0.29
Climax	605 x1212	91-242	0.20
Questa	758 x1212	212	0.11
Fremstfjell	300 x 500	30-212	0.035

The abundances of molybdenum and copper in the analysed samples described in Chapter 4, as well as the average analyses of samples from the boreholes and trenches, are presented in Tables 7,8,9. Molybdenum and copper show their highest values in the granitic samples (Table 7), but it is worth noting that the mineralized veins themselves were not selected for analysis and thus the data only represent the disseminated mineralization values.

From Tables 8 and 9 the average Mo and Cu for the trenches are seen to be more than three times those of the boreholes which may reflect poor core splitting or biased chip sampling or both. The highest molybdenum values occur in boreholes 4, 5 and 6 (inner zone) where several metres of analysed core have > 500 ppm Mo and > 500 ppm Cu (see Tables 10, 11).

Boreholes 2 and 9 also show significant copper values (Table 11).

The boreholes + trenches average value of 353 ppm Mo (Table 9) is well below 1200 ppm (0.2% MoS_2), the lowest limit suggested by Clark (1972) for economic porphyry molybdenum deposits. Although the values of copper (Table 8) are higher than molybdenum (Table 9), it should be noted that the analysed core was selected on the basis of it containing visible molybdenite and/or coarse grains of chalcopyrite. The core that has not been analysed could also contain molybdenum and, possibly more significantly, copper, and if it was analysed the picture may be changed (but probably for the worse).

There are not enough data to show clearly the shape and configuration of the ore body. However, if one considers a simple model for the ore body to be a diamond shaped surface area of 500 x 300 m (Fig. 26) with an estimated depth of 120 m, then:

$$\text{the volume} = \tfrac{1}{2} \times 500 \times 300 \times 120 = 9 \times 10^6 \text{ m}^3$$

If the density of the rock is assumed to be 2.8, then the mass of the ore body = $9 \times 10^6 \times 2.8 = 25.2 \times 10^6$ tonnes and these 25.2×10^6 tonnes of:

average 0.035 wt.% Mo and
0.043 wt.% Cu, representing
8820 tonnes Mo metal
10800 tonnes Cu metal

Table 7: Mo and Cu concentrations of all analysed samples referred to in Chapter 4.

Sample No.	Mo ppm	Cu ppm
Basalt-rhyolite		
N5	10	7
N16	8	3
N17	8	5
N1	8	14
N15	8	11
γ3	7	39
γ4	1	9
γ1	5	10
γ2	12	7
Gabbro and diorite		
B7	15	101
N6	23	36
B7/c	7	114
N7	13	7
B7/d	6	3
B7/a	21	2
B7/b	7	3
4/8/8	1	7
4/8/9	1	35
E2	10	11
4/8/14	3	9
N4	8	6
4/8/10	6	11
4/8/15	13	21
C5	12	340
N2	8	11
N8	10	16
CYP	5	110
Trondhjemite		
A1	625	15
H1	72	56
J1/b	33	8
F1	13	130
D4	37	114
N13	10	8
J1/a	15	10
D5	15	42
J2	5	18
B3	1	72
H2	8	11
B1/b	1	16
D2	10	11
A2	27	29
A3	1	5

Table 7 ctd.

Sample No.	Mo ppm	Cu ppm
B5	11	15
B6/a	10	4
D6	67	98
B4	1	142
Ao	129	139
A4	121	15
A5	41	6
B2/d	48	4
D3	25	8
Granite		
T5/j	467	1017
T1/a	154	229
B/5	53	170

Sample No.	Mo ppm	Cu ppm
T1/d	35	248
T5/c	136	602
T5/b	512	628
T5/f	44	301
T6/e	35	70
T2/g	75	292
T5/o	825	121
T3/b	148	7
Dolerite		
N20	2	5
Md	15	22
N3	13	10

Table 8: Mo and Cu analyses of the borehole cores

B.H. number	Number of samples *	Mo ppm	Cu ppm
1(0-30 m)	15	224	252
2(0-70 m)	35	248	664
3(0-40, 56-90)	32	110	325
4(0-123, 190-202)	69	161	383
5(0-130, 250-268)	84	374	854
6(10-30, 50-70, 110-197)	64	209	228
7(80-90, 106-116, 120-140)	20	60	299
8(60-90, 120-130)	20	148	110
9(20-90)	35	61	642
Average B.H.1-9	. .	177	417

*2 metre core samples averaged to give the analysed values

Table 9: Mo and Cu analyses of trench samples

Trench number	Number of samples *	Mo ppm	Cu ppm
1/80	11	300	258
2/80	24	152	486
3/80	25	698	277
4/80	3	2072	772
5/80	10	209	362
6/80	3	268	228
2/83[x]	50	403	866
7/83[x]	70	122	331
Average Trenches		528	448
Overall average Boreholes + Trenches		353	433

* 1 metre sample
x blasted in 1983

Table 10 : Mo analytical results from the borehole cores

B.H. number	No. of samples that contain > 500 ppm	No. of samples that contain > 1000 ppm
1	2	0
2	2	0
3	0	0
4	1	0
5	16	4
6	5	0
7	0	0
8	0	0
9	0	0

Table 11 : Cu analytical results from the borehole cores

B.H. number	No. of samples that contain > 500 ppm	No. of samples that contain > 1000 ppm
1	1	0
2	13	7
3	2	0
4	11	7
5	16	34
6	8	1
7	1	0
8	1	0
9	9	5

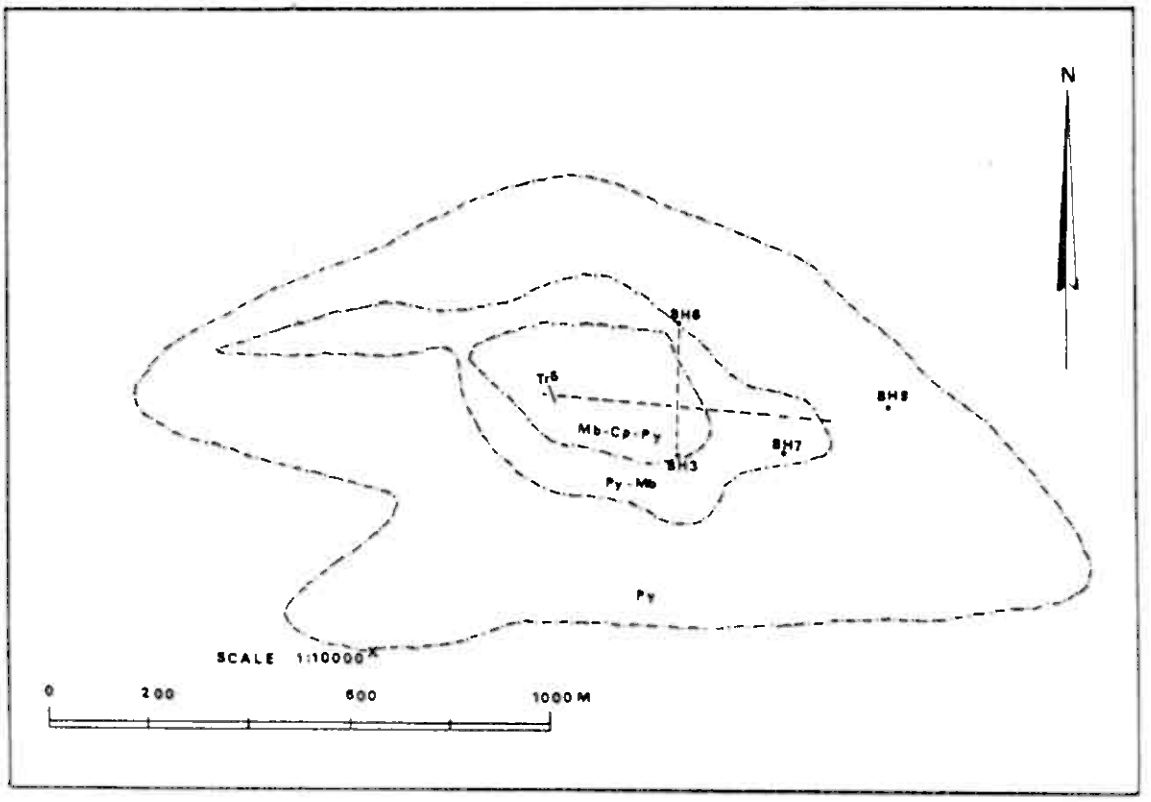

Fig 26 Estimated limits of the potential ore body used in tonnage calculation

These results very probably err on the optimistic side but the analyses were carried out only for molybdenum and copper. Nothing is known of, for example, gold and silver concentrations. However, from the current investigations it is difficult to imagine that the Fremstfjell mineralization could become an economically viable Mo deposit in the foreseeable future.

CHAPTER 6

Summary and Conclusions

The Fremstfjell area comprises a thrust sheet of Lower Palaeozoic rocks (greenstones) thrust onto Precambrian gneisses of the Grong Culmination of the Baltic Shield. The greenstones consist of metavolcanic (basalt-rhyolite) and metasedimentary rocks. These rocks are intruded by a trondhjemite complex with which Mo-Cu mineralization is associated. The intrusive rocks comprise mainly trondhjemite (a leucocratic rock composed of oligoclase, quartz and sparse biotite), minor gabbro (which, in the field area occurs as xenolithic blocks and screens enclosed in and veined by trondhjemite), diorite and granitic rocks which have K-feldspar as an important constituent and which host the mineralization. A sharp, intrusive or chilled contact between granite and trondhjemite has not been observed even in fresh drill cores and trondhjemite may pass gradationally into granite. The latest phase of magmatic activity was the intrusion of a set of dolerite dykes, now schistose metagreenstones. These dykes are never Mo-Cu mineralized, even when the immediately adjacent rocks are riddled with molybdenite veins. Thus it seems that molybdenum mineralization pre-dates the dykes and their subsequent metamorphism.

The gabbro-trondhjemite association which hosts the Mo-Cu mineralization at Fremstfjell occurs commonly elsewhere in the Norwegian Caledonides. Goldschmidt (1916) suggested that similar rocks in the Trondheim region are derived from basaltic magma by fractional crystallization. However, this

model is difficult to apply in the Trondheim region as well as in the Fremstfjell area, because there are significant compositional gaps in the magmatic rock series and anomalously small volumes of basic and intermediate rocks (Size, 1979).

Several other models have been proposed for the origin of trondhjemites:-

i) Trondhjemites are integral parts of ophiolite complexes similar to the oceanic plagiogranites of Coleman and Peterman (1975). The chemistry of the trondhjemites considered in the current work suggests a continuum from true trondhjemitic plagiogranite through to more typical continental potassic granite. However, the Fremstfjell rocks show higher values of K_2O than the ophiolite associated rocks and are not pre-tectonic, as would be the case with ophiolites, so this model is unlikely to be valid for the study area.

ii) Partial melting of greywackes could provide the source of trondhjemite magma. Flysch-type greywackes and associated volcaniclastic rocks are common in the Norwegian Caledonides where they show differing effects of metamorphism and recrystallization (Size, 1979). Trondhjemitic magma has been produced experimentally by partial fusion of greywacke (Albuquerque, 1977). However, as the average greywacke contains about 67% SiO_2 and 2% K_2O, initial minimum partial melts would inevitably be granitic in composition and the liquid would only become trondhjemitic as partial melting proceeded. Large quantities of granitic rocks in the map area and elsewhere in the region are not evident.

iii) A third model could involve partial fusion of gneisses and granites of the continental crustal margin. However, the minimum melt of such source rocks would be enriched in K_2O and even with progressive melting of these rocks at higher temperatures, the K_2O content would probably not be diluted enough for the liquid to resemble trondhjemite.

The Follestad trondhjemite of the Trondheim region has an initial $^{87}Sr/^{86}Sr$ ratio of 0.7039, which is indicative of a less radiogenic source than continental gneisses and granite (Peterman and Barker, 1976). The high Al_2O_3 and low K_2O contents of Fremstfjell trondhjemites and those from elsewhere in the Norwegian Caledonides equally requires a primitive source. The volume relations and compositional gaps preclude a simple mantle partial melt-fractional crystallization model for the origin of the suite and therefore the only acceptable alternative appears to be a two stage model in which mantle derived rocks such as island-arc basalts or ocean-floor low-K tholeiites with low $^{87}Sr/^{86}Sr$ initial ratios are themselves partially melted, probably in a continental accretionary environment (Size, 1979). Discriminant diagrams, such as Ti/Cr v Ni, Ti v Zr, Zr/Y v Zr and Nb v SiO_2 (Figs. 15,17,18,22) strongly support this interpretation and suggest that these rocks were generated in an island-arc showing both tholeiitic and oceanic characters.

The volcanic association of basalt-basaltic andesite-andesite-rhyolite in the Fremstfjell area suggests that such an arc would have been a relatively mature one.

In the Fremstfjell area the igneous association and the economic mineralogy with indistinct mineral zoning and poorly defined alteration pattern are all suggestive of a porphyry type occurrence. The ore mineral assemblage and the chemistry of its host rocks are comparable with the calc-alkaline molybdenum deposits described by Westra and Keith (1981) associated with volcano-plutonic arcs in plate collision zones. The initial cylindrical form of such deposits could have been distorted by tectonism to give the present lensoid shape of the occurrence at Fremstfjell.

The close relationship between plate subduction, arc magmatism and the genesis of porphyry ore deposits (porphyry copper and stockwork molybdenum) is well documented (Sillitoe, 1972; Westra and Keith, 1981). There are two fundamentally different models for the genesis of porphyry ore deposits, one involving concentrations of metals from partial melts derived from descending lithospheric slabs at destructive plate margins (Sillitoe, op.cit) and a second involving the concentration of metals from crustal rocks by circulating hydrothermal solutions generated by the emplacement of large, sufficiently wet, intrusive bodies (Aprahamian, 1976). However, these models are not mutually exclusive and the present author considers that a combination of these processes is most likely to have occurred.

The metals contained in porphyry deposits may have been largely derived from lithospheric oceanic crust or upper mantle and extracted by partial melting of the lithosphere

during subduction (Sillitoe, 1972). According to this model the metals were initially abstracted from the mantle at constructive plate margins and were carried to the destructive plate margins as components of layers 1, 2 and 3 of the oceanic crust (Sillitoe, op. cit.). The metals released during partial melting would concentrate in chloride-rich fluid phases associated with the roof-zone of certain intrusions. The fluid phases would be released upwards during consolidation of the magma to give rise to the typical upright cylindrical forms of porphyry copper and molybdenum mineralization.

Fluid inclusion and isotope studies in porphyry systems suggest that early mineralization and alteration are carried out by hot saline fluid mostly of magmatic origin. The structural controls for fluid migration are provided by stockwork fractures caused by hydraulic fracturing of the host rocks and by inter-grain permeability. Later mineralization and alteration are produced by fluids involving progressively greater amounts of meteoric waters becoming involved in circulating convective cells generated by the magmatic heat source. The majority of the Cu, Mo and perhaps also S, is probably derived from the magma, but one cannot tell whether the ultimate source was deep continental crust, mantle or subducted oceanic crust.

REFERENCES

ALBUQUERQUE, C.A.R. de, 1977: Geochemistry of the tonalitic and granitic rocks of the Nova Scotia plutons.
Geochim. Cosmochim. Acta, v. 41, p. 1-13.

ALI, S.M., 1977: The Geology of the Homogar Group Volcanic Rocks, Southern Red Sea Hills, Sudan.
Unpublished M.Phil. thesis, Portsmouth Polytechnic, England.

ANDREASSON, P.G., SOLYOM, Z. and ROBERTS, D., 1979: Petrochemistry and tectonic significance of basic and alkaline-ultrabasic dykes in the Leksdal Nappe, northern Trondheim region, Norway.
Norges geol. Unders. 348, 47-71.

ANDERSON, T.B., AUSTRHEIM, H., STURT, B.A., PEDERSEN, S. and KJAERSRUD, K., 1982: Rb-Sr whole rock ages from Magerøy, North Norwegian Caledonides.
Norsk geol. Tidsskr., Vol. 62, pp. 79-85.

APRAHAMIAN, F., 1976: Porphyry Copper Case Study.
Open University Press, Milton Keynes, 80 p.

ARTH, J.G. and HANSON, G.N., 1975: Geochemistry and origin of the early Precambrian crust of northeastern Minnesota.
Geochim. Cosmochim. Acta, 39, 325-362.

ARTH, J.G., BARKER, F., PETERMAN, Z.E. and FRIEDMAN, I., 1978: Geochemistry of the gabbro-diorite-tonalite-trondhjemite suite of southwest Finland and its implications for the origin of tonalitic and trondhjemitic magmas. J. Petrology, Vol. 19, pp. 289-316.

AUKES, P.G., REYMER, A.P.S., de REUTER, G.W.M., STEL, H. and ZWART, H.J., 1979: The geology of the Lierne district, northeast of the Grong Culmination, central Norway. Norges geol. Unders. 354, 115-129.

BAILEY, E.H. and STEVENS, R.E., 1960: Selective staining of K-feldspar and plagioclase on rock slabs and thin sections. Am. Min., v. 45, p. 1020-1025.

BARKER, F., 1979: Trondhjemite: Definition, Environment and Hypothesis of Origin, p. 1-12. In: Barker (ed.), Trondhjemite, Dacites and Related Rocks. Elsevier Scientific Publishing Company, Amsterdam.

BARKER, F. and ARTH, J.G., 1976: Generation of trondhjemitic-tonalitic and Archean bimodal trondhjemitic-basalt suites. Geology, 4, 596-600.

BARKER, F. and MILLARD, H.T., 1979: Geochemistry of the type trondhjemite and three associated rocks, Norway, p. 518-529. In: Barker (ed.), Trondhjemite, Dacites and Related Rocks. Elsevier Scientific Publishing Company, Amsterdam.

BARTH, T.F.W. and REITAN, P.H., 1963: The Precambrian of Norway.
The Precambrian, Vol. 1, 27-80.

BATTEY, M.H. and McRITCHIE, W.D., 1973: A geological traverse across the pyroxene-granulites of the Jotunheim in the Norwegian Caledonides.
Norsk geol. Tidsskr. 53, 237-265.

BATTEY, M.H. and McRITCHIE, W.D., 1975: The petrology of the pyroxene-granulite facies of the Jotunheim, Norway.
Norsk geol. Tidsskr. 55, 1-49.

BECCALUVA, L., OHNENSTETTER, D. and OHNENSTETTER, M., 1979: Geochemical discrimination between ocean-floor and island-arc tholeiites application to some ophiolites.
Can. J. Earth Sci., 16, pp. 1874-1882.

BILHORN, W.W., 1983: Molybdenum.
Engineering and Mining Journal, Vol. 184, no. 3, p. 70-72.

BROWN, G.C., HUGHES, D.J. and ESSON, J., 1973: New X.R.F. retrieval techniques and their application to U.S.G.S. standard rocks.
Chem. Geol., 11, 223-229.

BRUECHNER, HANNES K., 1979: Precambrian ages from the Geiranger-Tafjord-Grotli area of the Basal Gneiss Region, West Norway.
Norsk geol. Tidsskr. 59, 141-153.

CANN, J.R., 1969: Spilites from the Carlsberg ridge, Indian Ocean.
J. Petrol. 10, 1-19.

CAWTHORN, R.G., STRONG, D.F. and BROWN, P.A., 1976: Origin of corundum-normative intrusive and extrusive magma.
Nature, 259, 102-104.

CLARK, K.F., 1972: Stockwork molybdenum deposits in the western cordillera of North America.
Econ. Geol., v. 67, p. 731-758.

COLEMAN, R.G., 1977: Ophiolites.
Springer-Verlag: Berlin, Heidelberg, New York. 229 p.

COLEMAN, R.G. and PETERMAN, Z.E., 1975: Oceanic plagiogranite.
J. Geophys. Res. 80, pp. 1099-1108.

COX, K.G., BELL, J.D. and PANKHURST, R.J., 1979: The interpretation of igneous rocks.
London, George Allen and Unwin, 450 p.

CRAIG, J.R. and VAUGHAN, D.J., 1981: Ore microscopy and ore petrography.
New York, Chichester: Wiley and Sons, 406 p.

DAY, F.H., 1963: The chemical element in nature.
London Harrap and Co. Ltd., 372 p.

DEER, W.A., HOWIE, R.A. and ZUSSMAN, J., 1966: An introduction to the rock forming minerals.
Longman-London, 528 p.

DEWEY, J.F., 1969: Evolution of the Appalachian/Caledonian Orogen.
Nature, Volume 222, pp. 124-129.

DEWEY, J.F. and KAY, M., 1969: Appalachian and Caledonian evidence for drift in the North Atlantic. In R.A. Phinney (Ed.), The History of the Earth's Crust, Princeton Univs. Press, New Jersey, 161-167.

FERRARA, G., INNOCENTI, F., RICCI, C.A. and SEMI, G., 1976: Ocean floor affinity of basalts from Apennine ophiolites: geochemical evidence.
Chemical Geology, 17, p. 101-111.

FOSLIE, S. Geological maps prepared during 1922-1927 and published at 1:100 000 scale by Norges Geologiske Undersøkelse as follows: Namsvatnet med en del air Frøyningsfjell, Oslo 1957, Tunnsjø, Oslo 1958, Sanddøla, Oslo 1958, Trones, Oslo 1958, Nordli, Oslo 1959.

FOSLIE, S. and STRAND, T., 1956: Namsvatnet med en del av Frøyningsfjell.
Norgesgeol. Unders. no. 196, 82 p.

FURNES, H., ROBERTS, D., STURT, B.A., THON, A. and GALE, G.H., 1979: Ophiolite fragments in the Scandinavian Caledonides.
Proc. Intern. Ophiolite Symp. Geol. Survey Cyprus, p. 582-600.

☆ See page 167

GALE, G.H. and PEARCE, J.A., 1982: Geochemical patterns in Norwegian greenstones.
Can. J. Earth Sci., 19, 385-397.

GALE, G.H. and ROBERTS, D., 1974: Trace element geochemistry of Norwegian Lower Palaeozoic basic volcanics and its tectonic implications.
Earth and Planetary Science Letters, 22, pp. 380-390.

GANSTER, M.W., 1976: Evidence for the localized accumulation of hydrothermal fluids at the Henderson molybdenum deposit, Empire, Colorado (abs.).
Geol. Soc. America, Abstracts with Programs, v. 8, no. 6, p. 880.

GEE, D.G., 1974: Comments on the metamorphic allochthon in northern Trøndelag, Central Scandinavian Caledonides.
Norsk geol. Tidsskr. 54, 435-440.

GEOLOGICAL MAP OF SUDAN, 1981: Scale 1:2 000 000.
Compiled by the Geological and Mineral Resources, Department, Khartoum.

GJELSVIK, T., 1968: Distribution of major elements in the wall rocks and the silicate fraction of the Skorovas pyrite deposit, Grong area, Norway.
Econ. Geol. 63, 217-231.

GOLDSCHMIDT, V.M., 1916: Geologish. Petrographische studien im Hochgebirge de südlichen Norwegens, iv. Übersicht der eurptivgeoteine im kaledonischen Gebirge zwischen Stavanger und Trondhem.
Vidensk. Selsk Skr. 1. Mat Naturv. Kl. No. 2, 1-140.

GOLDSCHMIDT, V.M., 1954: Geochemistry.
Oxford Clarendon Press, 730 p.

GREILING, R., 1975: Der Südrand des Børgefjell-Fensters.
Zeit. deutschen geol. Ges. 126, 155-165.

GRIFFIN, W.L., TAYLOR, P.N., HAKKINEN, J.W., HEIER, K.S., IDEN, I.K., KROGH, E.J., MALM, O., OLSEN, K.I., ORMAASEN, D.E. and TUETEN, E., 1978: Archaean and Proterozoic crustal evolution in Lofoten-Vesterålen, N. Norway.
Jl. geol. Soc. London, Volume 135, pp. 629-647.

HALLS, C., REINSBAKKEN, A., FERRIDAY, I., HAUGEN, A. and RANKIN, A., 1977: Geological setting of the Skorovas ore body within the allochthonous volcanic stratigraphy of the Gjersvik Nappe, Central Norway.

Inst. Min. Metall. and Geol. Soc. London. Special publication no. 7, p. 128-151.

HART, S.R., GLASSLEY, W.E. and KARIG, D.E., 1972: Basalts and sea floor spreading behind the Mariana island arc.
Earth Planet. Sci. Lett., 15, 12-18.

HATCH, F.W., WELLS, A.K. and WELLS, M.K., 1972: Petrology of the igneous rocks (13th ed.).
George, Allen and Unwin, London.

HESS, H.H., 1960: The Stillwater igneous complex, Montana.
Geol. Soc. Amer., Mem., 80, 1-230.

HOBBS, B.E., MEANS, W.D. and WILLIAMS, P.F., 1976: An Outline of Structural Geology.
John Wiley and Sons, New York. 571 p.

HOLLAND, C.H. and STURT, B.A., 1970: On the occurrence of Archaeocyathids in the Caledonian metamorphic rocks of Sørøy, and their stratigraphical significance.
Norsk geol. Tidsskr., Vol. 50, pp. 341-355.

HOLTEDAHL, Olaf, 1960: (Editor) Geology of Norway.
N.G.U., No. 208.

HUGHES, V.J., 1973: Late precambrian volcanic rocks of Avalon, New Foundland - a spilite/keratophyre province: Recognition and implications.
Can. J. Earth Sci., 10, 272-282.

IRVINE, T.N. and BARAGER, W.R.A., 1971: A guide to the chemical classification of the common volcanic rocks.
Can. J. Earth Sci. 8, 523-548.

JACOBSEN, S.B. and HEIER, K., 1978: Rb-Sr isotopes systematics in metamorphic rocks, Kongsberg sector, South Norway.
Lithos, Vol. 11, pp. 257-276.

JAKES, P. and GILL, J., 1970: Rare earth elements and the island-arc tholeiite series.
Earth Planet. Sci. Lett. 9, pp. 17-28.

JENKINS, R. and de VRIES, J.L., 1967: Practical X-ray spectrometry.
Eindhoven, Philips, 182 p.

KOLLUNG, S., 1979: Stratigraphy and major structures of the Grong District, Nord.Trøndelag.
Norges geol. Unders. 354, 1-51.

KRAUSKOPF, K.B., 1979: Introduction to Geochemistry, (2nd ed.).
McGraw-Hill, Inc. U.S.A. 617 p.

KULLING, O., 1972: In: Strand, T. and Kulling, O. (eds). Scandinavian Caledonides. Wiley-Interscience, London, p. 147-302.

KUNO, H., 1969: Andesite in time and space. In: A.R. Mc Birney (ed.), "Proceeding of the andesite conference", p. 13-20, Bull. 65, Dept. Geology and Mineral Industries, State of Oregon.

KURODA, P.K. and SANDELL, E.B., 1954: Geochemistry of molybdenum. Geochim. Cosmochim. Acta, v. 6, p. 35-63.

KVALE, A., 1960: The nappe area of the Caledonides in western Norway. In Guide A7 and to excursions A7 and C4. 21st International geol. Cong. Norden 1960, 43 p. Norges geol. Unders. 212e.

LEAKE, B.E., 1978: Nomenclature of amphiboles. American Mineralogist, 63 pp. 1023-1052.

LOWELL, J.D. and GUILBERT, J.M., 1970: Lateral and vertical alteration-mineralization zoning in porphyry ore deposits. Econ. Geol., v. 65, p. 373-408.

LUTRO, O., 1979: The geology of the Gjersvik area, Nord-Trøndelag, central Norway. Norges geol. Unders, 354, 53-100.

MALM, O.A. and ORMAASEN, D.E., 1978: Mangerite-charnockite intrusive in the Lofoten-Vesterålen area, North Norway: Petrography, chemistry and petrology.
Norges geol. Unders. 338, 83-114.

MASON, B., 1966: Principles of geochemistry.
John Wiley and Sons Inc., U.S.A., 329 p.

MIYASHIRO, A., 1973: Metamorphism and metamorphic belts.
London: George Allen and Unwin. pp. 1-479.

MIYASHIRO, A., 1973: The Troods ophiolite complex was probably formed in an island arc.
Earth Planet. Sci. Lett. 19, 218-224.

MUTSHLER, F.E., WRIGHT, E.G., LUDINGTON, S. and ABBOTT, J.T., 1981: Granite molybdenite systems.
Econ. Geol., v. 76, p. 874-897.

NAKAMURA, N., 1974: Determination of REE, Ba, Fe, Mg, Na and K carbonaceous and ordinary chondrite.
Geochim. Cosmochim. Acta., 38, p. 757-775.

NORRISH, K. and CHAPPEL, B.W., 1967: X-ray fluorescence spectrography. In: Zussmann (ed.). Physical methods in determinative mineralogy, Academic Press, London.

N.G.U. 1975: Trondhjemitt. Prosjektet. Bekkesedimenter, HNO_3-Løselig Mo.
Sanddøla. Nesavatna, Nord Trøndelag. Scale 1:20 000.

N.G.U. 1981: IP. Gradient målinger, Søndre del av Grongfeltet, Grong, Nord Trøndelag. Unpublished map. Scale 1:5000.

O'CONNOR, J.T., 1965: A classification for quartz-rich igneous rocks based on feldspar ratios.
U.S. Geol. Surv. Prof. Paper 525B, 79-84.

OFTEDHAL, C., 1956: Om Grongkulminasjonen og Grongfeltets Skyvedekker.
Norges geol. Unders. no. 195, p. 57-64.

OFTEDHAL, C., 1958: A theory of exhalative-sedimentary ores.
Geol. För. Stockh. Förh., 80, 1-19.

OFTEDHAL, C., 1980: Geology of Norway.
Norges geol. Unders. 348, 47-71.

OLERUD, S. and SANDSTAD, J.S., 1983: Geology of the Skrukkelia molybdenite deposit, northwestern margin of the Oslo Graben, Norway.
Norges geol. Unders. 387, p. 1-20.

PASTEELS, P., DEMAIFFE, D. and MICHOT, J., 1979: U-Pb and Rb-Sr geochronology of the eastern part of the south Rogaland igneous complex, South Norway.
Lithos, Vol. 12, pp. 199-208.

PEARCE, J.A., 1975: Basalt geochemistry used to investigate past tectonic environment on Cyprus.
Tectonophysics, 25, 41-67.

PEARCE, J.A., 1980: Geochemical evidence for the genesis and eruptive setting of lavas from Thethyan ophiolites. In: Panagioton, A. (ed.). Ophiolites Proceeding International Ophiolite Symposium, Cyprus, 1979.
The Geological Survey of Cyprus, Nicosia, p. 261-272.

PEARCE, J.A., 1982: Trace element characteristics of lavas from destructive plate boundaries. In: Thorpe, R.S. (ed.) Orogenic andesites.
J. Wiley and Sons, p. 525-548.

PEARCE, J.A. and CANN, J.A., 1971: Ophiolite origin investigated by discriminant analysis using Ti, Zr and Y.
Earth Planet. Sci. Lett., 12, 339-349.

PEARCE, J. and CANN, J.R., 1973: Tectonic setting of basic volcanic rocks determined using trace element analysis.
Earth Planet. Sci. Lett., 19, 290-300.

PEARCE, J. and GALE, G.H., 1977: Identification of ore-deposition environment from trace-element geochemistry of associated igneous host rocks.
Inst. Min. Metall. special publication 7, 14-24.

PETERMAN, Z.G. and BARKER, F., 1976: Rb-Sr whole rock age of trondhjemite and related rocks of the S.W. Trondheim region, Norway.
U.S. Geol. Surv. report 76-670, 1-13.

PHILPOTTS, J.A., SCHNETZLER, C.C. and HART, S.R., 1969: Submarine basalts: some K, Rb, Sr, Ba, rare-earth, H_2O and CO_2 data bearing on their alteration, modification by plagioclase and possible source materials.
Earth and Planet. Sci. Lett., 7, p. 293.

RÅHEIM, A., GALE, G. and ROBERTS, D., 1979: Rb/Sr ages of basement gneisses and supracrustal rocks of the Grong area, Nord Trøndelag, Norway.
Norges geol. Unders. 354, 131-142.

RAMBERG, H., 1967: The Scandinavian Caledonides as studied by centrifuged dynamic models.
Bull. Geol. Inst., Univ. Uppsala, v. 43, p. 1-72.

RAMSAY, D.M. and STURT, B.A., 1976: The syn-metamorphic emplacement of the Magerøy Nappe.
Norsk geol. Tidsskr. 56, 291-307.

RAMSAY, D.M. and STURT, B.A., 1977: A sub-Caledonian unconformity within the Finnmarkian nappe sequence and its regional significance.
Norges geol. Unders. 334, 107-116.

READ, H.H., 1970: Rutley's elements of mineralogy.
George Allen and Unwin (26 ed.), London, 560 p.

REYMER, A.P.S., 1979: Age determination on reworked crystalline basement of the Grong culmination, Norway.
Norges geol. Unders. 354, 143-149.

ROBERTS, D., 1975: The Stokkvola conglomerate - a revised stratigraphical position.
Norsk geol. Tidsskr., 55, 361-371.

ROBERTS, D., 1978: Caledonides of south central Norway. In Caledonian-Appalachian Orogen of the North Atlantic region.
Geol. Survey of Canada Paper 78-12, 31-37.

ROBERTS, D. and GALE, G.H., 1978: The Caledonian-Appalachian Iapetus Ocean. In: Tarling, D.H. (ed.) Evolution of the Earth's crust.
Academic Press, London, New York, 255-342.

ROBERTS, D. and STURT, B.A., 1980: Caledonian deformation in Norway.
Jl. geol. Soc. London, vol. 137, pp. 241-250.

ROBINS, B., 1982: The geology and petrology of the Rognsund intrusion, west Finnmark, northern Norway.
Norges geol. Unders., 371, pp. 1-55.

ROBIN, B. and GARDNER, P.M., 1974: Synorogenic layered basic intrusion in the Seiland Petrographic Province, Finnmark.
Norges geol. Unders., 312, pp. 91-130.

ROSE, A.W., HAWKES, H.E. and WEBB, J.S., 1979: Geochemistry in mineral exploration (2nd ed.).
Academic Press, 657 p.

RUI, I., 1972: Geology of the Røros district, south-eastern Trondheim region, with special study of the Kjøliskarvene-Holtsjøen area.
Norsk geol. Tidsskr., 52, 1-21.

RYAN, P.A. and STURT, B.A., 1981: Early Caledonian orogenesis in North-western Europe.
Abstract, Uppsala Caledonide Symposium, Terra Cognita 1, 1, 71.

SAUNDERS, A.D., TARNEY, J., MARCH, N.G. and WOOD, D.A., 1979: Ophiolites as ocean crust or marginal basin crust: a geochemical approach.
Proc. Int. ophiolite symp., Cyprus, pp. 193-204.

SCHERMERHORN, L.J.G., 1973: What is keratophyre?
Lithos 6, p. 1-11.

SHERVAIS, J.W., 1982: Ti/Y plots and the petrogenesis of modern and ophiolitic lavas.
Earth Planet. Sci. Lett., 59, 101-118.

SHEPPARD, S.M.F., 1977: Identification of the origin of ore forming solutions by the use of stable isotopes.
Inst. Min. Metall. and Geol. Soc. London, special publication no. 7, p. 14-24.

SIGMOND, E.M.O., 1978: Sanda. Description of the 1:250 000 geological map.
Norges geol. Unders., 341, 1-94.

SIGMOND, E.M. and ANDRESEN, A., 1976: A Rb-Sr isochron age of meta-andesites from Skorpehie, Suldal, south Norway.
Norsk geol. Tidsskr., Vol. 56, pp. 315-319.

SILLITOE, R.H., 1972: A plate tectonic model for the origin of porphyry copper deposits.
Econ. Geol., v. 67, p. 184-197.

SILLITOE, R.H., 1980: Types of porphyry molybdenum deposits.
Mining Mag., Volume June, p. 550-553.

SIZE, W.B., 1979: Petrology, geochemistry and genesis of the type area trondhjemite in the Trondheim Region, Central Norwegian Caledonides.
Norges geol. Unders. 351, pp. 51-76.

SMITH, F.G., 1963: Physical geochemistry.
Addison-Wesley Inc., U.S.A., 624 p.

SPRY, A., 1969: Metamorphic textures.
Pergamon Press Ltd., Oxford, 350 p.

STURT, B.A. and RAMSAY, D.M., 1965: The alkaline complex of the Breivikbotn area, Sørøy, northern Norway.
Norges geol. Unders., 231, 142 p.

STURT, B.A., PRINGLE, I.R. and RAMSAY, D.M., 1978: The Finnmarkian Phase of the Caledonian Orogeny.
J. Geol. Soc. London 135, 597-610.

STURT, B.A. and ROBERTS, D., 1978: Caledonides of northernmost Norway (Finnmark).
Geol. Surv. Canada, Paper (78-13).

SUTULOV, A. (ed.), 1975: International Molybdenum Encyclopedia, Vol. 1, Intermet Publications, Santiago De Chile.

STEPHENS, M.B., 1980: Spilitization, element release and formation of massive sulphides in the Stekenjokk volcanites, central Swedish Caledonides.
Norges geol. Unders. 360, 159-193.

TAYLOR, S.R., 1969: Trace element chemistry of andesites and associated calc-alkaline rocks. In: Proceeding of the andesite conference. McBinney (Ed.), Bull. 65, Department of Geology and Mineral Industries, State of Oregon, pp. 43-63.

VOKES, F.M., 1978: Introduction: in Mineral deposits of Europe. V. 1, (ed. Bowie, S.H.U., Kvalheim, A. and Haslam, H.W.). Mineralogical Society of London.

VOKES, F.M., 1979: Rapport over befaring av Mo-Cu mineraliseringer i området omkring Fremstfjellet (Fremsttjern-Smalltjern - Kroktjern-Amøbetjern); Sanddøla Området, Grong-feltet.
Unpublished report, Grong Gruber A/S.

VOKES, F.M. and GALE, G.H., 1976: Metallogeny Relatable to Global Teconics in Southern Scandinavia.
Geological Association of Canada. Special Paper No. 14, pp. 413-441.

WALLACE, S.R., MACKENZIE, W.B., BLAIR, R.G. and MUNCASTER, N.K., 1978: Geology of the Urad and Henderson molybdenite deposits, Clear Greek County, Colorado, with a section on A comparison of these deposits with those at Climax, Colorado.
Econ. Geol., v. 73, p. 325-368.

WESTRA, G. and KEITH, S.B., 1981: Classification and genesis of stockwork molybdenum deposits.
Econ. Geol., v. 76, p. 844-873.

WILSON, A.D., 1955: Rocks and Mineral Analysis.
Bull. Geol. Surv. Gt. Britain, 9, pp. 56-58.

WILLSON, J.R. and OLESEN, N.Ø., 1975: The form of the Fongen-Hyllingen gabbro complex, Trondheim region, Norway.
Norsk geol. Tidsskr., 55, 423-439.

WINKLER, H.G.H., 1974: Petrogenesis of metamorphic rocks.
New York, Heidelberg, Berlin: Springer, 3rd ed.

WOLFF, F.Chr., 1967: Geology of the Meråker area as a key to the eastern part of the Trondheim region.
Norges geol. Unders., 245, 123-146.

WOLFF, F.Chr., 1980: Excursions across part of the Trondheim region, Central Norwegian Caledonides, F.Chr. Wolf (ed.).
Norges geol. Unders., 356, 115-167.

YODER, H.S. and TILLEY, C.E., 1962: Origin of basalt magmas: An experimental study of natural and synthetic rock system.
J. Petrol., 3, 342-532.

ZACHRISSON, E., 1969: Caledonian geology of north Jamtland, southern Vasterbotten; Koli stratigraphy and main tectonic outlines.
Sveriges Geol. Unders., v. C644, p. 1-32.

ZWAAN, K.B. and ROBERTS, D., 1978: Tectonostratigraphic succession of the Finnmarkian Nappe Sequence, north Norway.
Norges geol. Unders., 343, 53-72.

GALE, G., 1975: Geology and sulphide mineralization in the Sanddøla-Gaizervann area, Grong, Nord-Trøndelag.
Norges geol. Unders., report 1293 (unpubl.).

Appendix 1: Petrographic data

1.a Greenstone. N5, N16, N15, 3/10, 4/7, 7/11, Y3, Y4, Y1, Y2, 4/8/12, 4/8/13, 4/8/5, 4/8/6, 4/8/7.

1.b Gabbro and diorite. B7, N6, B7/c, B7/d, B7/a, B7/b, 4/8/14, N4, 4/8/15, 3/20, C5, N2, N8, CYP.

1.c Trondhjemite. H1, J1/b, F1, J1/a, J2, H2, B5, B6/a, A4, B3, A5, B2/d.

1.d Granite. T5/j, T1/a, T5/c, T5/b, T5/f, T6/e, T3/b, 2/2, 2/8, 6/3o.

1.e Dolerite dyke. N20, Md, N3.

1.f Conglomerate. 4/8/1.

1.a Greenstone

Sample Number	Rock type	Petrography	Fabric	Analysis
N5	Metabasalt	chl+plg+opq+hbl+ep+ser+cab+sph	extensively chloritized, schistose, originally fine-grained	XRF
N16	Schistose basalt	plg+chl+ep+cab+opq+ser+trem+act+sph	sheared, schistose, recrystallised and veined by carbonate and quartz	XRF
N15	Basaltic andesite	plg+bio+hbl+opq+ep+ser+chl+cab+sph+ap+trem+act ±qtz	porphyritic	XRF
3/10	Basaltic andesite	plg+bio+hbl+opq+ep+ser+cab+chl+trem+sph+qtz	massive, biotite rich rock	
4/7	Basaltic andesite	plg+bio±hbl+opq+ep+ser+chl+trem±stil±qtz		
7/11	Andesite	plg+bio+opq+chl+ep+ser+sph±qtz+cab±trem±act		
Y3	Andesite	plg+qtz+bio+opq+ep+chl+act+trem+cab+sph+ap±zr	strong mylonitic fabric, pressure shadows. Typical greenschist facies mineral paragenesis	XRF
Y4	Sodic rhyolite	plg+qtz+opq+chl+trem+ep+mus+ser+sph±zr±ap		XRF
Y1	Sodic rhyolite	plg+qtz+opq±bio±mus+chl+ser+ep+cab+sph±trem	slightly sheared. recrystallised but with relict porphyritic texture	XRF
Y2	Sodic rhyolite	plg+qtz+opq+py+ser+chl+ep+sph+trem	submylonitic texture and veined by quartz	XRF
4/8/12	Altered rhyolite	plg+qtz+ep+mus+chl+cab+sph+zr+opq	schistose	
4/8/13	Sheared rhyolite	plg+qtz+chl+ser+mus+ep+py+cab+opq+sph	veined by quartz albite veins	

Sample Number	Rock type	Petrography	Fabric	Analysis
4/8/5	Calcareous marl	(1) ep+opq+plg+trem+cab ±qtz (2) cab+ep+plg+opq+trem +qtz (3) cab+plg+ep+qtz+opq+ sph	laminated 1.2.3 are thin beds <1 cm in thickness	
4/8/6	Interbedded calcareous sandstone and siltstone	(1) qtz+qtz pebbles+qtz fragments in a recrystallized calcareous matrix: cab+ep+trem+sph+opq (2) fine matrix of ep+ trem+qtz+sph+plg+ opq+other rock fragment+cab+ep	interbedded	
4/8/7	Calcareous metasediment	cab+ep+opq+trem+qtz+ap	laminated and veined later carbonate vein	
1.b Gabbro and diorite				
B7	Hornblendite	hbl+plg+pyrx+opq+bio+ chl+ep+sph+ap±scp (plagioclase range from albite-andesine)	uralitized and saussuritized	XRF
N6	Cumulate gabbro	pyrx+hbl+mag+plg±bio± ol+ep+chl+sph+act+trem		XRF
B7/c	Hornblendite	hbl+plg+opq+ep+chl+ trem+act+sph	recrystallized	XRF probe
B7/d	Gabbro	plg+hbl+pyrx+opq+ep+ chl+sph+ap	primary structure with incipient recrystallization	XRF
B7/a	Hornblende gabbro	plg+hbl+pyrx+opq+epd+ chl+ser+sph+ap	massive with ophitic texture	XRF
B7/b	Pyroxenite	aug+hbl±hyp+plg+act+ trem+chl+ep+opq+sph+ ap±scp	uralitized with crude layering probably of cumulate origin	XRF
4/8/14	Gabbro	plg+hbl+pyrx+opq+ser+ ep+chl+sph	recrystallized	XRF

Sample Number	Rock type	Petrography	Fabric	Analysis
N4	Pyroxenite	pyrx+plg+trem+opq+hbl+ep+sph	pyroxenes show exsolution lamellae and cumulate texture	XRF and probe
4/8/15	Microgabbro	plg+hbl+opq+bio+ep+act+trem+ser+chl+sph+qtz+ap		XRF
3/20	Hornblende gabbro	plg+pyrx+hbl+opq+bio+ser+ep+chl+trem+act+sph+ap	ophitic texture	
	veined by carbonate vein	cab+chl+hbl+plg+qtz	glide twinning	
C5	Diorite	plg+trem+bio+opq+ser+ep+ap+chl+sph	altered	XRF
N2	Quartz diorite	plg+trem+qtz+bio+ser+ep+opq+chl+ap+sph	sheared	XRF
N8	Quartz diorite	plg+qtz+bio+trem+ep+ser+opq+chl+sph+ap		XRF
CYp	Quartz diorite	plg+qtz+trem+sph+opq+ap+ep+ser+chl		XRF
1.c	Trondhjemite			
H1	Trondhjemite	plg+qtz+ep+opq+bio+chl+trem+act+mus+ser+sph+ap	veined by quartz and chlorite-schistose and strained	XRF
J1/b	Schistose trondhjemite	plg+qtz+ep+opq+trem+act+ser+sph+ap	schistose	XRF
P1	Foliated trondhjemite	plg+qtz+ep+ser+chl+mus+opq+sph	altered and metamorphosed	XRF probe
J1/a	Porphyritic trondhjemite	plg+qtz+ep+ser+hbl+trem+act+sph+ap	veined by quartz and chlorite parallel to the foliation	XRF probe
J2	Trondhjemite	plg+qtz+ep+ser+py+sph+ap	veined by quartz and sericite	XRF
H2	Trondhjemite	plg+qtz+chl+ser+ep+cab+opq+sph+ap+py+al		XRF probe

Sample Number	Rock type	Petrography	Fabric	Analysis
B5	Trondhjemite	plg+qtz+per+opq+ser+ep+chl+sph+mus+ap	granular	XRF probe stained for feldspar
B6/a	Trondhjemite	plg+qtz+per+opq+ser+ep+mus+chl+act+trem+sph+ap	veined and sheared	XRF stained for feldspar
A4	Trondhjemite	plg+qtz+opq+ser+ep+chl+mus+sph+ap+zr	recrystallized	XRF stained for feldspar
B3	Trondhjemite	plg+qtz+per+bio+opq+ser+ep+chl+mus+sph+ap	plagioclase is zoned and the rock is sheared	XRF
A5	Trondhjemite	plg+qtz+opq+ser+ep+chl+mus+sph+ap		XRF
B2/d	Trondhjemite	plg+qtz+per+ser+ep+sph+ap+chl+zr	granular	XRF
1.d Granite				
T5/j	Granite	kfs(per+mic)+plg+qtz+mus+opq+ser+ep+ap + sph+cab	moderately sheared	XRF
T1/a	Sheared granite	per+plg±or+qtz+ser+ep+opq+sph+ap+chl+hem+cab	greenschist assemblage	XRF probe stained for feldspar
T5/c	Granite	kfs(per+mic)+plg±or+qtz+mus±bio+opq+ser+ep+sph+ap+zr±act±trem	feldspar are zoned and show mortar structure	XRF stained for feldspar
T5/b	Graphic granite	kfs(mic+per)+or+plg+qtz±mus+ser+ep+opq+sph+ap+chl+cab	micrographic intergrowth	XRF probe

Sample Number	Rock type	Petrography	Fabric	Analysis
T5/f	Granite	kfs(per±or)+plg+qtz+ mus±bio+ser+ep+opq+sph+ ap+act+trem+cab+zr	moderately sheared	XRF
T6/e	Sheared granite	plg+qtz+mus+ser+ep+sph+ opq+cab		XRF stained for feldspar
T3/b	Granite	kfs(per±mic)+plg+qtz± mus+ser+ep+opq+sph	slightly altered and recrystallized	XRF probe stained for feldspar
2/2	Aplite granite	plg+per+qtz±mus+ser+ep +opq+sph+ap±chl	chilled against basic material	
2/8	Granite	per+plg+or+qtz+mus+ ser+ep+opq+sph+zr		
6/30	Granite	kfs(per+mic±or)+plg+ qtz+mus+bio+ser+ep+opq +sph+zr+cab	micrographic texture	stained for feldspar
1.e Dolerite dyke				
N20	Dolerite	ep+plg+ser+chl+act+sph +opq+cab	altered	XRF
M4	Dolerite	ep+plg+ser+act+opq+qtz +chl+sph		XRF
N3	Porphyritic dolerite	ep+ser+plg+chl+act+ trem+sph+opq+cab+qtz±ap	intensively altered	XRF
4/8/1	Conglomerate	plg+qtz+opq - trondhjemitic boulder plg+qtz+opq+bio+sph+ ser+ep+chl plg+qtz+chl+opq+sph+ser +ep+cab	pebbles boulder semi pelitic matrix	

Abbreviations used:

qtz = quartz

kfs = K-feldspar

mic = microcline

per = perthite

or = orthoclase

plg = plagioclase

mus = muscovite

bio = biotite

ser = sericite

stil = stilpnomelane

chl = chlorite

hbl = hornblende

trem = tremolite

act = actinolite

ep = epidote

cab = carbonate

scp = scapolite

pyrx = pyroxene

ol = olivine

ap = apatite

sph = sphene

opq = opaque minerals (pyrite + magnetite)

py = pyrite

zr = zircon

hem = hematite

mag = magnetite

aug = augite

hyp = hypersthene

al = allanite

Appendix 2: Mineral analyses

2.a Pyroxene analyses (N4)

	N4/1	N4/2	N4/3	N4/4	N4/5	N4/6	N4/7	N4/8	N4/9	N4/10
SiO_2	51.70	52.14	51.10	52.72	53.33	52.59	51.62	52.63	51.51	52.81
Al_2O_3	1.70	1.06	1.26	0.66	0.73	0.54	0.94	0.39	1.98	1.23
FeO	5.94	6.19	5.52	6.10	6.00	7.33	7.11	7.04	6.29	6.61
MgO	13.94	14.09	14.06	14.18	14.43	13.66	13.09	13.17	13.68	14.02
CaO	23.51	23.52	23.14	23.43	23.79	22.72	22.82	23.23	23.26	22.92
Na_2O	0.62	-	-	-	0.56	0.53	-	-	-	0.42
TiO_2	0.01	0.18	-	0.14	0.16	0.13	0.14	-	0.44	0.34
MnO	-	0.12	0.14	-	-	0.32	0.22	0.26	0.13	-
Cr_2O_3	-	0.19	0.15	0.14	-	0.16	-	0.13	-	-
Total	97.42	97.49	95.37	97.37	99.00	97.98	95.94	96.85	97.29	98.35
ionic $\frac{Mg}{(Mg+Fe)}$	80.70	80.22	81.95	80.56	81.14	76.85	76.64	76.92	79.48	79.08

2.b Amphibole analyses (B7/c, N4, J1/a)

	B7C/1	B7C/2	B7C/3	N4/1	N4/2	J1a/1	J1a/2	J1a/3	J1a/4
SiO_2	41.53	41.29	40.32	41.13	49.99	56.80	55.12	60.07	50.76
Al_2O_3	11.43	11.67	12.09	11.04	4.67	1.18	1.16	0.69	5.98
FeO	14.86	14.32	13.04	11.09	11.07	8.78	8.49	7.76	9.86
MgO	11.49	11.64	12.21	14.42	15.63	18.07	17.72	15.86	13.72
CaO	11.61	11.28	11.47	9.08	12.33	12.70	12.30	11.40	13.53
Na_2O	1.90	1.96	2.42	0.56	0.85	-	-	-	-
K_2O	0.66	0.69	0.81	2.29	0.36	0.11	0.10	0.11	0.43
TiO_2	1.98	2.13	2.47	1.75	0.59	-	-	-	-
MnO	0.19	0.22	0.15	-	-	0.27	0.29	0.26	0.26
Cr_2O_3	-	-	-	-	0.13	-	0.11	-	-
Total	95.65	95.20	94.98	91.36	95.62	97.91	95.29	96.15	94.54

2.c Feldspar analyses (BH8, F1, J1/a, H2, B5, T5/b, T3b)

	B8	F1	J1/a	H2	B5/1	B5/2	B5/3	B5/4	T5/b	T3/b
SiO_2	68.66	66.75	67.15	67.51	67.94	68.08	67.15	58.87	63.60	64.53
Al_2O_3	19.30	19.41	19.71	19.28	19.29	19.36	19.39	20.76	17.94	20.98
FeO	-	0.25	0.13	-	0.17	-	0.11	0.83	0.11	-
CaO	0.20	0.15	0.18	0.16	0.08	0.13	-	9.86	-	0.26
Na_2O	11.45	11.30	11.17	11.61	11.61	11.99	11.27	7.39	0.45	10.41
K_2O	0.09	0.39	0.56	-	0.15	-	0.26	-	16.19	0.96
Total	99.70	98.25	98.90	98.56	99.24	99.56	98.18	97.71	98.29	97.14

2.d Epidote analyses (BH8, B7/c, F1, J1/a, H2, T1/a, T5/b)

	BH8/1	BH8/2	BH8/3	BH8/4	BH8/5*	B7C/1	B7C/2	F1/1	J1a/1	J1a/2
SiO_2	38.75	37.51	37.44	38.42	21.51	36.92	38.15	36.94	37.22	36.91
Al_2O_3	24.82	20.04	23.65	23.36	13.51	23.12	21.37	19.14	22.29	19.83
FeO	9.95	14.88	10.89	11.16	6.46	11.20	12.37	15.84	12.66	15.28
MgO	-	-	-	-	0.58	-	1.42	-	-	-
CaO	22.69	21.90	22.15	22.38	6.79	22.57	20.84	21.99	21.88	20.37
TiO_2	-	-	0.28	0.19	0.89	0.14	-	-	-	-
MnO	0.12	-	0.18	-	-	0.13	0.16	-	0.12	-
Cr_2O_3	-	-	-	0.15	-	0.14	0.13	-	-	-
CuO	-	-	-	-	0.38	-	-	-	-	-
Total	96.33	94.33	94.59	95.66	50.12	94.22	94.44	93.91	94.17	92.39

2.d continued

	H2/1	H2/2*	H2/3*	H2/4*	T1a/1	T1a/2	T1a/3	T1a/4	T5b/1	T5b/2
SiO_2	36.79	29.43	24.68	29.01	38.37	38.37	39.14	37.67	37.47	33.00
Al_2O_3	21.69	13.10	13.16	12.41	21.89	21.36	27.52	23.08	22.37	21.34
FeO	13.36	11.60	10.35	10.44	12.96	14.09	6.92	11.51	10.16	11.40
MgO	-	0.60	0.23	0.23	-	-	-	-	-	-
CaO	21.82	9.75	6.90	8.46	22.85	22.64	23.58	22.60	22.33	21.45
TiO_2	0.13	0.29	0.94	0.80	-	0.21	-	0.23	-	-
MnO	0.15	-	0.45	0.35	-	-	-	-	-	-
Cr_2O_3	-	-	-	-	-	-	0.14	-	-	-
CuO	-	0.40	1.70	0.74	-	-	-	-	-	-
Total	93.94	65.17	58.41	62.44	96.07	96.67	97.30	95.09	94.33	87.19

*Allanite, REE not determined

GEOLOGICAL MAP OF FREMSTFJELL AREA, GRONG DISTRICT, CENTRAL NORWAY

MAP 1

12°51.07'E

13°00'

64°30'N

64°28.20'

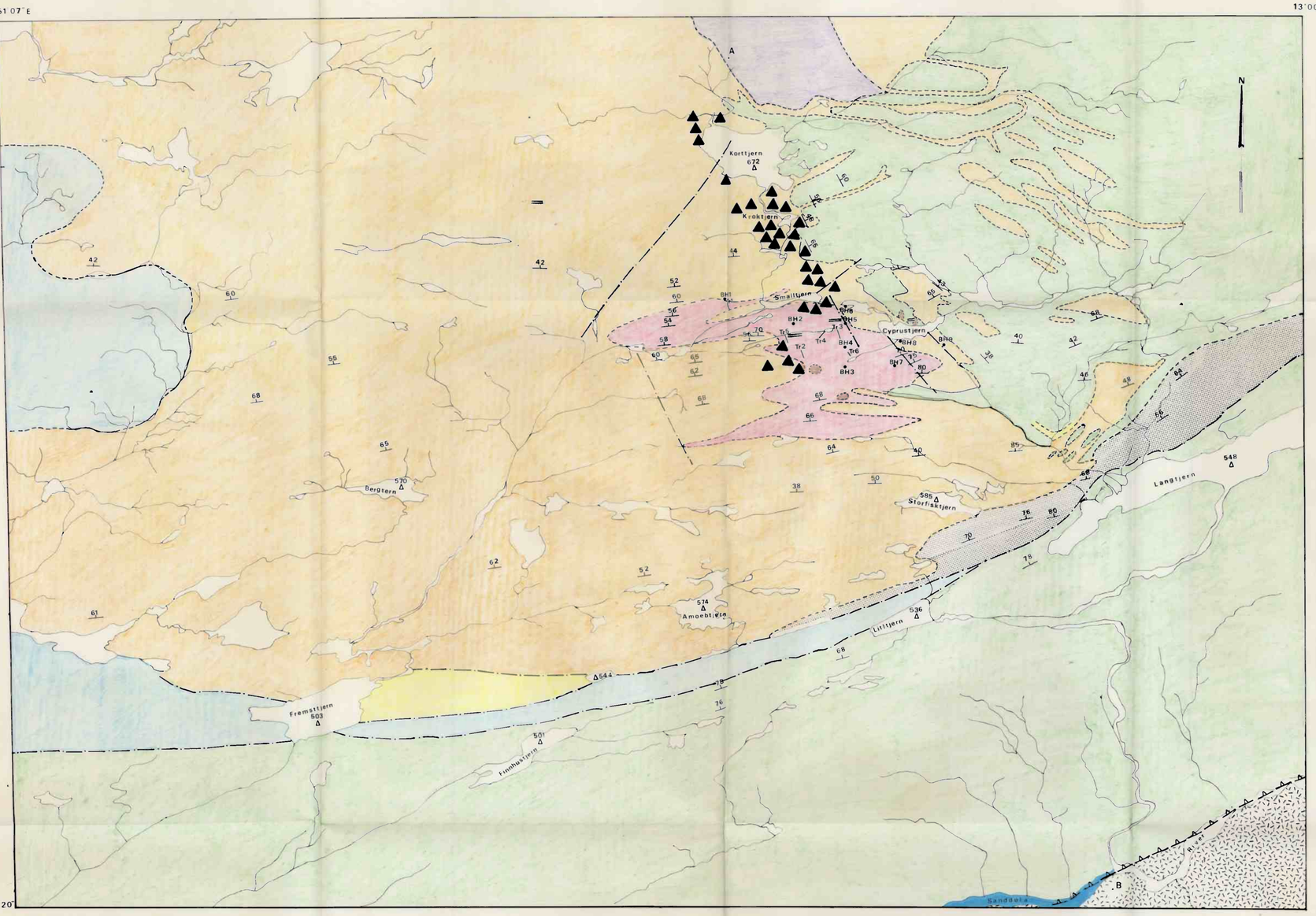

Legend

- Conglomerate
- Dolerite Dyke Trend
- Granite
- Trondhjemite
- Diorite
- Gabbro/Gabbroic Blocks
- Calcareous Metasediment
- Rhyolite
- Basalt and basaltic andesite
- Basement (granitic gneiss of Baltic Shield)
- Thrust Fault
- Normal or high angle reverse fault
- Geological boundary (certain and uncertain)
- Dip and strike of foliation
- 8H1 Borehole
- Tr1 Trench
- 548 Spot height in metres

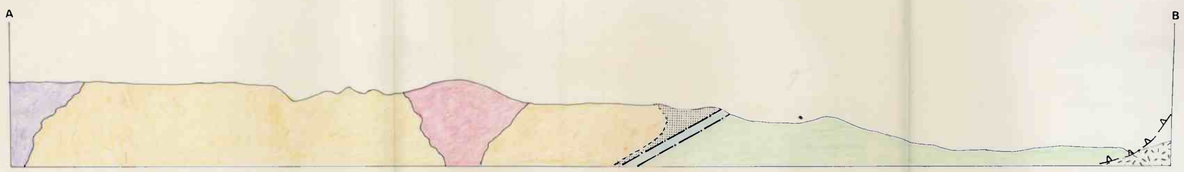

SCALE 1:10000

0 200 600 1000 M

MAPPED BY
ABDEL R I MOHAMED.1984

SAMPLE POINT AND MINERALIZATION ZONING MAP

FREMSTFJELL AREA

MAP 2

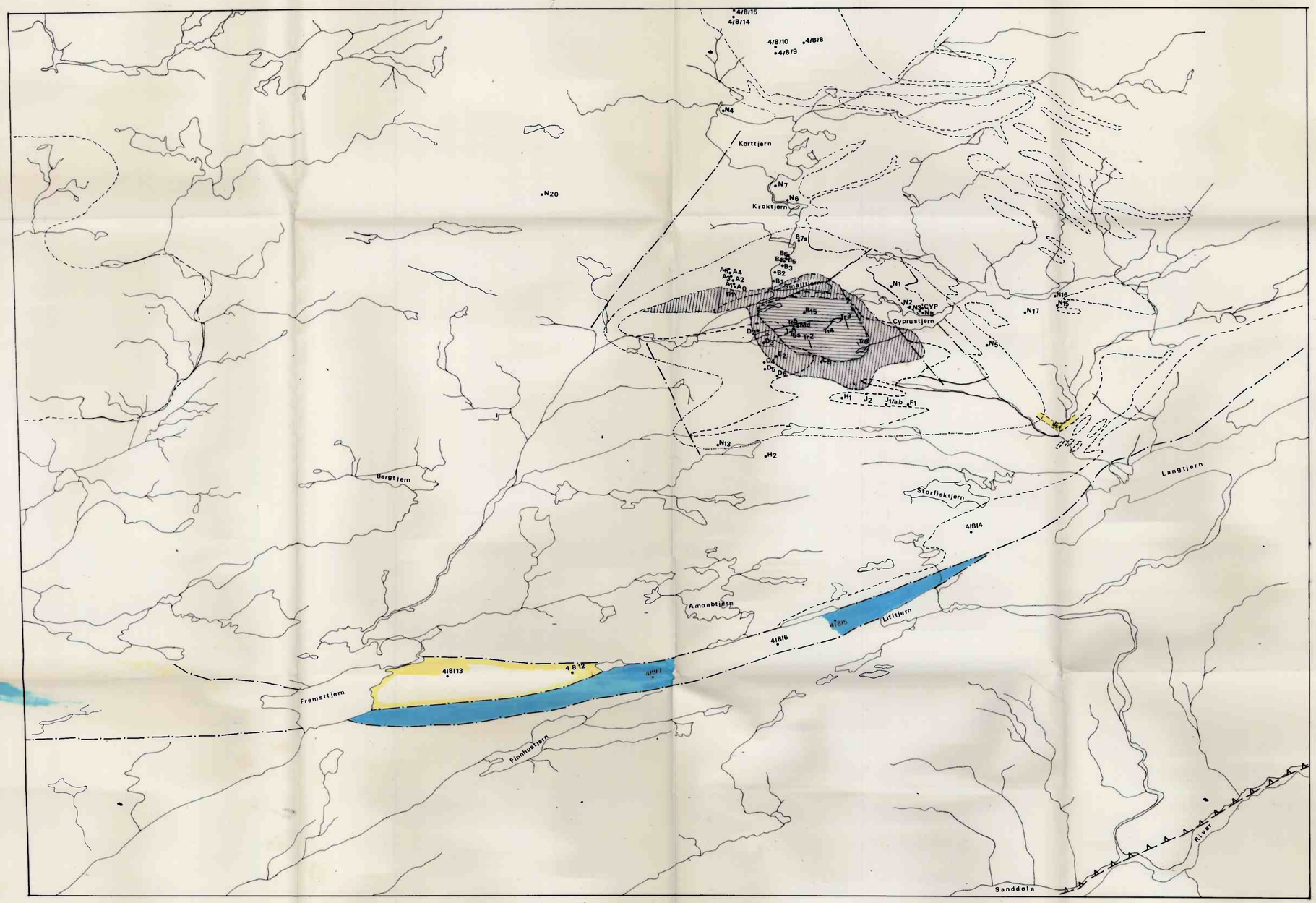

LEGEND

- Inner zone with Mb. Cp. Py
- Intermediate zone with Mb. Py
- Outer zone with Py
- Thrust Fault
- Normal or high angle reverse fault
- Geological boundary (certain and uncertain)
- Mineral zone boundary
- Tr1 — Trench
- A1 / 4/8/8 — Sample collected at surface
- B7s — Location of samples B7, B7/a, B7/b, B7/c, B7/d
- T5s — Location of samples T5/b, T5/c, T5/f, T5/j, T5/o
- Xs — Location of samples x1, x2, x3, x4

SCALE 1:10,000

0 200 600 1000 M

MAPPED BY:
ABDEL R I MOHAMED. 1984